Zoological Journal of the Linnean Society, 2008, **152**, 655–706. With 42 figures

A species complex within the isopod genus *Haploniscus* (Crustacea: Malacostraca: Peracarida) from the Southern Ocean deep sea: a morphological and molecular approach

WIEBKE BRÖKELAND[1]* and MICHAEL J. RAUPACH[2]

[1]*Forschungsinstitut Senckenberg, Abteilung DZMB, Südstrand 44, 26382 Wilhelmshaven, Germany*
[2]*Zoologisches Forschungsmuseum Alexander Koenig, Adenauerallee 160, 53113 Bonn, Germany*

Received 1 August 2006; accepted for publication 2 July 2007

Seven new species of the genus *Haploniscus* from the deep Scotia and Weddell Seas are presented, combining morphological and molecular data (mitochondrial 16S rDNA and nuclear 18S rDNA). ***Haploniscus cassilatus* sp. nov.**, ***H. cucullus* sp. nov.**, ***H. weddellensis* sp. nov.**, ***H. procerus* sp. nov.** and ***H. kyrbasia* sp. nov.** are characterized by a prominent rostral process, the size and shape of which vary among species. The rostrum of ***H. microkorys* sp. nov.** is distinctly smaller than that of the former species, while ***H. nudifrons* sp. nov.** does not possess a rostrum. The status of the latter as separate species is obvious, owing to the stronger morphological differences. DNA was sequenced from three of the other five species. Genetic distances together with the more subtle morphological variation justify the erection of separate species. Overall morphological variations between these species are small yet noticeable and include, among others, the rostrum, the shape of the pleotelson and setation of pereopods. Our molecular data sets reveal detailed phylogenetic insights within the *Haploniscus cucullus* complex, supporting the monophyly of all species. We found *p*-distances of at least 0.0732 (16S rDNA) and 0.0140 (complete 18S rDNA) between pairs of species and show that both genes can be used as a marker for DNA taxonomy.

ADDITIONAL KEYWORDS: 16S rDNA – 18S rDNA – DNA taxonomy – Haploniscidae – *Haploniscus cucullus* complex – molecular phylogeny – sibling species.

INTRODUCTION

DNA-based studies of phylogeny and genetic differentiation of deep-sea organisms are scarce. Nevertheless, recent genetic studies show that the number of species known from the deep sea may increase as a result of the existence of cryptic species (Etter & Rex, 1990; France & Kocher, 1996; Etter *et al*., 1999, 2005; Quattro *et al*., 2001; Weinberg *et al*., 2003; Raupach & Wägele, 2006), because speciation processes may be less coupled to morphology than to other phenotypic aspects, e.g. differences in ecology or life history (Knowlton, 1993, 2000). For asellote isopods, the dominating crustacean taxon in the deep sea, some additional aspects can be important and influence speciation. Asellotes are usually small animals, display a reduced mobility (even though some can swim, e.g. species of the Munnopsidae) and have no free-living larvae. This probably reduces gene flow and increases the probability for speciation events (Raupach & Wägele, 2006). The first molecular studies of the genus *Acanthaspidia* gave evidence for cryptic, reproductively isolated species (Raupach & Wägele, 2006).

Taxonomic discrimination of closely related species often relies on subtle morphological characteristics, making routine identification difficult. However, it has long been recognized that analysis of DNA sequences might be used to discriminate species, but

*Corresponding author.
E-mail: wbroekeland@senckenberg.de

that it is important to use meaningful gene sequences (Hebert *et al*., 2003; Tautz *et al*., 2003). Nevertheless, it must be emphasized that the power of DNA sequences for identifying species is limited when species pairs have very recent origins, and sequences from only one specimen and one locus will not be sufficient for an unequivocal assignment to a particular group, and more specimens have to be analysed (e.g. Bucklin, Bentley & Franzen, 1998; Ward *et al*., 2005).

The present study describes a small group of *Haploniscus* species from the Southern Ocean deep sea, which are essentially similar in morphological respect, but show considerable variation in size and shape of the rostral process. The isopod family Haploniscidae is a typical deep-sea taxon, and only few species are known to occur above 1000 m water depth. The phylogenetic relationships within the family are still unresolved. By far the largest of the haploniscid genera (currently 69 species, including those species described in the following), *Haploniscus* forms a depository for species that cannot be allocated to one of the six other and more clearly defined genera of the family (Lincoln, 1985a, b; Brökeland & Wägele, 2004) and needs to be revised. This depends on redescription of most *Haploniscus* species, as the original descriptions are often inadequate and lack essential information, especially regarding the appendages. The analysed specimens were conspicuous among the haploniscid material in the deep-sea samples obtained during the ANDEEP I & II expeditions to the Scotia and Weddell Seas, Southern Ocean. In addition to morphological characters we used partial mitochondrial 16S rDNA and complete nuclear 18S rDNA as molecular characters for inference of phylogenetic relationships and distinction between species.

MATERIAL AND METHODS

Sampling

During the Expeditions ANT XIX/3 + 4 (ANDEEP I and II, Antarctic benthic deep-sea biodiversity) with *RV Polarstern* in the Southern Ocean samples were obtained by means of an epibenthic sledge (Brenke, 2005) (Fig. 1). All samples were fixed in 96% precooled ethanol immediately and kept at –20 °C for at least 48 h before sorting to ensure proper fixation and prevent DNA digestion (e.g. Dreyer & Wägele, 2001, 2002). Specimens were partly sorted on board or later in the laboratory in the Zoological Museum of the University of Hamburg.

Taxonomic methods

Species were identified using a Leica MZ 7.5 dissecting microscope and illustrated using a Leitz Dialux compound microscope, equipped with a camera lucida. Total body length was measured in lateral

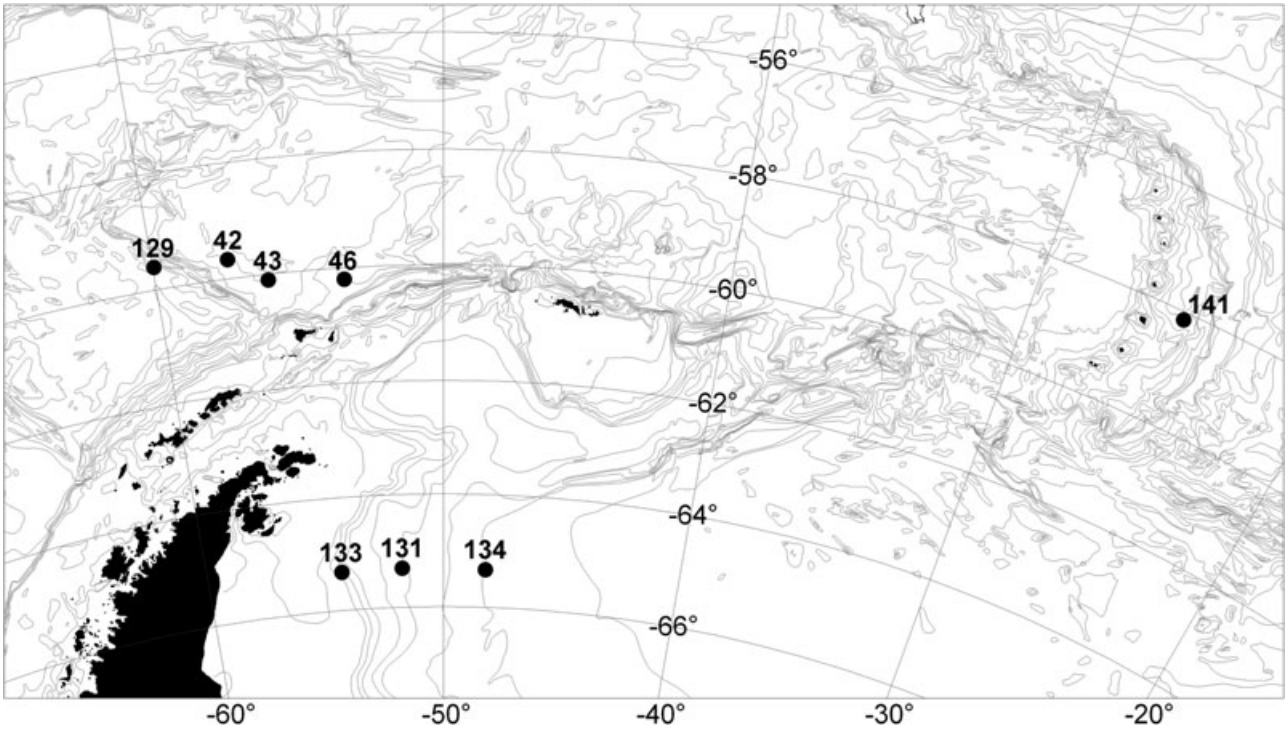

Figure 1. Station map, showing localities, where the *Haploniscus* species were sampled.

Table 1. Individual codes and GenBank accession numbers for gene sequences of examined specimens (for locality details see Taxonomy)

Species (locality)	Individual code	16S rDNA GenBank accession No.	18S rDNA GenBank accession No.
Antennuloniscus armatus (station 42-2)	HA55	AY693397	AY461468 (Raupach *et al*., 2004)
Haploniscus cassilatus (station 46-7)	HA2	AY693400	
Haploniscus cassilatus (station 46-7)	HA34	AY693405	
Haploniscus cassilatus (station 46-7)	HA35	AY693406	
Haploniscus cassilatus (station 46-7)	HA36	AY693407	DQ435679
Haploniscus cassilatus (station 46-7)	HA37	AY693408	
Haploniscus cassilatus (station 46-7)	HA38	AY693409	
Haploniscus cucullus (station 42-2)	HA24	AY693401	
Haploniscus cucullus (station 42-2)	HA26	AY693402	
Haploniscus cucullus (station 42-2)	HA27	AY693403	
Haploniscus cucullus (station 42-2)	HA28	AY693404	
Haploniscus cucullus (station 42-2)	HA56	AY693411	AY461465 (Raupach *et al*., 2004)
Haploniscus cucullus (station 43-8)	HA39	AY693410	
Haploniscus cucullus (station 43-8)	HA68	AY693413	
Haploniscus cucullus (station 42-2)	HA70	AY693414	
Haploniscus microkorys (station 134-4)	HA450	AY693421	AY461467 (Raupach *et al*., 2004)
Haploniscus nudifrons (station 129-2)	HA402	AY693419	DQ435680
Haploniscus weddellensis (station 133-3)	HA73	AY693415	
Haploniscus weddellensis (station 133-3)	HA78	AY693416	
Haploniscus weddellensis (station 133-3)	HA79	AY693417	
Haploniscus weddellensis (station 133-3)	HA80	AY693418	DQ535681
Mastigoniscus sp. 1 (station 42-2)	HA51	AY693398	
Mastigoniscus sp. 1 (station 42-2)	HA57	AY693399	AY461469 (Raupach *et al*., 2004)

view from the anterior edge of the head to the posterior medial tip of the pleotelson. Length of the pleotelson was measured medially from the anterior margin to posterior margin; the anterior margin was defined as the line between the anterior angles of the pleotelson because this segment is usually fused middorsally with pereonite 7. The length of the head was measured without rostral process. Generally, length/width ratios refer to the greatest length and width of the limb or segment. Because of the differing degree of curvature of the specimens, pleotelson and head were illustrated in plain dorsal view for comparison. The differentiation in peduncular and flagellar articles of the antennae follows Lincoln (1985a) and Wägele (1983). The maxilliped as well as male pleopods 1 and 2 are illustrated in dorsal view, because the dorsal side of these limbs is more richly structured (e.g. setation, sculpture) than the ventral side.

Molecular studies

DNA isolation and polymerase chain reaction

DNA was extracted on board from several dissected legs of the specimens, using the QIAmp© Tissue Kit (Qiagen GmbH) and following the recommended extraction protocol. Specimen vouchers are deposited in the Zoological Museum Hamburg.

Total genomic DNA of 23 specimens (see Table 1) of the Haploniscidae was amplified using the widely applicable primer pair 16Sar (5′-CGCCTGTTTATC AAAAACAT-3′) and 16Sbr (5′-CCGGTCTGAACTC AGATCACG 3′) (Palumbi *et al*., 1991). Amplifications were performed in 25-μL reactions containing 2.5 μL 10× Qiagen PCR buffer, 2.5 μL dNTPs (2 mmol μL^{-1}), 0.3 μL of each primer (50 pmol μL^{-1}), 1–2 μL of DNA template, 5 μL Q-Solution©, 0.2 μL Qiagen *Taq* (5 U μL^{-1}), filled up to 25 μL with sterile H_2O, on a Progene Thermocycler (Techne Ltd). The temperature profile of the PCR consisted of an initial denaturation of 94 °C (5 min), followed by 38 cycles of 94 °C (45 s), 44 °C (45 s) and 72 °C (80 s). Three microlitres of amplified product was controlled by electrophoresis in an agarose gel (1%) with ethidium bromide using DNA size standards. The remaining PCR product was purified with the QIAquick© PCR Purification Kit (Qiagen GmbH). Beside parts of the mitochondrial 16S rRNA gene, complete 18S rDNA sequences of three different species of the analysed Haploniscidae were amplified (see Table 1). Primers and PCR

conditions are given in Raupach, Held & Wägele (2004) and Raupach & Wägele (2006).

DNA sequencing

Chain-termination cycle sequencing (Sanger, Nicklen & Coulson, 1977) was performed using a Thermo-Sequenase Fluorescent Labelled Primer Cycle Sequencing Kit (Amersham Pharmacia Biotech) on a Primus96^{plus} Thermocycler (MWG-Biotech AG). For sequencing the 16S amplification product, fluorescently labelled primers with the same sequence as for amplification were used (Palumbi *et al*., 1991). Cycle sequencing conditions were: 2 min at 94 °C (initial denaturation), followed by 30 cycles of denaturation at 94 °C for 25 s, annealing at 56–58 °C for 25 s, and extension at 70 °C for 35 s. Primers and sequencing conditions used for the 18S rDNA sequences have been described elsewhere in detail (Raupach *et al*., 2004). A LI-COR 4000 (LI-COR Inc.) was used for automated sequencing; gels were proofread using the image analysis software of the automated sequencer. Double stranded sequences were assembled with the program AlignIR v1.2. All new 16S rDNA and 18S rDNA sequences can be retrieved from GenBank as indicated in Table 1.

Sequence alignment and phylogenetic analyses

All 23 partial 16S rDNA sequences were aligned using MUSCLE version 3.6 (Edgar, 2004) with default settings, generating an alignment of 530 bp. In addition to the three new sequenced 18S rDNA sequences we included four already published sequences of the Haploniscidae in our analyses (see Table 1). The 18S rDNA sequences were also aligned using MUSCLE, engendering an alignment of 2220 bp. Both alignments are available from the authors.

Both alignments were tested for nucleotide bias using a chi-square test of base composition homogeneity across taxa implemented in PAUP*4.0b10 (Swofford, 2001). Phylogenetic trees were reconstructed by Bayesian analysis using the program MrBayes v3.1 (Huelsenbeck & Ronquist, 2001). Markov chain Monte Carlo analyses were run for 10 million generations using random starting trees. Trees were sampled every 100 cycles, yielding 19 300 trees of the Markov chain after discarding 35 000 generations for both data sets. Statistical node support was assessed by posterior proabilities. Appropriate likelihood models were determined using the Akaike Information Criterion (AIC) (Akaike, 1974) implemented in MODELTEST version 3.7 (Posada & Crandall, 1998). The determined models of nucleotide substitution were used as parameter sets for the Bayesian analyses. In addition, PAUP*4.0b10 was employed for calculating pairwise genetic distances.

TAXONOMY

FAMILY HAPLONISCIDAE HANSEN, 1916

GENUS *HAPLONISCUS* RICHARDSON 1908

Synonymy: Haploniscus Richardson, 1908: 75; Vanhöffen, 1914: 557; Hansen, 1916: 28; Menzies, 1956: 8; 1962: 94; Wolff, 1962: 50; Birstein, 1963a: 41, b: 817; 1971: 180; Menzies & George, 1972: 107; Chardy, 1974: 1138; 1977: 897; Lincoln, 1985a: 14, b: 659; Kussakin, 1988: 363; Brökeland & Wägele, 2004: 2; George 2004: 351.

Type species: Nannoniscus bicuspis Sars, 1877, by original designation.

Diagnosis: Haploniscidae with pereonite 2–4 angles not produced anteriorly; pereonites 5–7 fused with each other and pleotelson middorsally, lateral margins separated; pereonites 6 and 7 of subequal length. Not conglobating. Clypeus not produced anteriorly. Pleotelson with two angular posterolateral processes. Antenna 2 with six conspicuous, freely articulating peduncular articles; article 3 with dorsal tooth-like projection; article 5 not inflated, cylindrical.

Remarks: No apomorphies of the genus *Haploniscus* are known and the diagnosis consists of plesiomorphic characters only. Consequently, the genus *Haploniscus* is not a monophyletic group, but a depository for species that cannot be placed in one of the other genera of the family. However, the revision of the genus depends on redescription of most *Haploniscus* species and is not the purpose of this study. Therefore, the newly described species are placed within *Haploniscus*, possessing none of the apomorphic characters of the other known genera and no unique morphological synapomorphies, which would justify the erection of a new genus.

HAPLONISCUS CUCULLUS COMPLEX

Composition: Haploniscus cassilatus sp. nov., *H. cucullus* sp. nov., *H. weddellensis* sp. nov., *H. procerus* sp. nov., *H. kyrbasia* sp. nov., *H. nudifrons* sp. nov., *H. microkorys* sp. nov.

Diagnosis: Body oval, length about 3× width. Head more than twice as long as wide, frontal margin concave. Anterior margin of pereonite 5 strongly serrated in intersegmental gap. Posterolateral processes of pleotelson short. Dorsal surface of pleotelson with two sharp longitudinal keels, ventral surface with cuticular bulge surrounding the branchial chamber and tapering towards anus. Antenna 1 with four flagellar articles. Peduncular articles of antenna 2 covered by cuticular scales. Mandibular palp article

3 with more than seven serrated spine-like setae. Carpus with ventral flagellate setae, apical and ventral combs of carpus spinose, pereopod 6 with dorsal flagellate seta subapically on carpus. Pleopod 1 without distal extensions or extensive sculpturing of apical part in adult males. Pleopod 2 endopod short, extending slightly beyond terminal margin of basipod.

Remarks: Five of the seven species described below, *H. cucullus*, *H. cassilatus*, *H. weddellensis*, *H. procerus* and *H. kyrbasia*, possess a rostrum that has a characteristic and complex basic shape, although its proportions vary between species. In dorsal view the rostrum has almost parallel lateral margins and tapers anteriorly into an acute spine. The dorsal surface of the rostrum has a shallow depression that is flanked by the sharp lateral margins and resembles a shovel. The anterior spine is curved dorsally in lateral view, and the lateral surfaces of the rostrum each have a shallow longitudinal depression. Across the ventral surface runs a shallow groove that is visible as a notch in lateral view. Posteriorly of the groove the rostrum is separated from the head by a sharp ventral notch. SEM pictures revealed that the rostrum is covered with small tubercles, each bearing several tiny sensory setae with the exception of the anterior spine and the small ventral part posteriorly of the shallow groove (Fig. 41). The rostrum is subject to interspecific variation. It differs in size and proportions. Besides, intraspecific variation of this structure can be observed. In relation to body size ovigerous females possess a smaller rostrum than other specimens belonging to the same species. Due to this conspicuous morphological similarity of the five species a close relationship between them may be assumed.

Apart from the rostrum *H. nudifrons* and *H. microkorys* share a number of characters with the other five species. All species are characterized by a relatively broad body shape, the concave frontal margin of the head, the short posterolateral processes of the pleotelson and the characteristic setation of the pereopods with flagellate setae on merus, carpus and propodus.

Pleopod 1 of adult males is similar to that of subadult males, the endopod of the male pleopod 2 is short, and sexual dimorphism is restricted to the pleopods. Scales on the peduncular articles of antenna 2 seem to be a common character as well. Although they were not visible under the compound microscope in some species, e.g. *H. cucullus*, these scales were found in a specimen of *H. cucullus* that was prepared for SEM studies. The size and number of scales is subject to interspecific variation, and perhaps also of intraspecific variation. The proportions of the peduncular articles of antenna 2 are variable as well; antenna 2 of *H. cassilatus* is relatively stout, whereas antenna 2 of *H. microkorys* is more slender. While the setation of the flagellar articles of antenna 2 is usually more strongly developed in males, such dimorphism could not be found in the two species where adult males and females were present: *H. cassilatus* and *H. weddellensis*. This corresponds to the generally weakly expressed sexual dimorphism of the group.

The size range of the species is large; the smallest adult specimens belonged to *H. weddellensis* and the biggest specimen was the *H. nudifrons* female (11.3 mm in length). However, it is difficult to determine the size range of most species due to lack of material. The size ranges of *H. cassilatus*, *H. cucullus* and *H. weddellensis* broadly overlap. Ovigerous females seem to be among the largest specimens of each species.

The setation of the pereopods includes flagellate spine-like setae ventrally on merus, carpus and propodus of all species, but their number varies within and between species. By far the most setae can be found in *H. microkorys*, while specimens of *H. cassilatus* possess only 1–3 flagellate setae on the ventral carpus. Because of the intraspecific variation, the number of setae is problematic as a diagnostic character; to define discrete character states a statistical analysis would be necessary. This is not possible at the moment, because not enough specimens were found of most species.

Where adult males were found, pleopods 1 and 2 looked more or less alike between species. In contrast to most species of the Haploniscidae, pleopod 1 of subadult and adult specimens does not differ greatly; it has to be dissected to identify the ontogenetic stage. In adult males the dorsal surface of pleopod 1 has two transversal grooves, which are only weakly indicated in the subadult stage V males (stages after Wolff, 1962).

The complex is named after the new species *Haploniscus cucullus*, whose holotype male (ZMH K40758) was the first specimen of the complex found in the samples and also the specimen in which the rostrum was most striking when first observed. Despite this, the species described in full detail below is *H. cassilatus* because the material of this species contained adult males, which is not the case for *H. cucullus*. For all other species only the characters that differ from those of *H. cassilatus* are described. Because only a single specimen of *H. nudifrons* and *H. microkorys* was found, the mouthparts of these species were not dissected to avoid damaging of the important diagnostic features of the head in the holotypes. The mouthparts themselves were found to hold no important diagnostic characters in the remaining species, except for the mandibular palp, which was

dissected carefully in *H. microkorys*, but was lost in *H. nudifrons*.

HAPLONISCUS CASSILATUS SP. NOV.

(Figs 2–7, 40A)

Holotype: Male, 3.9 mm; station 46-7, 60°38.33–38.06′S 53°57.38–57.51′W, 5639 m depth; ZMH K40756.

Paratypes: Same locality as holotype: four males, 3.5–3.9 mm; three ovigerous females, 3.5–3.6; 21 females, 2.4–3.6 mm, 36 juveniles, 1.4–2.5 mm; ZMH K40757.

Etymology: The species is named after the prominent rostrum; from Latin *cassis*, which means 'helmet', and *latus*, which means 'carrying'.

Diagnosis: Body oval, length 3.0× width. Head width 2.5× length, frontal margin concave, with prominent rostrum; rostrum covered with small tubercles, with dorsal depression and acute upturned frontal tooth, a deep ventral indentation between rostrum and frontal margin of head. Pereonites 3–5 broadest. Lateral margins of pleotelson convex, posterolateral processes short, not reaching terminal margin; dorsal surface of pleotelson with two sharp longitudinal keels, ventral surface with cuticular bulge surrounding the branchial chamber and tapering towards anus. Antenna 1 with four flagellar articles. Carpus with 1–3 flagellate spine-like setae, apical and ventral combs of carpus spinose, carpus of pereopods 5 and 6 with dorsal flagellate seta. Pleopod 1 with nearly continuous distal margin. Endopod of pleopod 2 as long as basipod. Uropods not reaching terminal margin.

Description of female paratype: Body oval. Margins of pereonites straight, smooth. Pereonites 3–5 broadest. Pleotelson length 0.2× body length, tapering distally, distance between pleotelson processes 2.1× anterior margin width; terminal margin convex. Cuticle of body smooth.

Antenna 1 (Fig. 3) length 0.3× body length, article 1 broadest, length 1.5× width, article 2 length 1.3× article 1 length, width 0.5× article 1 width, both articles with several broom and simple setae; article 3 length 0.4× article 2 length, with simple seta; flagellum article 1 shortest, with broom seta; articles 2–4 of subequal length, article 2 with simple seta, article 3 with one aesthetasc and one simple seta, article 4 with two aesthetascs and two simple setae.

Antenna 2 (Fig. 3) length 0.7× body length, articles 1 and 2 slightly wider than long, with simple seta, article 3 about as long as wide, length 2.0× article 2 length, with short dorsal tooth and several simple setae, article 4 length 0.8× article 3 length, 1.1× width, article 5 length 1.5× article 3 length, 0.9× article 6 length, 2.4× width, article 6 length 1.6× article 3 length, 4.0× width, both articles with several simple and some broom setae, articles 4–6 covered with numerous triangular scales; flagellum length 0.7× peduncle length, 14-articulated, each article with several simple setae.

Mandible (Fig. 4) incisor with five blunt teeth, lacinia mobilis of left mandible with five teeth, right mandible with stout serrated spine-like seta instead, spine row comprising two serrated and four simple spine-like setae; molar tooth row with about seven teeth and eight setulated setae proximally, cuticular ledge tapering off forming a tooth on both sides, right mandible with row of six accessory teeth proximally of cuticular ledge; palp article 2 with three serrated spine-like setae proximally of insertion of article 3, article 3 with ten serrated spine-like setae of increasing length.

Maxilla 1 (Fig. 3) outer lobe with seven simple and five serrated spine-like setae and several simple setae on lateral and medial margin and surface; inner lobe apically with several stout simple setae.

Maxilla 2 (Fig. 3) outer lobe with two long and two short simple spine-like setae apically, several simple setae on lateral margin; medial lobe with two long and one shorter simple spine-like setae and one serrated seta apically, medial margin with six spine-like setae; inner lobe with two apical serrated spine-like setae, three stout apical simple setae and numerous simple setae on surface and medial margin.

Maxilliped (Fig. 3) endite apical margin with three small fan setae and two short spine-like setae, ventral surface with numerous simple setae, separated apical medial margin dorsally with one simple spine-like seta, one serrated spine-like seta and row of simple setae, medial margin with four retinacula; epipod slightly longer than endite.

Pereopods (Figs 4–6): Basis with 3–4 long simple setae ventrally, basis of pereopods 2–6 with 1–2 broom setae dorsally. Ischium with three simple setae ventrally and dorsally (some broken off in type specimen). Merus with 3–4 setae apically and one simple seta ventrally, pereopods 5–7 with apical ventral flagellate seta, ventral seta on pereopods 5–7 spine-like. Ventral comb-like scale rows of carpus and propodus spinose; carpus with 1–3 flagellate setae and several simple setae, dorsal flagellate seta on pereopods 5 and 6; apical comb on carpus of pereopod 1 small and setose, apical combs on pereopods 2–7 comprising one small and one larger spinose comb. Propodus with 2–6 simple setae ventrally, pereopods 5–7 with 2–3 flagellate spine-like setae ventrally, pereopods 1–4 with mediodorsal simple seta. Dactylus with three lateral setae; accessory tooth acute.

Pleopods (Fig. 6): Pleopod 2 subcircular, with more than 40 setae on distal and lateral margins,

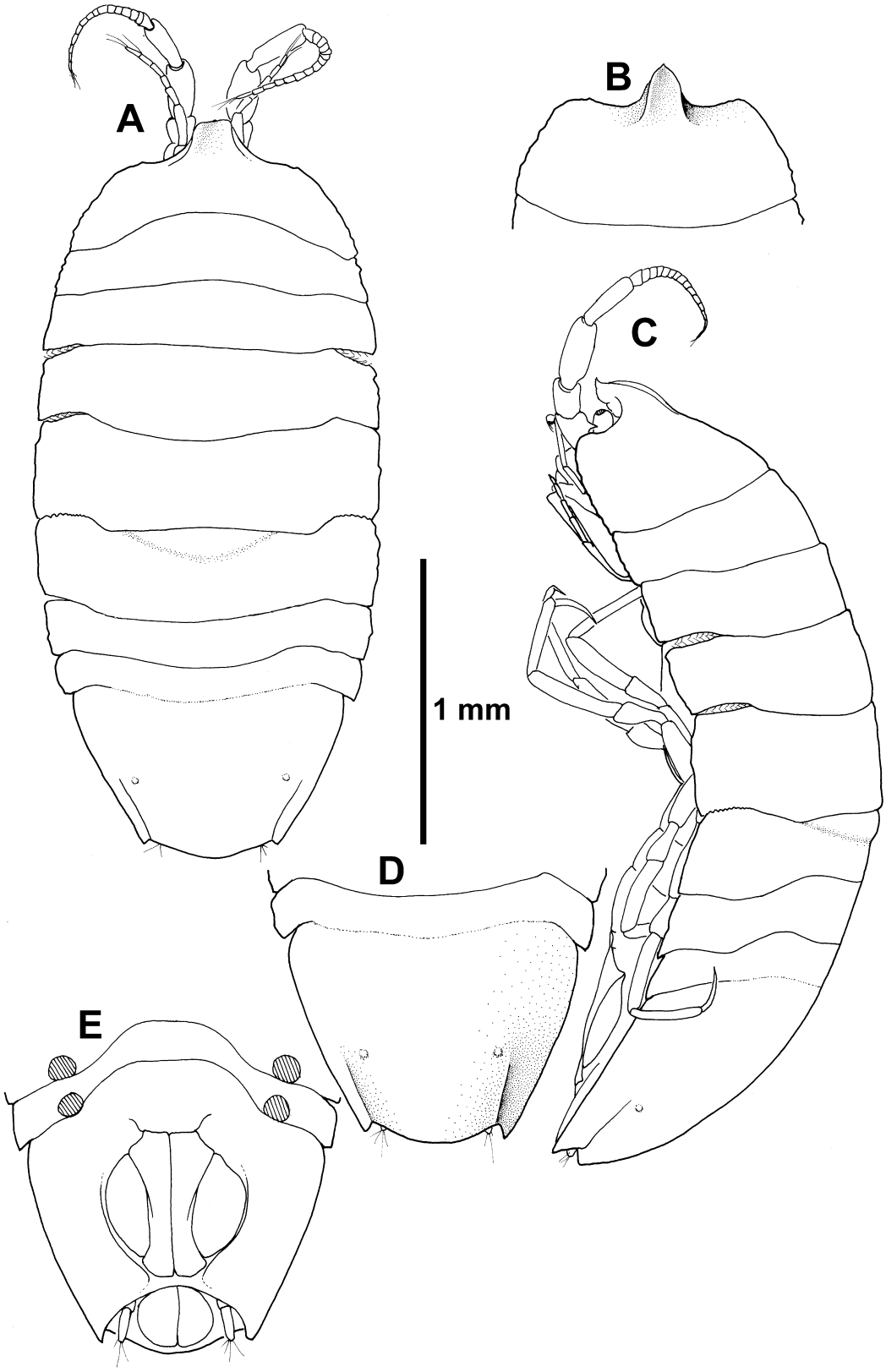

Figure 2. ***Haploniscus cassilatus*** **sp. nov.**, holotype, male, K40756, 3.9 mm: A, dorsal view; B, anterior body, straight dorsal view; C, lateral view; D, posterior body, straight dorsal view; E, posterior body, ventral view.

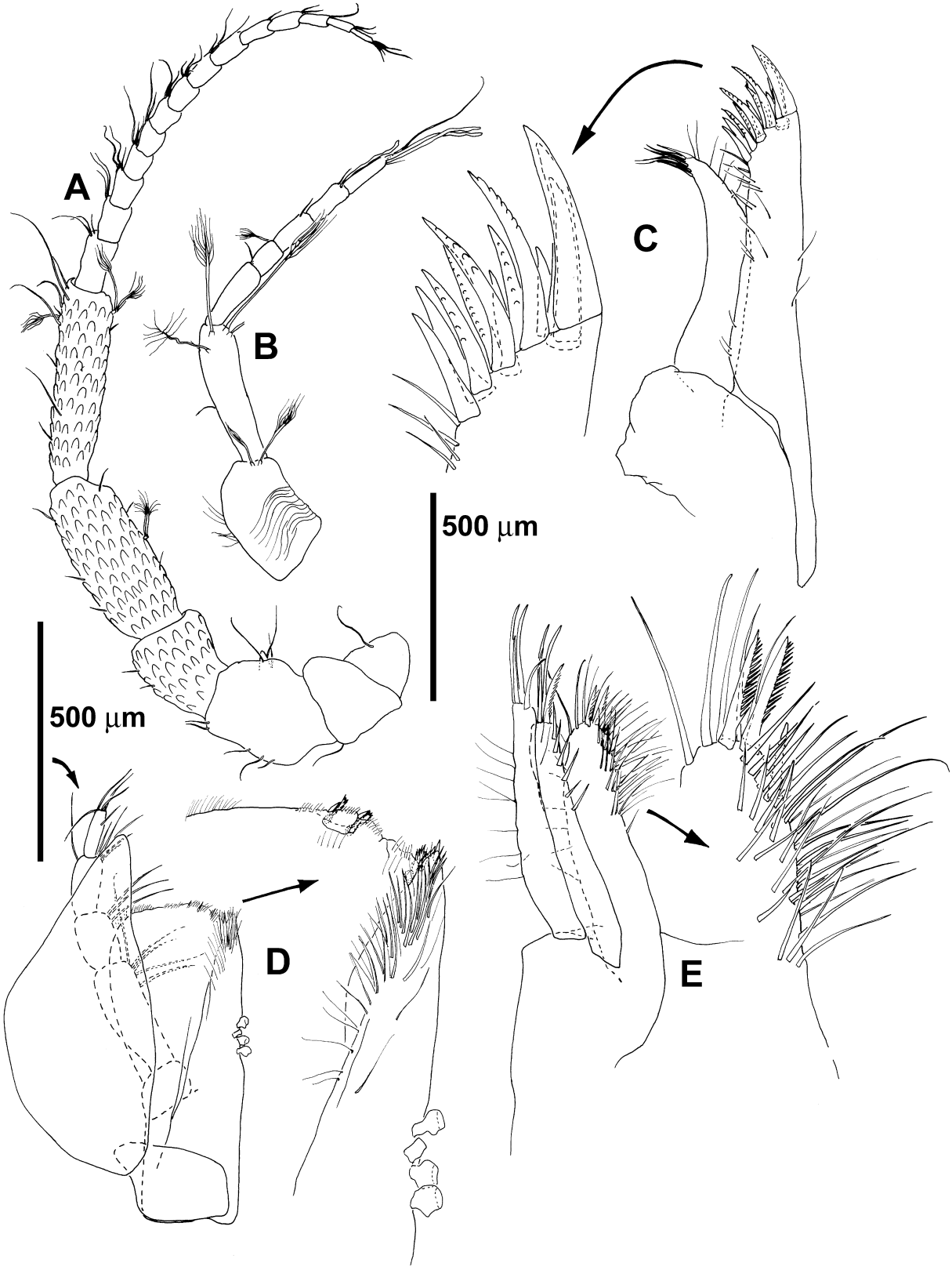

Figure 3. ***Haploniscus cassilatus*** **sp. nov.**, paratype, female, K40757, 3.6 mm: A, antenna 2; B, antenna 1; C, maxilla 1; D, maxilliped; E, maxilla 2.

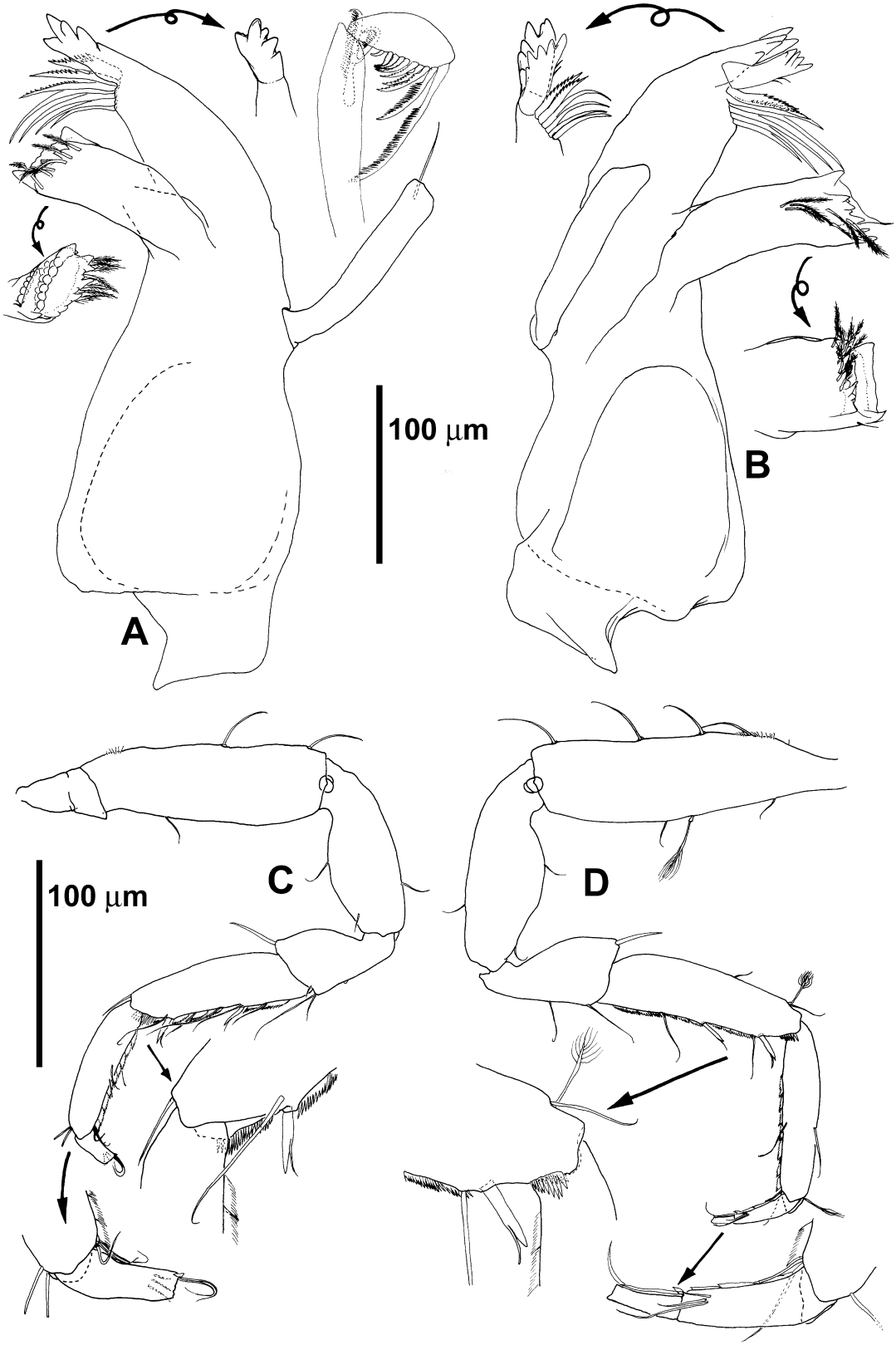

Figure 4. ***Haploniscus cassilatus*** **sp. nov.**, paratype, female, K40757, 3.6 mm: A, right mandible; B, left mandible; C, pereopod 1; D, pereopod 2.

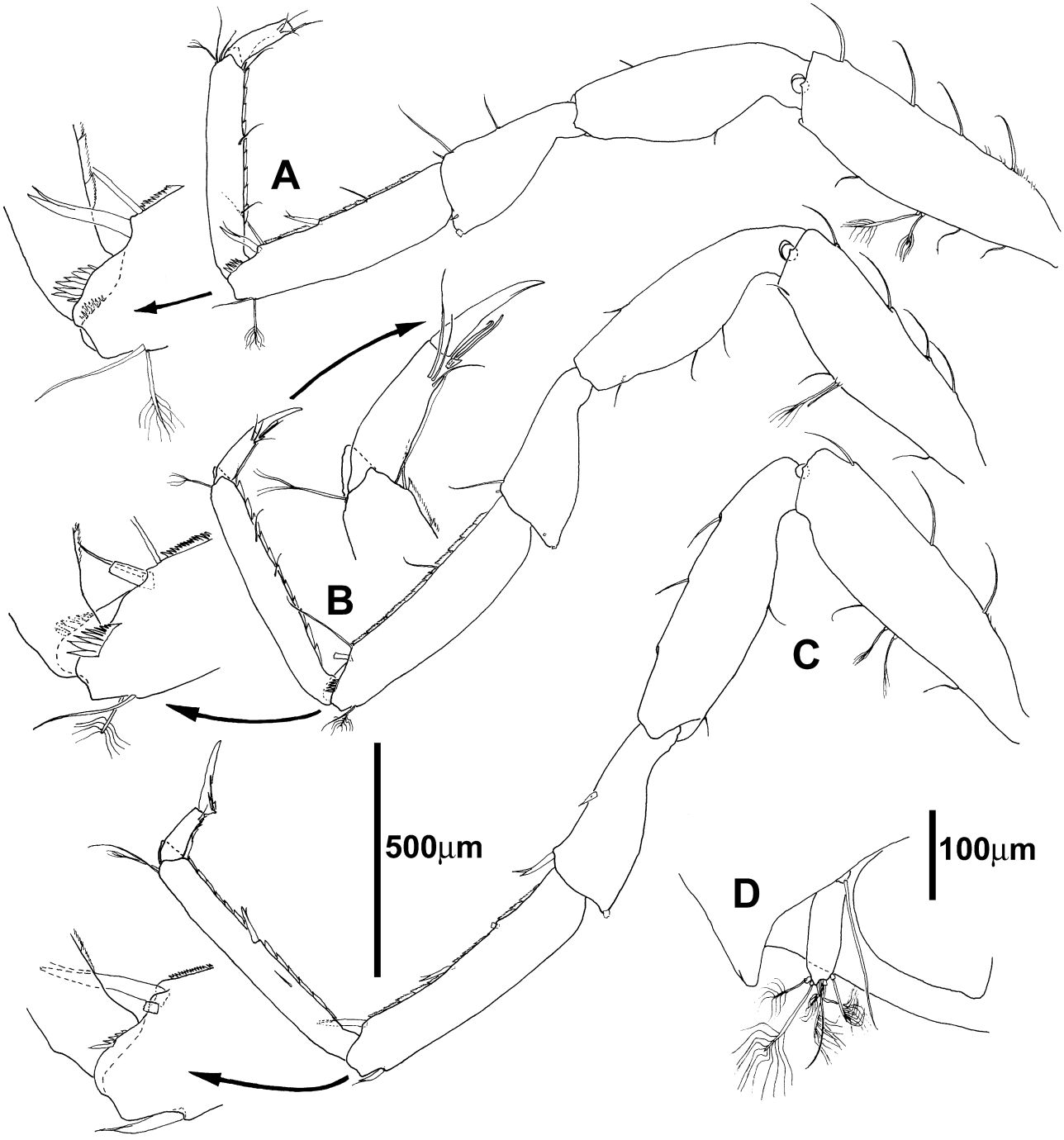

Figure 5. ***Haploniscus cassilatus*** **sp. nov.**, paratype, female, K40757, 3.6 mm: A, pereopod 3; B, pereopod 4; C, pereopod 5; D, paratype, male, K40757, 3.8 mm, uropod.

longest setae on distal margin. Pleopod 3 endopod length 1.6× width, with rounded distal margin; exopod small, length 1.8× width, 0.5× endopod length, width 0.4× endopod width, lateral margin rounded, with six simple setae and fringe of fine bristles. Pleopod 4 endopod length 1.6× width; exopod length 4.4× width, 0.6× endopod length, width 0.2× endopod width, lateral margin rounded with fringe of long bristles, plumose seta slightly longer than exopod. Pleopod 5 length 1.6× width.

Uropods (Fig. 2) not reaching terminal margin.

Description of male: The male (Figs 2, 7, 40A) differs from the female in the following characters.

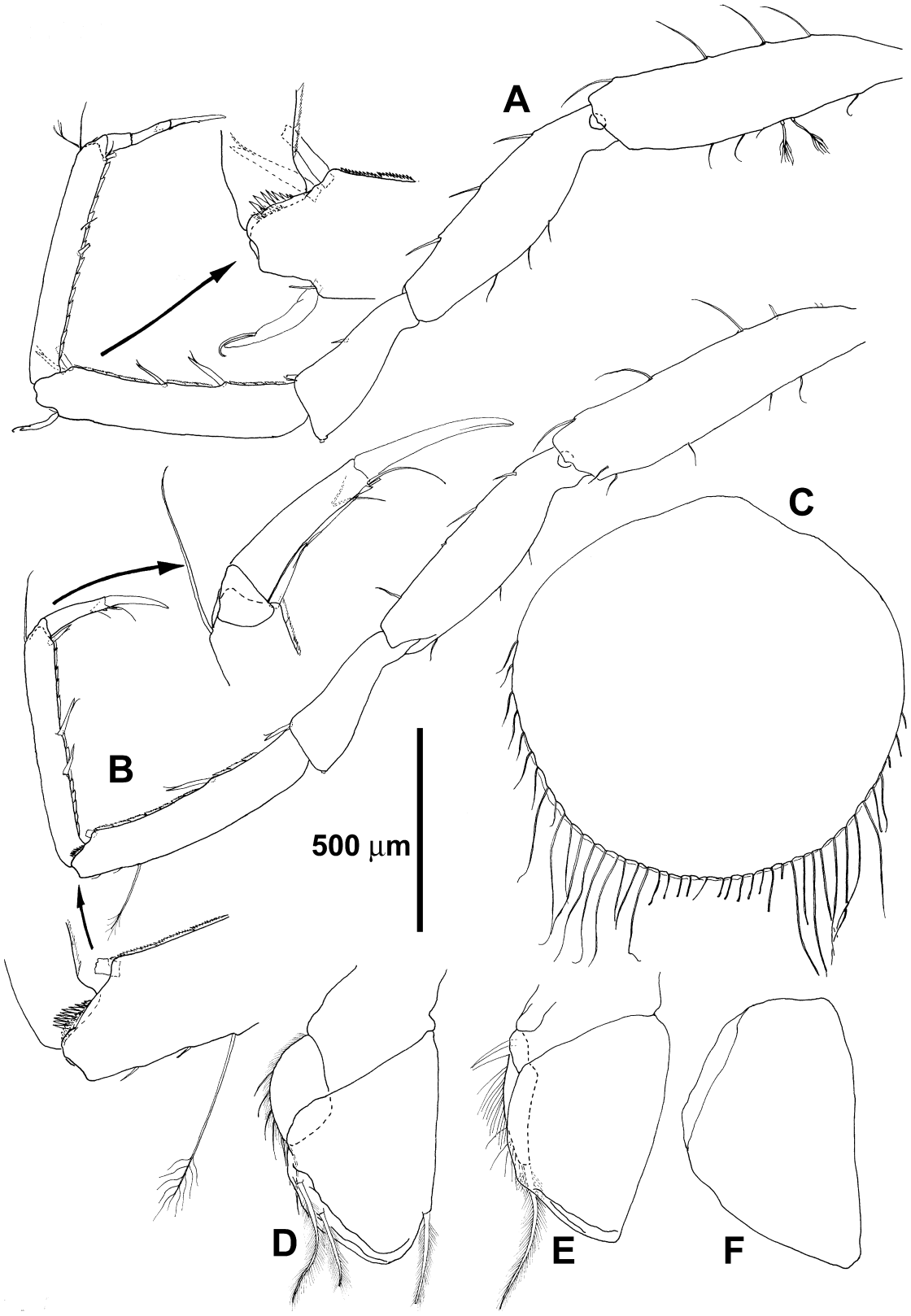

Figure 6. ***Haploniscus cassilatus*** **sp. nov.**, paratype, female, K40757, 3.6 mm: A, pereopod 6; B, pereopod 7; C, pleopod 2; D, pleopod 3; E, pleopod 4; F, pleopod 5.

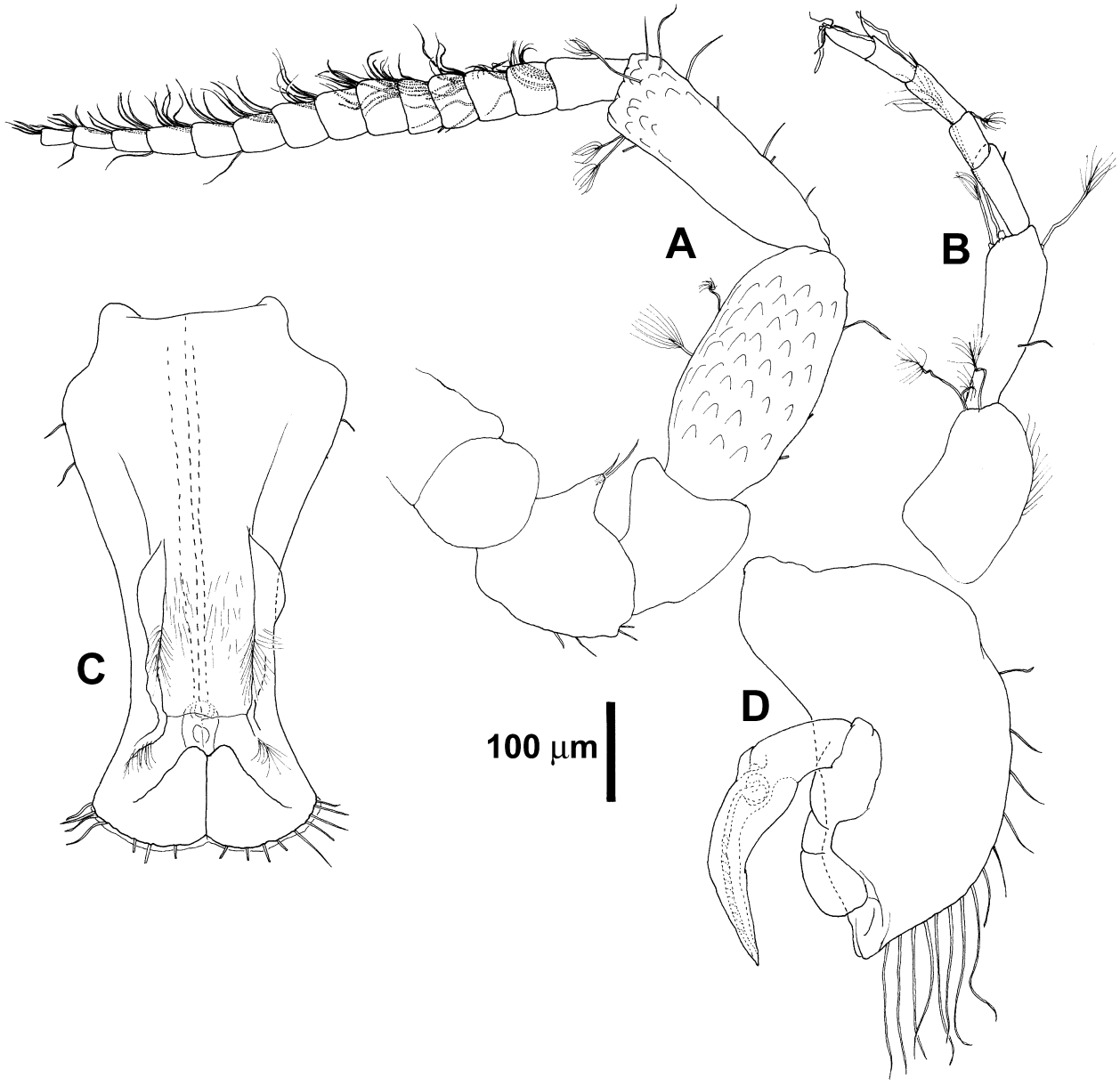

Figure 7. ***Haploniscus cassilatus*** **sp. nov.**, paratype, male, K40757, 3.9 mm: A, antenna 2; B, antenna 1; C, pleopod 1; D, pleopod 2.

Antenna 2 (Fig. 7) more stout, with more than 14 flagellar articles, flagellar articles with more setae.

Pleopod 1 (Fig. 7) length 1.9× width, broadest part in the proximal quarter, 1.9× broader than narrowest part, lateral margins with two simple setae, distal margins with about nine setae each, sympods distal margin continuous, ventral surface with mediolateral bulges covered with numerous bristles, transverse grooves in the distal third with several bristles. Pleopod 2 (Fig. 7) basipod length 2.1× width, with several simple setae on lateral and distal margin; endopod inserting in distal half of basipod, short, stout, as long as basipod, article 2 length about 3.0× article 1 length, expanding in the medial part, sperm duct reaching from endopod tip almost to proximal third of article 2, exopod small, inserting in the distal third of basipod.

HAPLONISCUS CUCULLUS SP. NOV.

(FIGS 8–14, 40B, 41)

Holotype: Subadult male, 5.3 mm; station 43-8, 60°27.13–27.19′S, 56°05.12–04.81′W, 4782 m depth, ZMH K40758.

Paratypes: Same locality as holotype: one ovigerous female, 5.4 mm; one female, 2.8 mm; one juvenile, 2.2 mm; ZMH K40759. Station 42-2, 59°40.30–40.32′S, 57°35.42–42.64′W, 3689 m depth: one ovigerous female, 5.9 mm; three females, 3.4–3.6 mm; eight juveniles, 3.3–3.6 mm; ZMH K40760.

Etymology: The name refers to the cap-like rostrum that is extraordinarily large in this species; the Latin *cucullus* means 'cap' or 'hood'.

Diagnosis: Body oval, length 3.0× width. Head width 2.5× length, frontal margin concave, with prominent rostrum; rostrum covered with small tubercles, with dorsal depression and acute upturned frontal tooth, a deep ventral indentation between rostrum and frontal margin of head. Pereonites 3–5 broadest. Lateral margins of pleotelson convex basally, concave distally, posterolateral processes short, not reaching terminal margin; dorsal surface of pleotelson with two sharp longitudinal keels, ventral surface with cuticular bulge surrounding the branchial chamber and tapering towards anus. Antenna 1 with four flagellar articles. Maxilliped with three retinacula. Carpus of pereopods 1–4 with 3–4 ventral flagellate setae, of pereopods 5–7 with 4–6 ventral flagellate setae, apical and ventral combs of carpus spinose, carpus of pereopods 5 and 6 with dorsal flagellate seta.

Description of female: H. cucullus differs from *H. cassilatus* in the following characters.

Rostrum (Fig. 13) slightly larger, less tapering distally, curved slightly stronger dorsally in lateral view.

Pleotelson (Fig. 8) lateral margin convex in basal half, concave in distal half, posterolateral processes slightly longer, distance between processes 1.6× anterior margin width.

Antenna 2 (Fig. 9) article 4 length 1.3× width, article 5 length 2.7× width, 0.8× article 6 length, article 6 length 1.8× article 3 length, 5.5× width.

Mandibular (Fig. 9) palp article 3 with about ten serrated spines.

Maxilliped (Fig. 10) with three retinacula.

Pereopods (Fig. 10, 11): Basis with 3–5 ventral setae. Merus with 1–2 medioventral simple setae on pereopods 5–7. Carpus of pereopods 1–4 with 3–4 ventral flagellate setae, pereopods 5–7 with 4–6 ventral flagellate setae.

Description of male: No adult males were found; the subadult male differs from the female in the following characters.

Pleopod 1 (Fig. 13) similar to that of *H. cassilatus*, but lacking the transversal grooves on the dorsal surface, due to immaturity. Penes present. Pleopod 2 sperm duct not developed.

HAPLONISCUS WEDDELLENSIS SP. NOV.

(FIGS 15–19, 40C)

Holotype: Male, 3.0 mm; station 133-3, 65°20.17–20.08′S, 54°14.30–14.34′W, 1314 m depth, ZMH K40761.

Paratypes: Same locality as holotype: 16 males, 2.6–3.0 mm; three ovigerous females 3.5–4.2 mm; nine females, 2.3–2.9 mm; 11 juveniles, 1.2–2.3 mm; ZMH K40762.

Etymology: Named after the type locality in the Weddell Sea.

Diagnosis: Body oval, length 3.0× width. Head width 2.5× length, frontal margin concave, with prominent rostrum; rostrum covered with small tubercles, with shallow dorsal depression and acute upturned frontal tooth, a deep ventral indentation between rostrum and frontal margin of head. Pereonites 3–6 broadest. Lateral margins of pleotelson convex basally, concave distally, posterolateral processes slightly exceeding terminal margin; dorsal surface of pleotelson with two sharp longitudinal keels, ventral surface with cuticular bulge surrounding the branchial chamber and tapering towards anus. Antenna 1 with four flagellar articles. Carpus of pereopods 1–4 with 2–4 ventral flagellate setae, of pereopods 5–7 with 2–3 ventral flagellate setae, apical and ventral combs of carpus spinose, carpus of pereopod 6 with dorsal flagellate seta.

Description of female: H. weddellensis differs from *H. cassilatus* in the following characters.

Rostrum (Fig. 16) shorter and broader, dorsal depression shallow. Pereonites 3–6 broadest. Pleotelson (Fig. 16) lateral margins convex basally, concave distally, posterolateral processes longer, exceeding terminal margin slightly, distance between processes 1.8× anterior margin width.

Antenna 2 article 5 length 1.6× article 3 length, 1.1× article 6 length, 2.1× width, article 6 length 1.4× article 3 length, 3× width.

Mandibular palp with about eight serrated setae.

Carpus with 2–4 ventral flagellate setae, only carpus of pereopod 6 with dorsal flagellate seta.

Description of male: Pleopods 1 and 2 (Fig. 19) are more or less identical with the pleopods of *H. cassilatus*.

HAPLONISCUS PROCERUS SP. NOV.

(FIGS 20–25, 40D)

Holotype: Female, 7.4 mm; station 131-3, 65°19.83–19.99′S, 51°31.61–31.23′W, 3553 m depth; ZMH K40763.

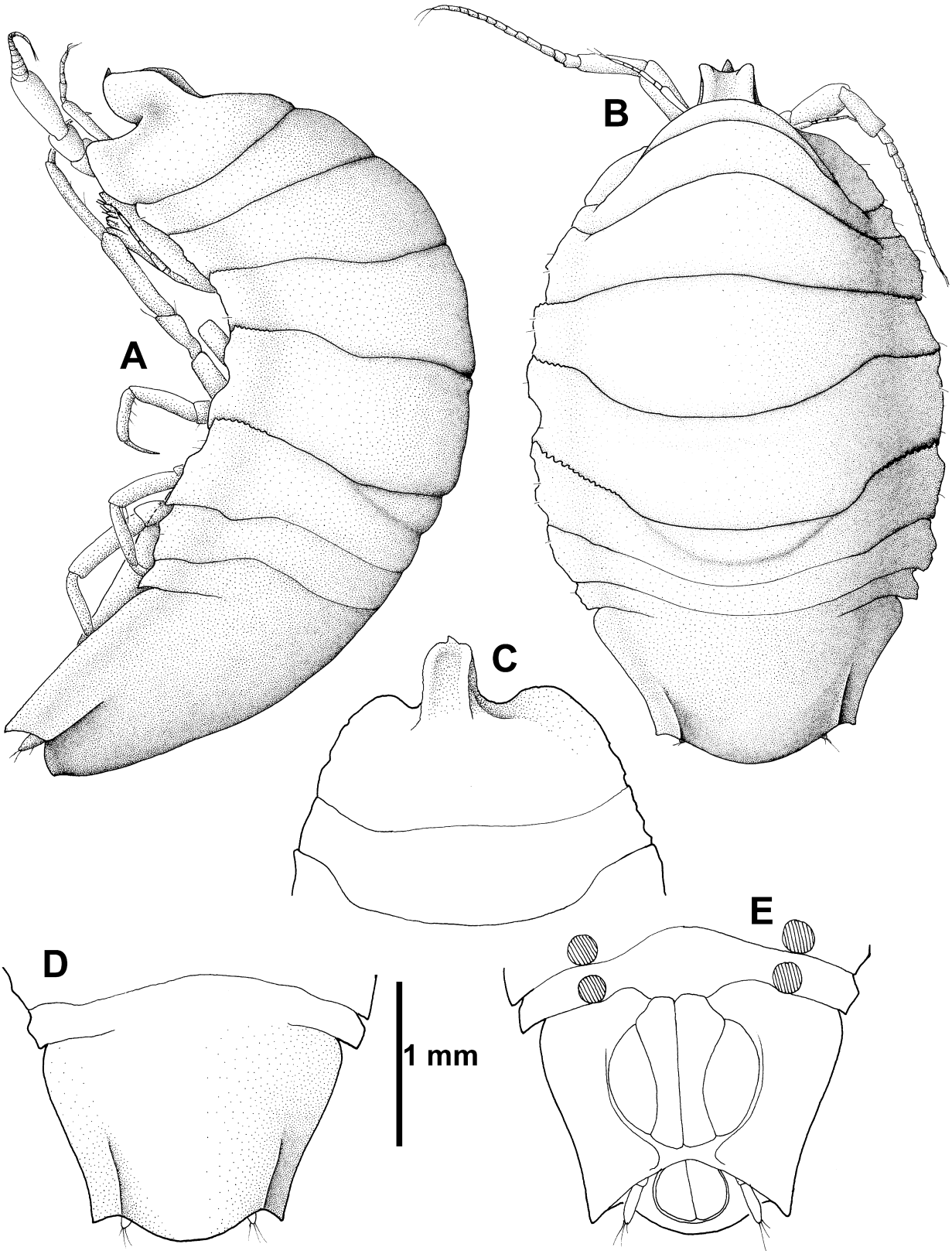

Figure 8. ***Haploniscus cucullus*** **sp. nov.**, holotype, male, K40758, 5.3 mm: A, lateral view; B, dorsal view; C, anterior body, straight dorsal view; D, posterior body, straight dorsal view; E, posterior body, ventral view.

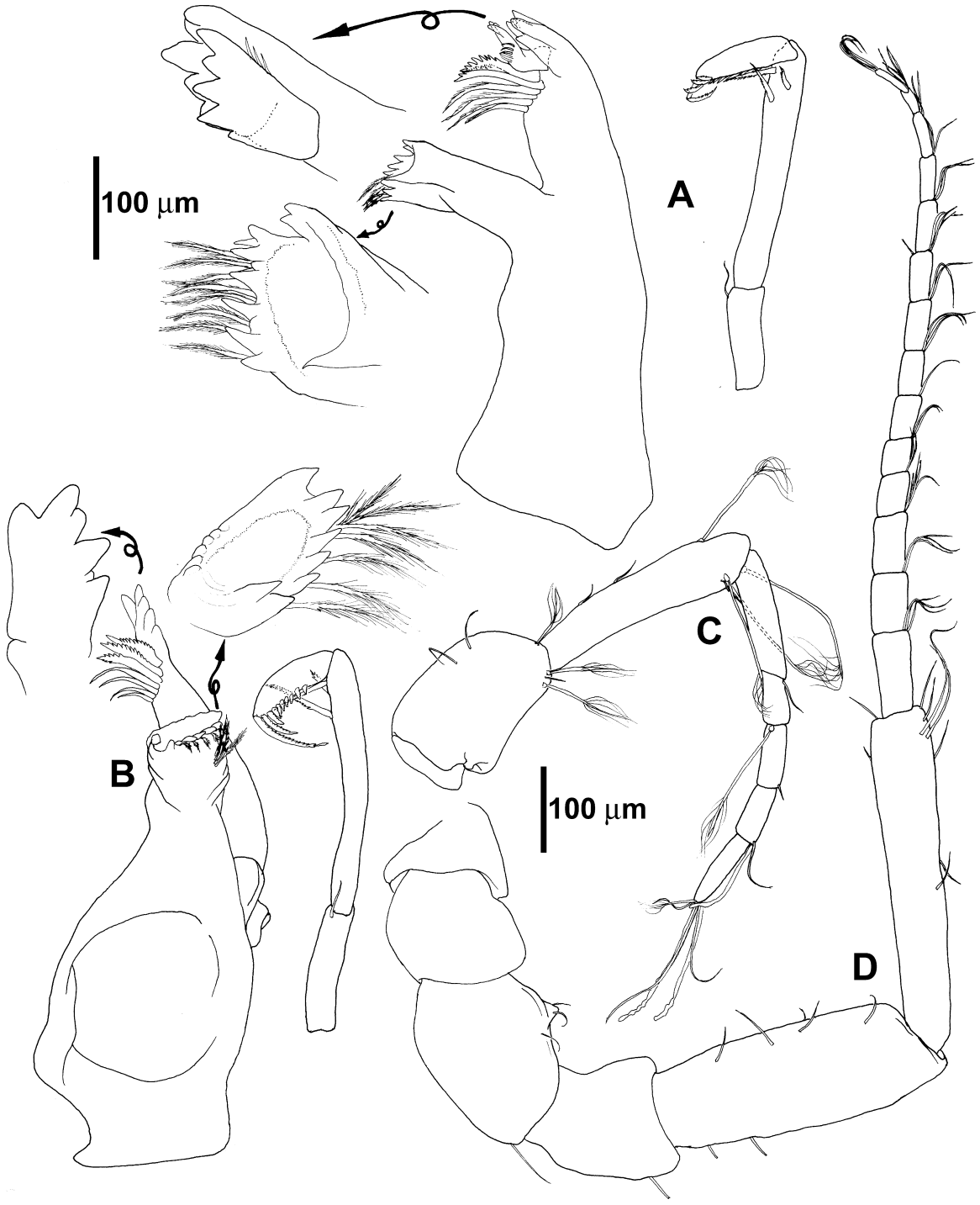

Figure 9. ***Haploniscus cucullus*** **sp. nov.**, paratype, female, K40759, 5.4 mm: A, left mandible; B, right mandible; C, antenna 1; D, antenna 2.

Paratype: Same locality as holotype: one female, 7.6 mm; ZMH K40764.

Etymology: The name refers to the rostrum, which is elongated in this species; the Latin term *procerus* means 'large', 'slender', 'long'.

Diagnosis: Body oval, length 3.0× width. Head width 2.5× length, frontal margin concave, with prominent rostrum; rostrum covered with small tubercles, with dorsal depression and acute upturned frontal tooth, a deep ventral indentation between rostrum and frontal margin of head. Pereonites 3–6 broadest. Lateral

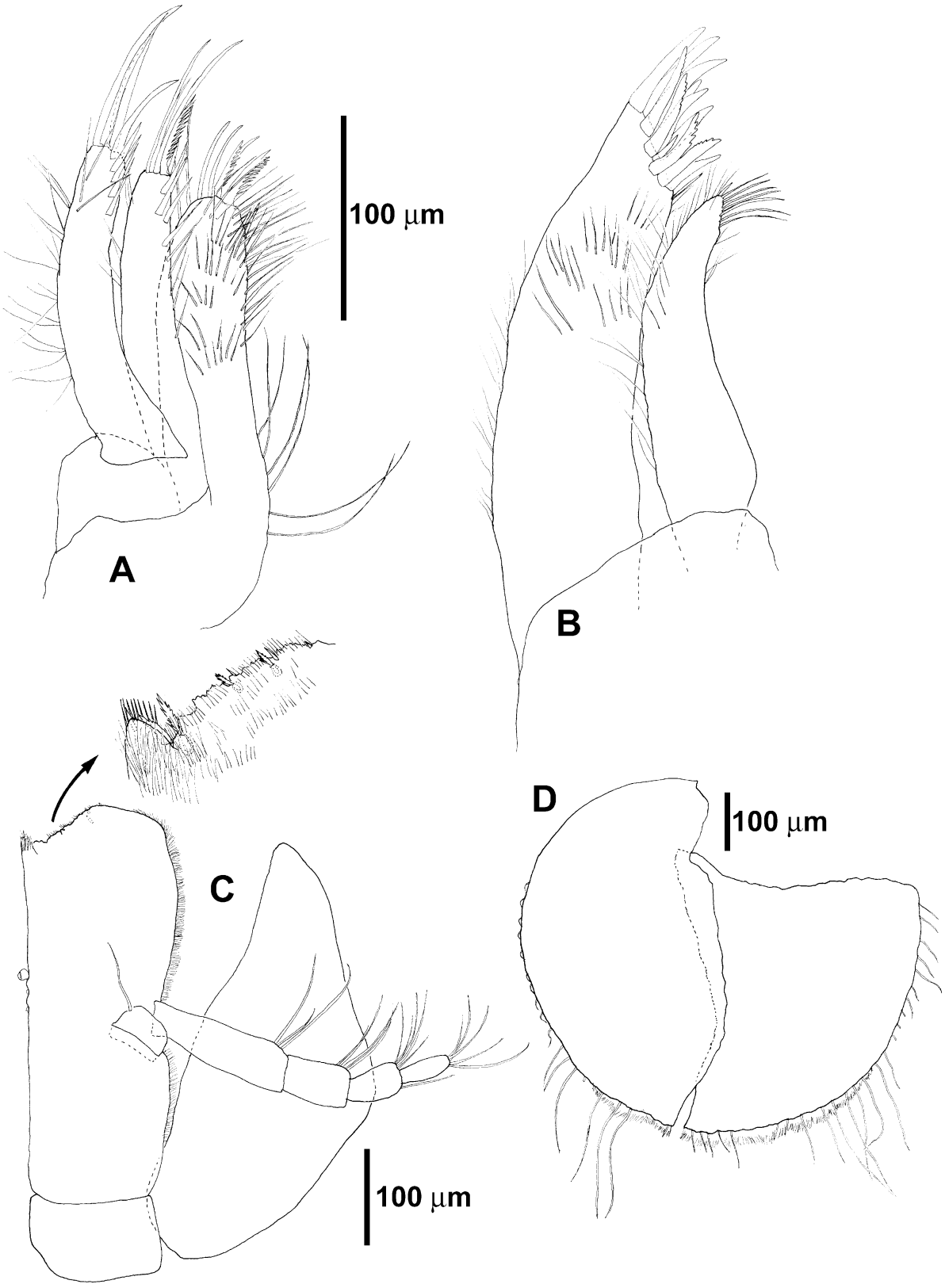

Figure 10. ***Haploniscus cucullus*** **sp. nov.**, paratype, female, K40759, 5.4 mm: A, maxilla 2; B, maxilla 1; C, maxilliped; D, pleopod 2.

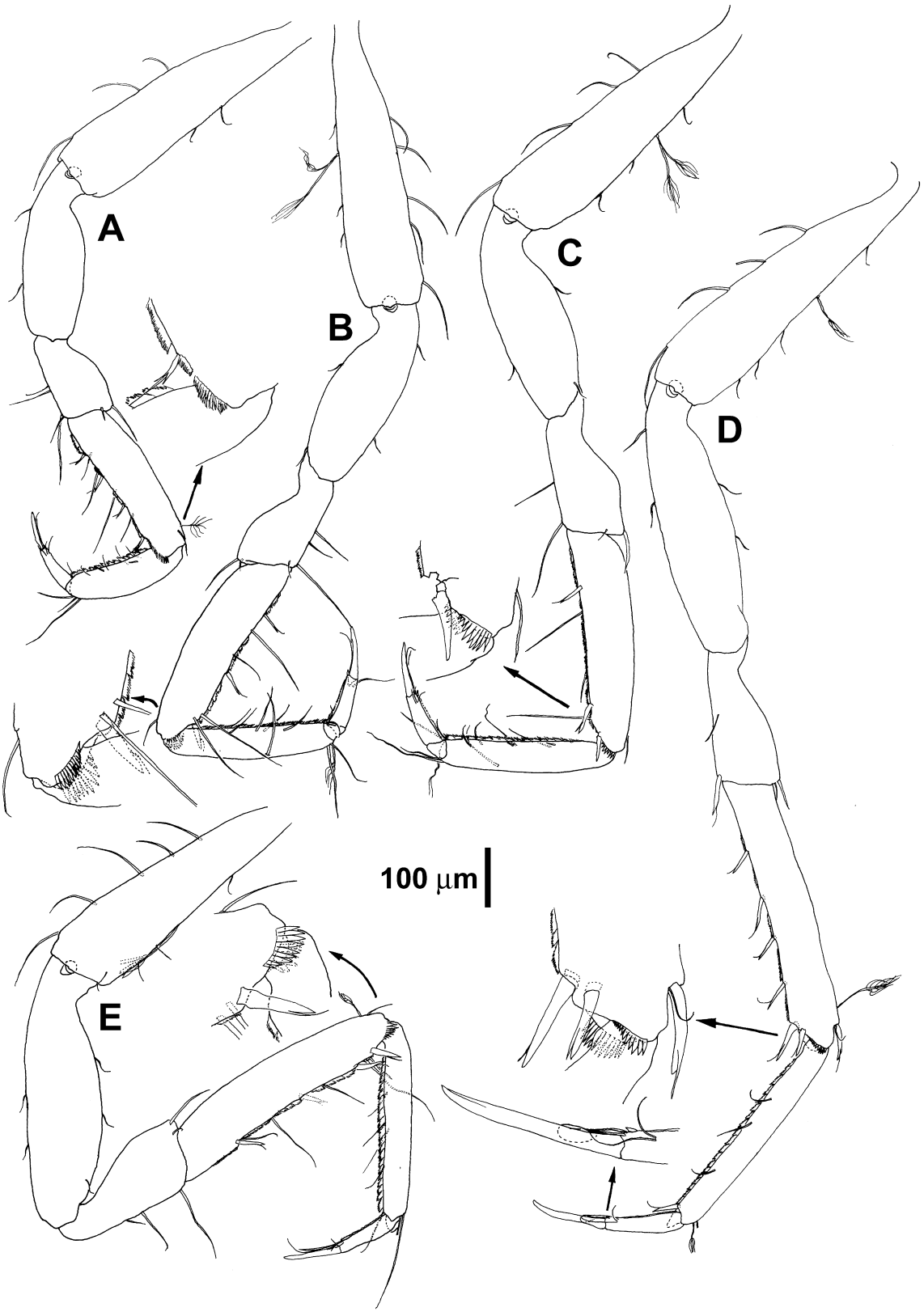

Figure 11. ***Haploniscus cucullus*** **sp. nov.**, paratype, female, K40759, 5.4 mm: A, pereopod 1; B, pereopod 2; C, pereopod 3; D, pereopod 5; E, pereopod 4.

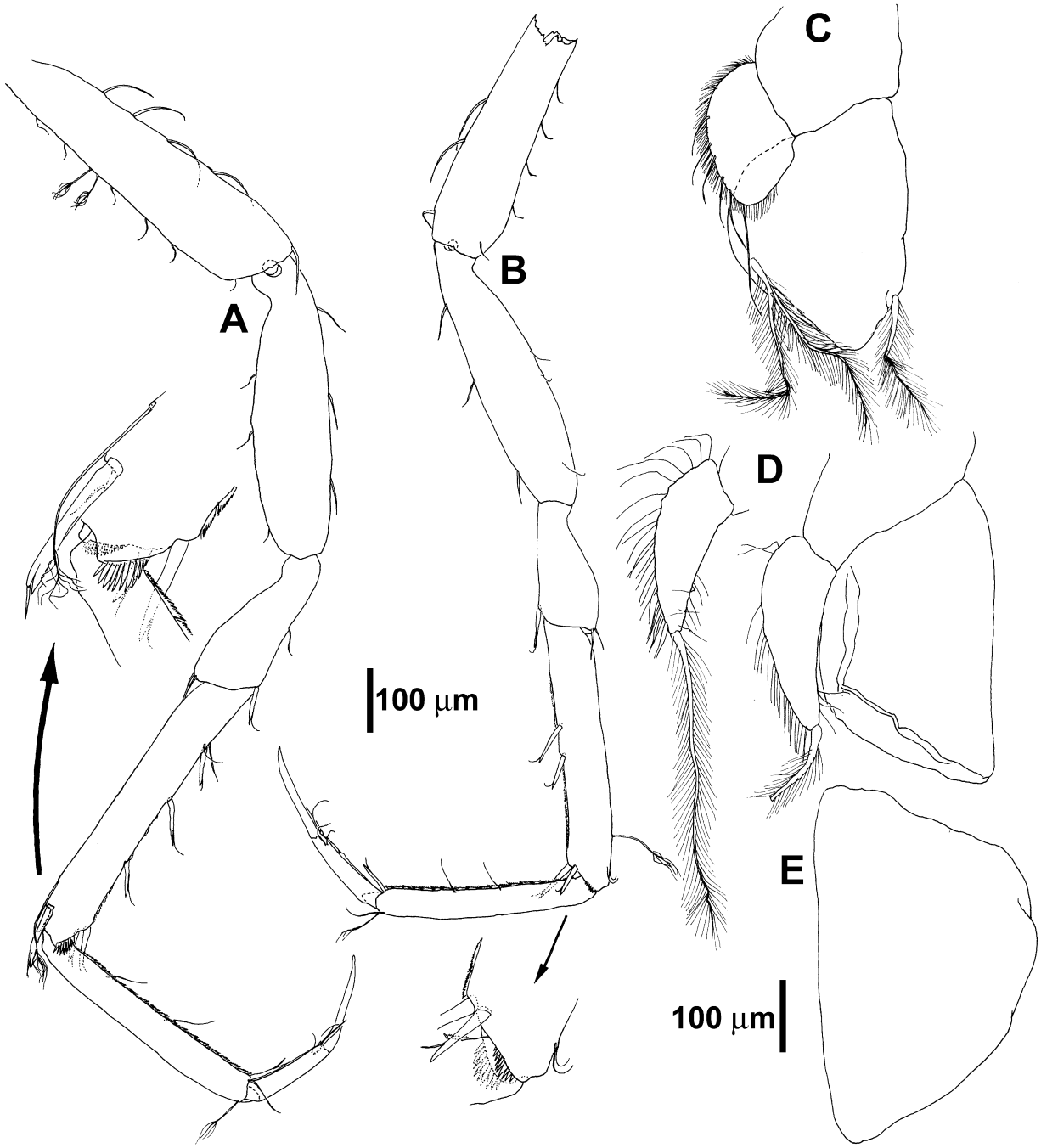

Figure 12. ***Haploniscus cucullus*** **sp. nov.**, paratype, female, K40759, 5.4 mm: A, pereopod 6; B, pereopod 7; C, pleopod 3; D, pleopod 4; E, pleopod 5.

margins of pleotelson convex basally, concave distally, posterolateral processes slightly exceeding terminal margin; dorsal surface of pleotelson with two sharp, pronounced longitudinal keels, ventral surface with cuticular bulge surrounding the branchial chamber and tapering towards anus. Antenna 1 with four flagellar articles. Maxilliped with three retinacula. Carpus of pereopods 1–4 with 4–5 ventral flagellate setae, of pereopods 5–7 with 7–8 ventral flagellate setae, apical and ventral combs of carpus spinose, carpus of pereopods 5–7 with dorsal flagellate seta.

Description of female paratype: H. procerus differs from *H. cassilatus* in the following characters.

Rostrum larger, less tapering, less vaulted, distal part elongated. Pereonites 3–6 broadest. Lateral

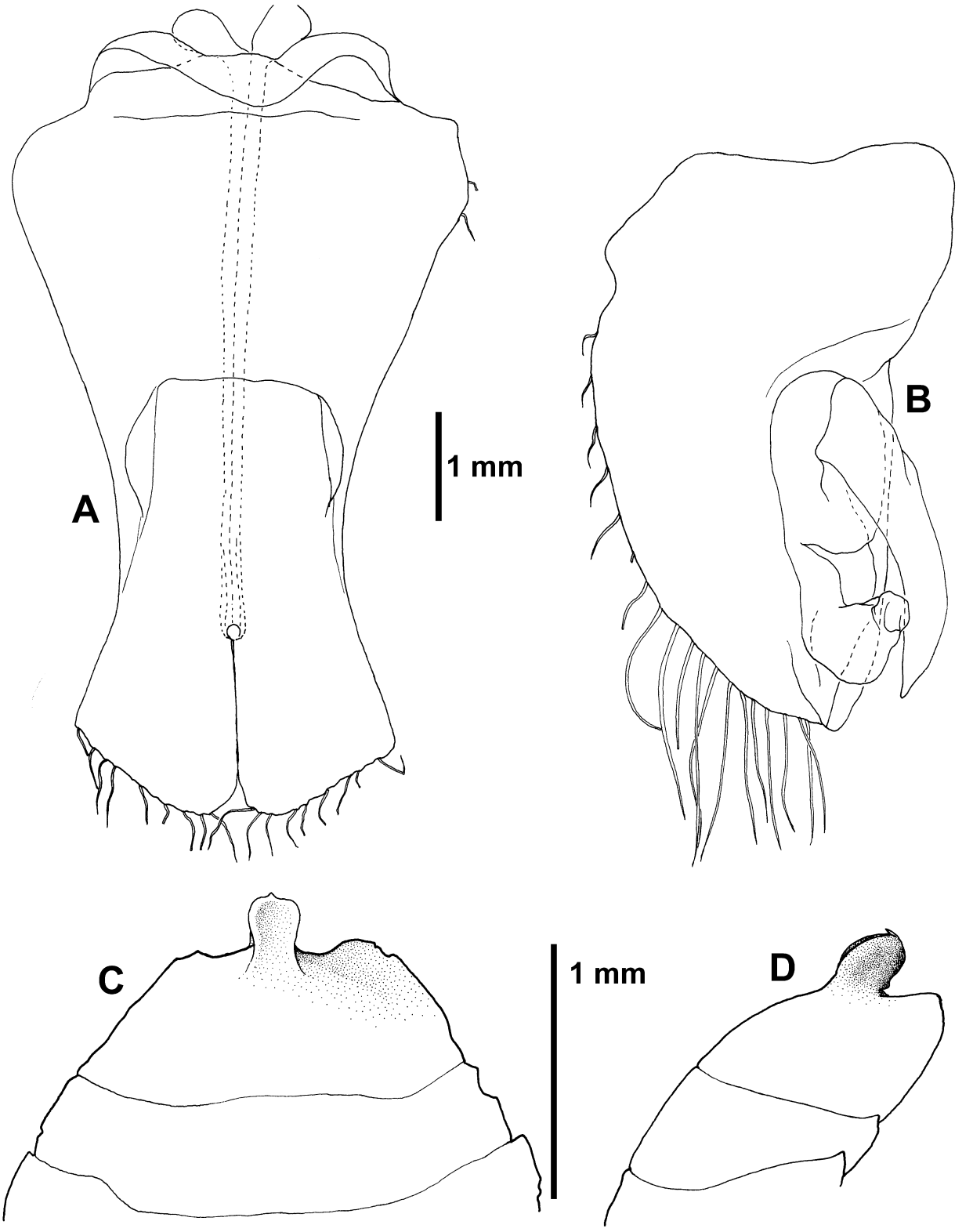

Figure 13. ***Haploniscus cucullus*** **sp. nov.**, holotype male, K40758, 5.3 mm: A, pleopod 1; B, pleopod 2; paratype female, K40760, 5.9 mm: C, anterior body, straight dorsal view; D, anterior body, lateral view.

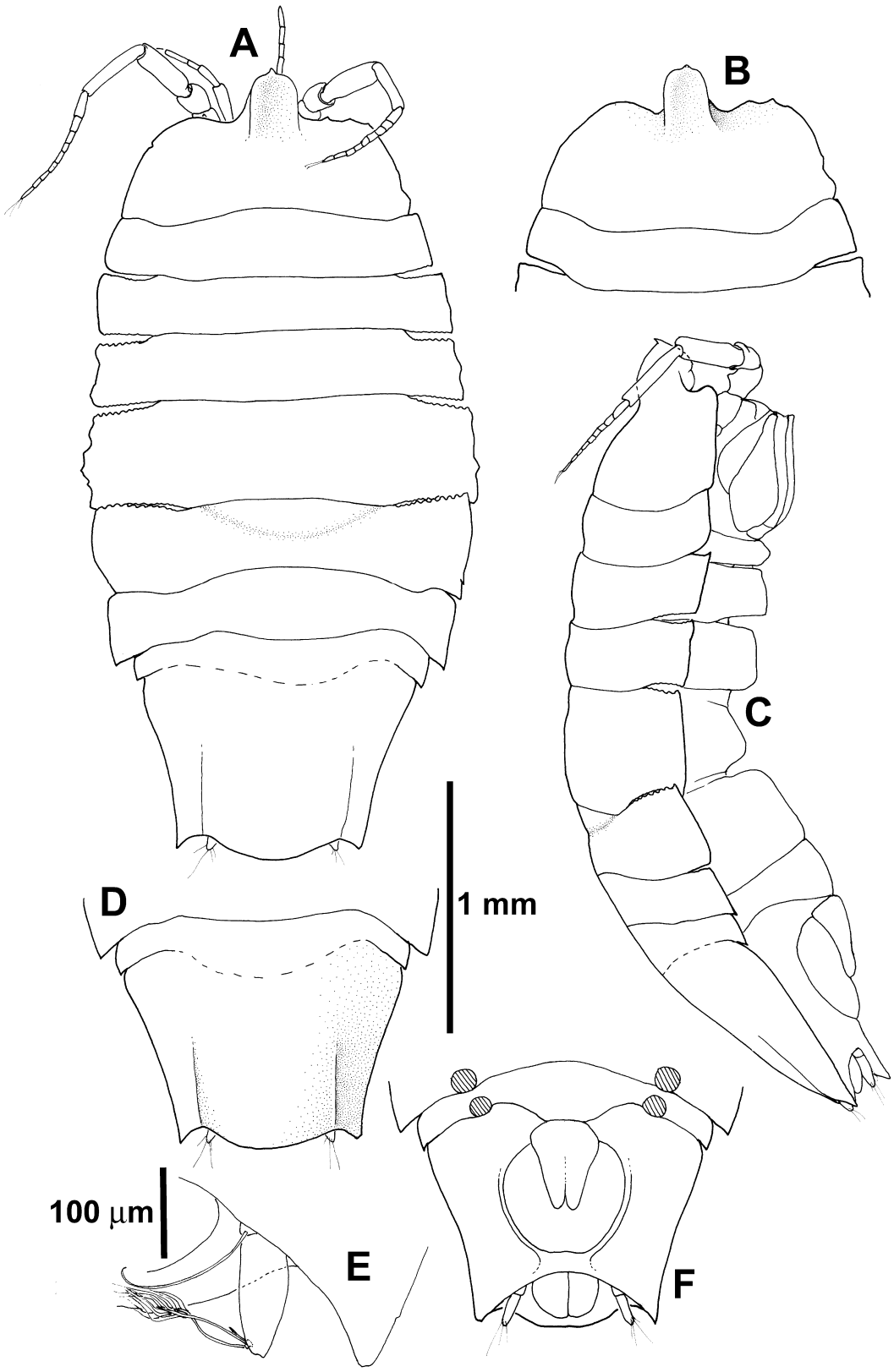

Figure 14. ***Haploniscus cucullus*** **sp. nov.**, paratype, juvenile male, K40760, 3.6 mm: A, dorsal view; B, anterior body, straight dorsal view; C, lateral view (pereopods omitted); D, posterior body, straight dorsal view; E, uropod; F, posterior body, ventral view.

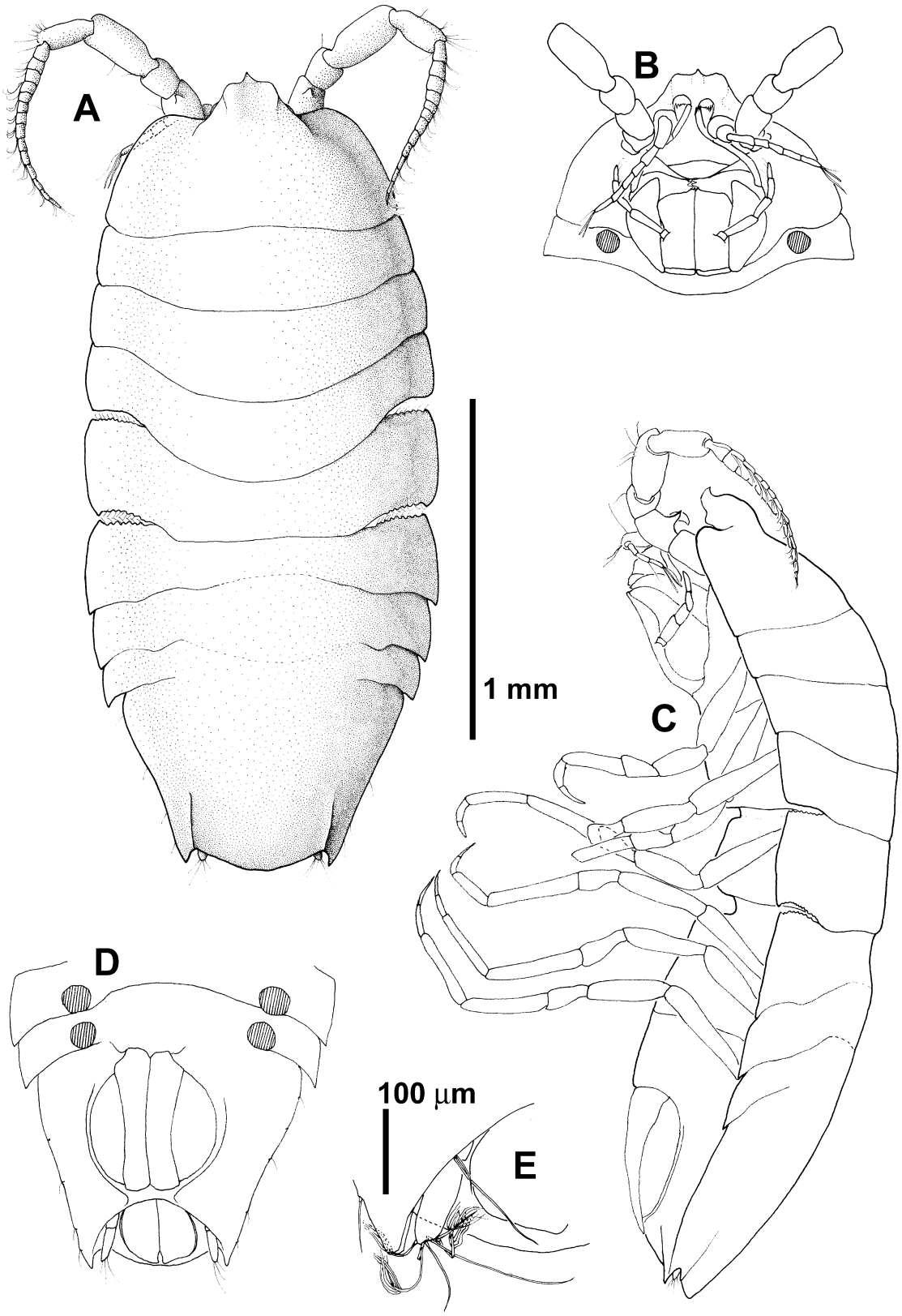

Figure 15. ***Haploniscus weddellensis*** **sp. nov.**, holotype, male, K40761, 3.0 mm: A, dorsal view; B, anterior body ventral view; C, lateral view; D, posterior body, ventral view; E, paratype, male, K40762, 2.8 mm, uropod.

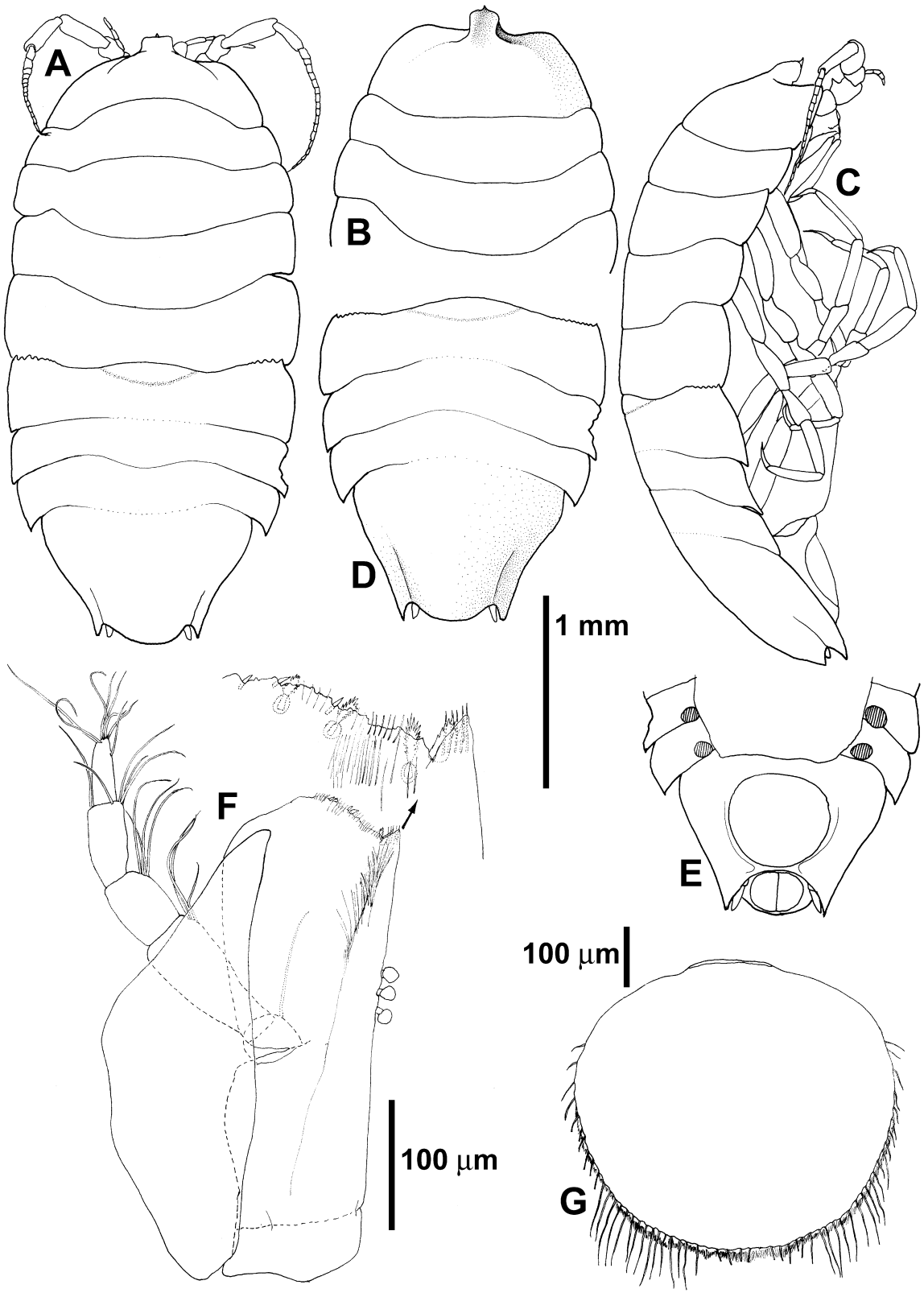

Figure 16. ***Haploniscus weddellensis*** **sp. nov.**, paratype, female, K40762, 4.2 mm: A, dorsal view; B, anterior body, straight dorsal view; C, lateral view; D, posterior body, straight dorsal view; E, posterior body, ventral view; G, pleopod 2; paratype, male, 2.8 mm: F, maxilliped.

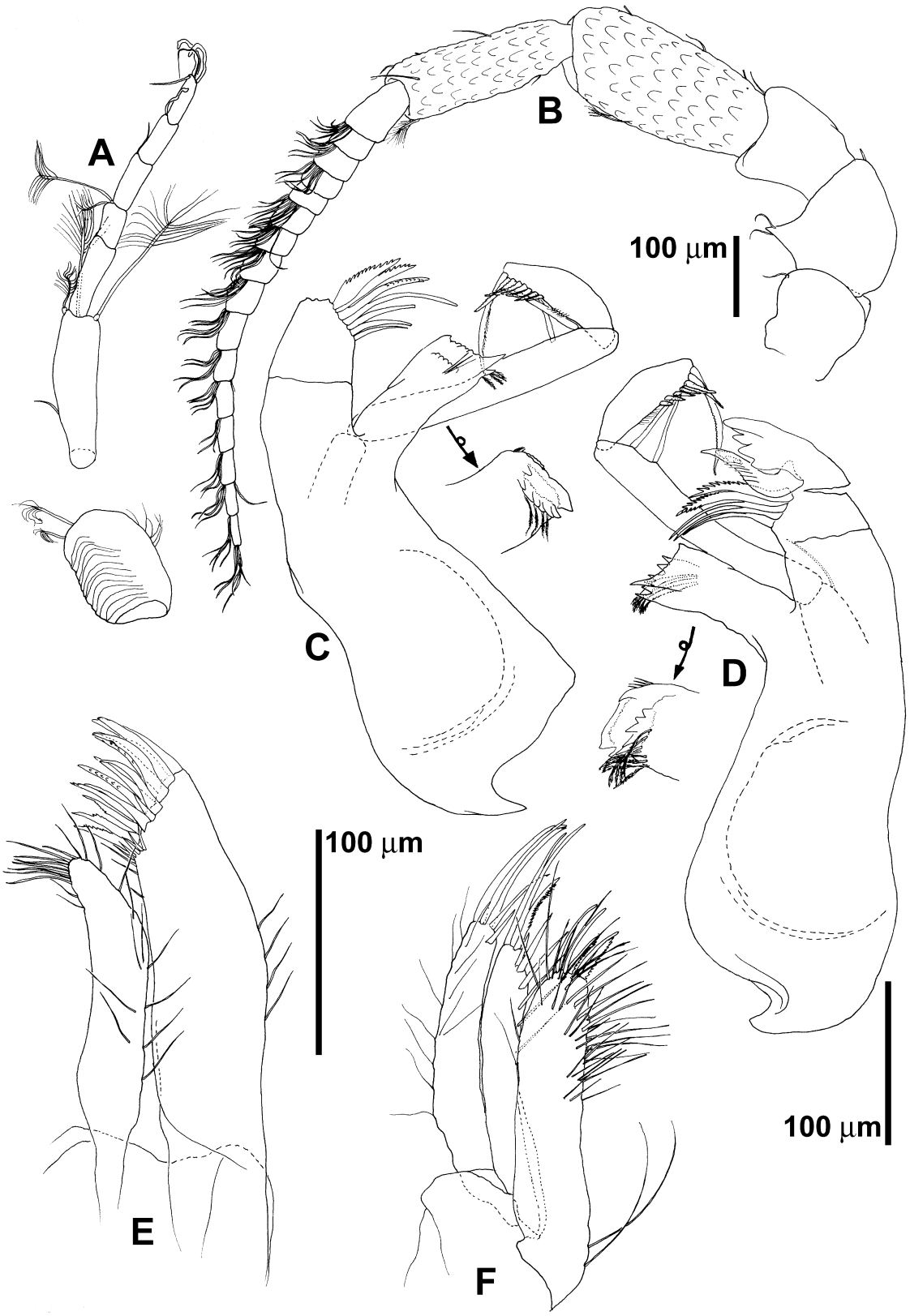

Figure 17. ***Haploniscus weddellensis*** **sp. nov.**, paratype, male, K40762, 2.8 mm: A, antenna 1; B, antenna 2; C, right mandible; D, left mandible; E, maxilla 1; F, maxilla 2.

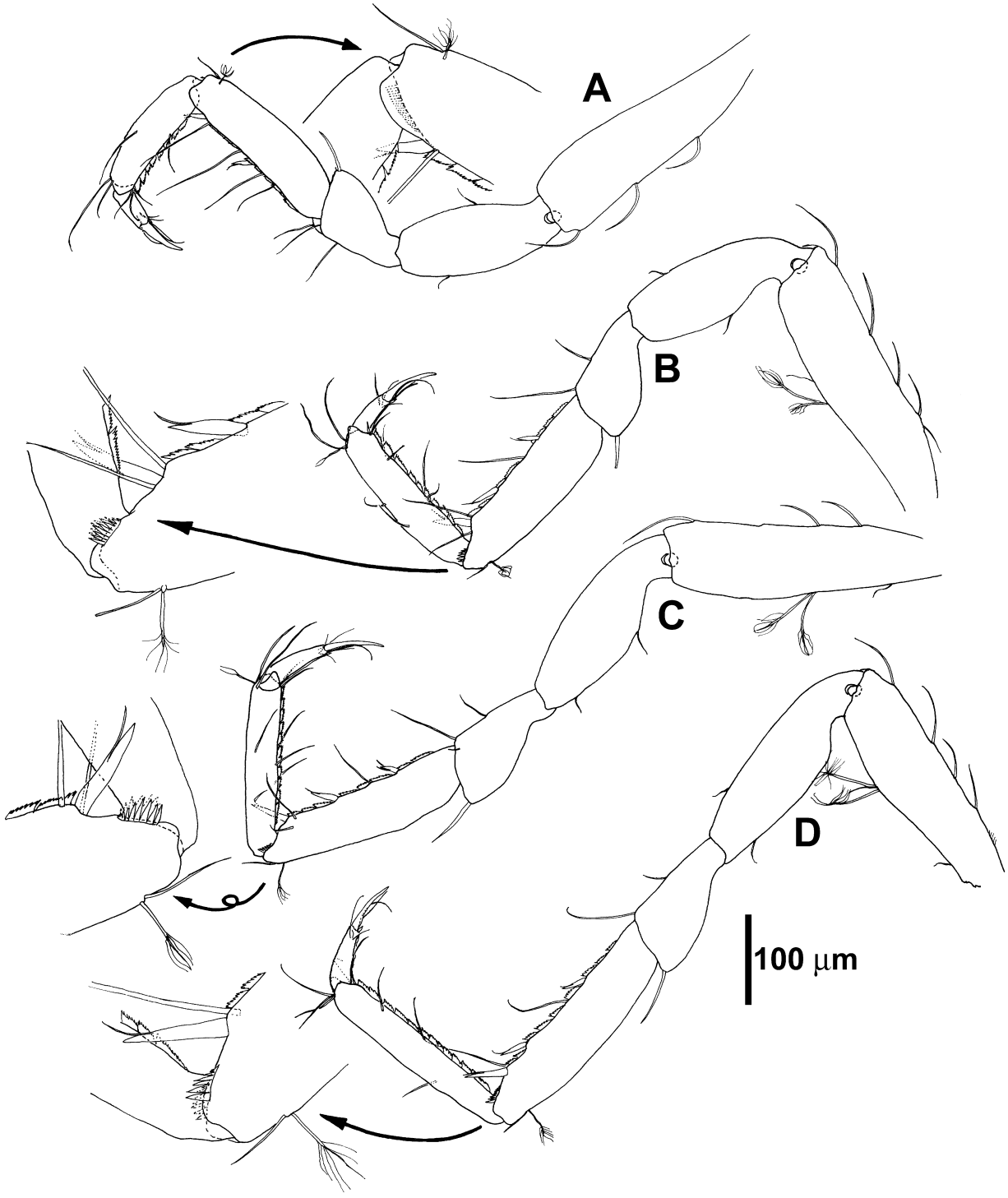

Figure 18. ***Haploniscus weddellensis*** **sp. nov.**, paratype, male, K40762, 2.8 mm: A, pereopod 1; B, pereopod 2; C, pereopod 3; D, pereopod 4.

margins of pleotelson convex basally, slightly concave distally, dorsal keels more pronounced, pleotelson processes slightly exceeding terminal margin, distance between processes 1.3× anterior margin width.

Antenna 2 (Fig. 21) article 4 length 0.7× article 3 length, 0.9× width, article 5 about as long as article 6, length 2× width, article 6 length 4.8× width. Scales small, more numerous.

Mandibular (Fig. 21) palp with 12 serrated setae.

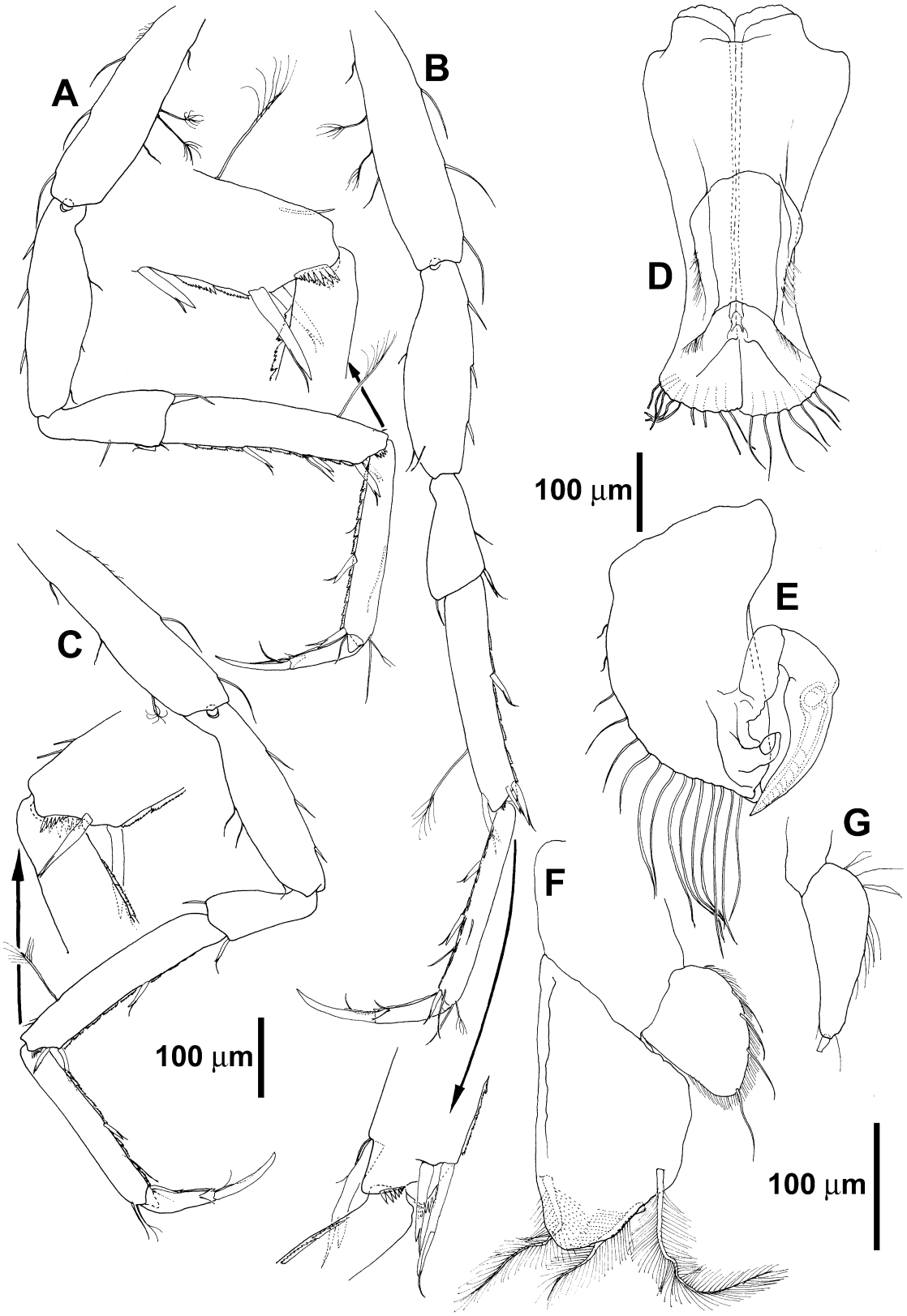

Figure 19. ***Haploniscus weddellensis*** **sp. nov.**, paratype, male, K40762, 2.8 mm: A, pereopod 5; B, pereopod 6; C, pereopod 7; D, pleopod 1; E, pleopod 2; F, pleopod 3; G, pleopod 4, exopod.

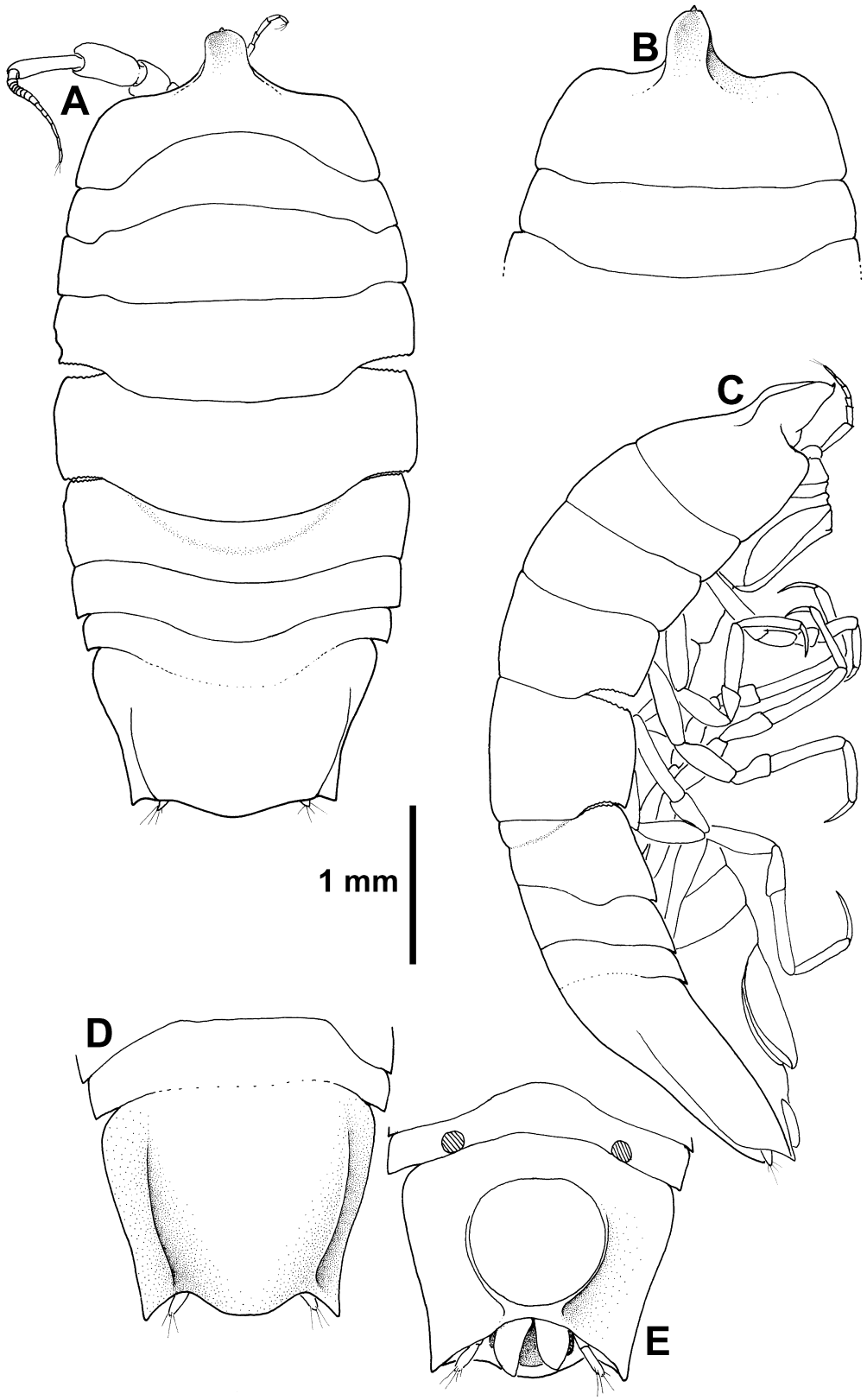

Figure 20. ***Haploniscus procerus*** **sp. nov.**, holotype, female, K40763, 7.4 mm: A, dorsal view, B, anterior body, straight dorsal view; C, lateral view; D, posterior body, straight dorsal view; E, posterior body, ventral view.

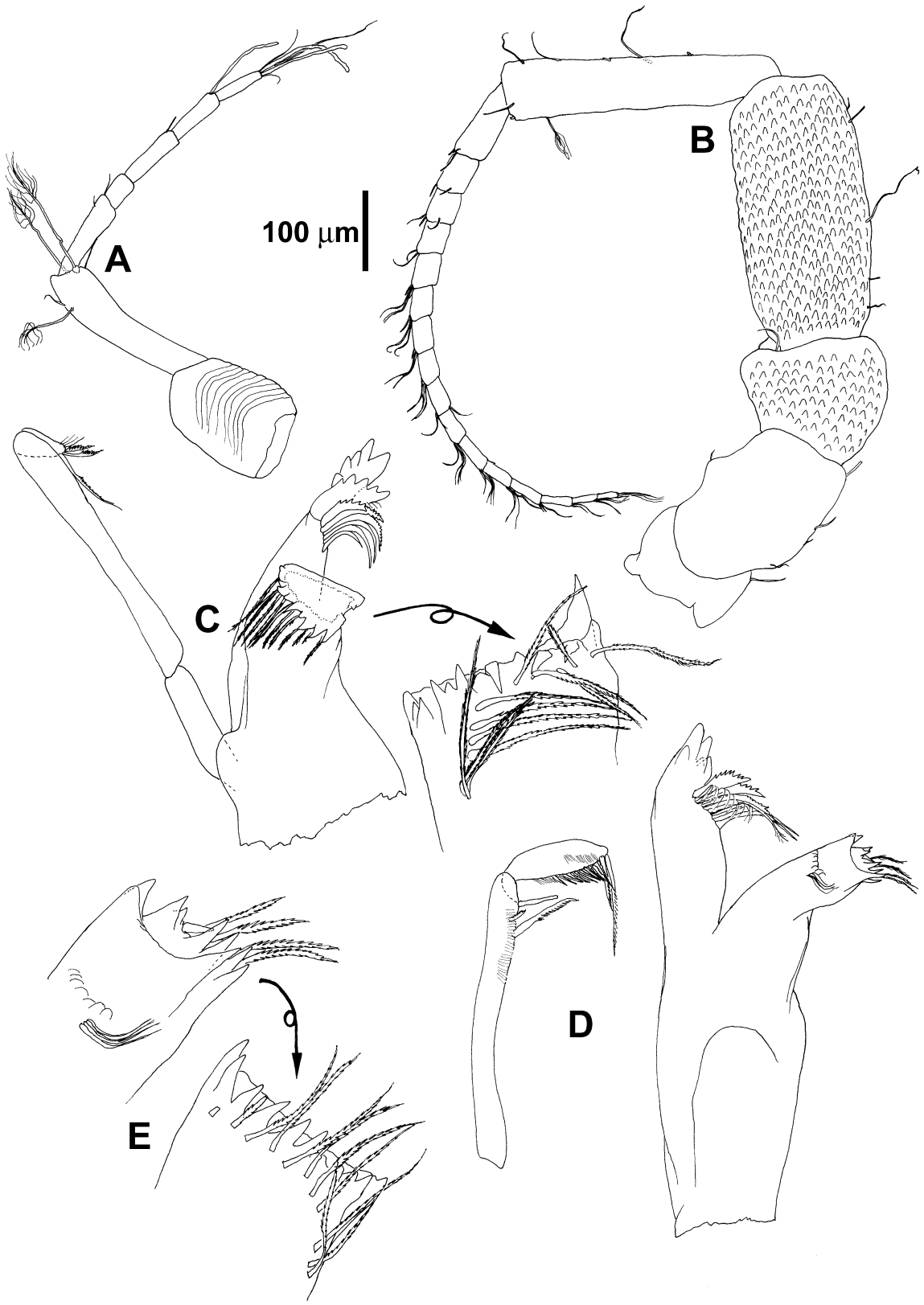

Figure 21. ***Haploniscus procerus*** **sp. nov.**, paratype, female, K40764, 7.6 mm: A, antenna 1; B, antenna 2; C, left mandible; D, right mandible; E, right mandible, detail of molar process.

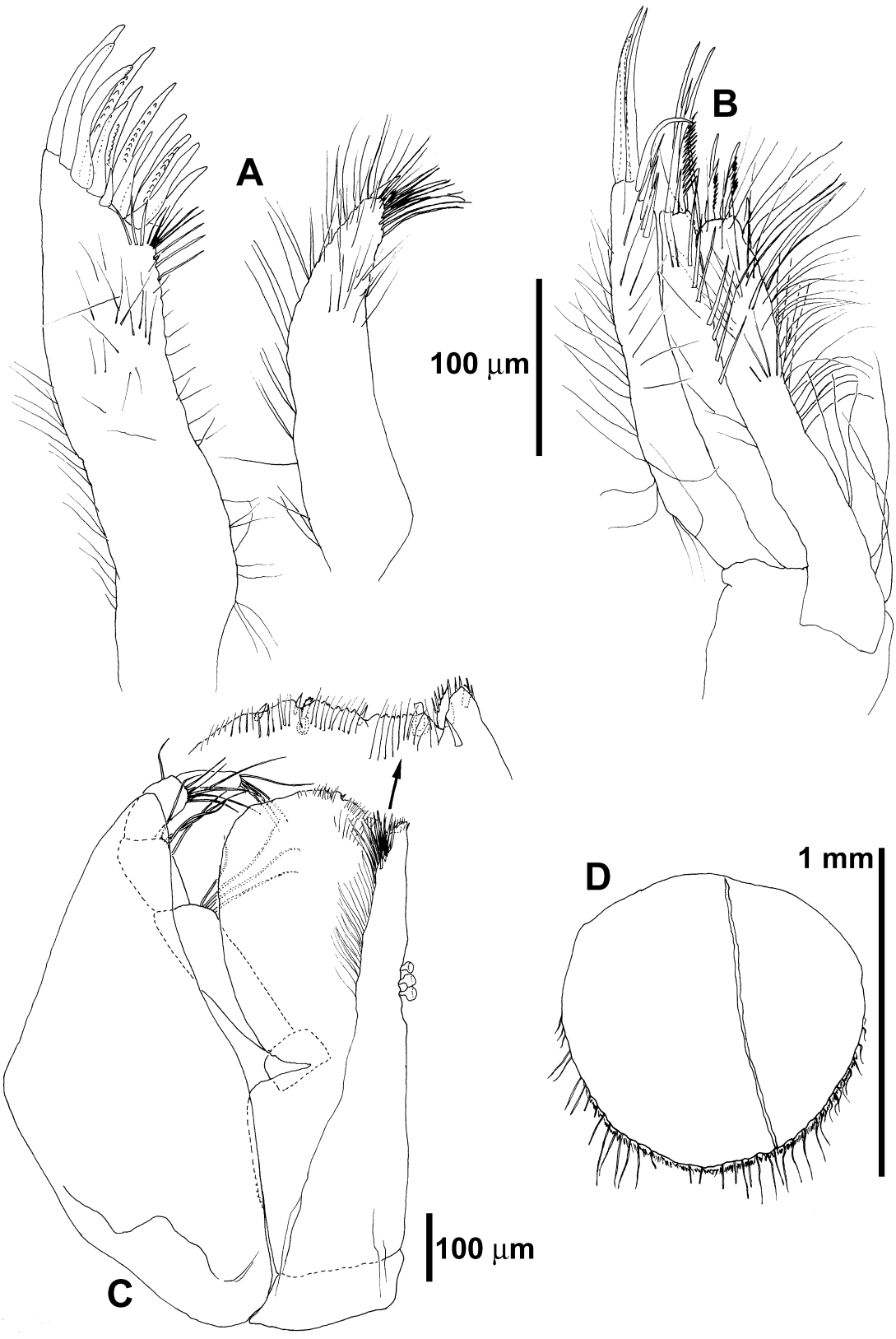

Figure 22. ***Haploniscus procerus*** **sp. nov.**, paratype, female, K40764, 7.6 mm: A, maxilla 1; B, maxilla 2; C, maxilliped; D, pleopod 2.

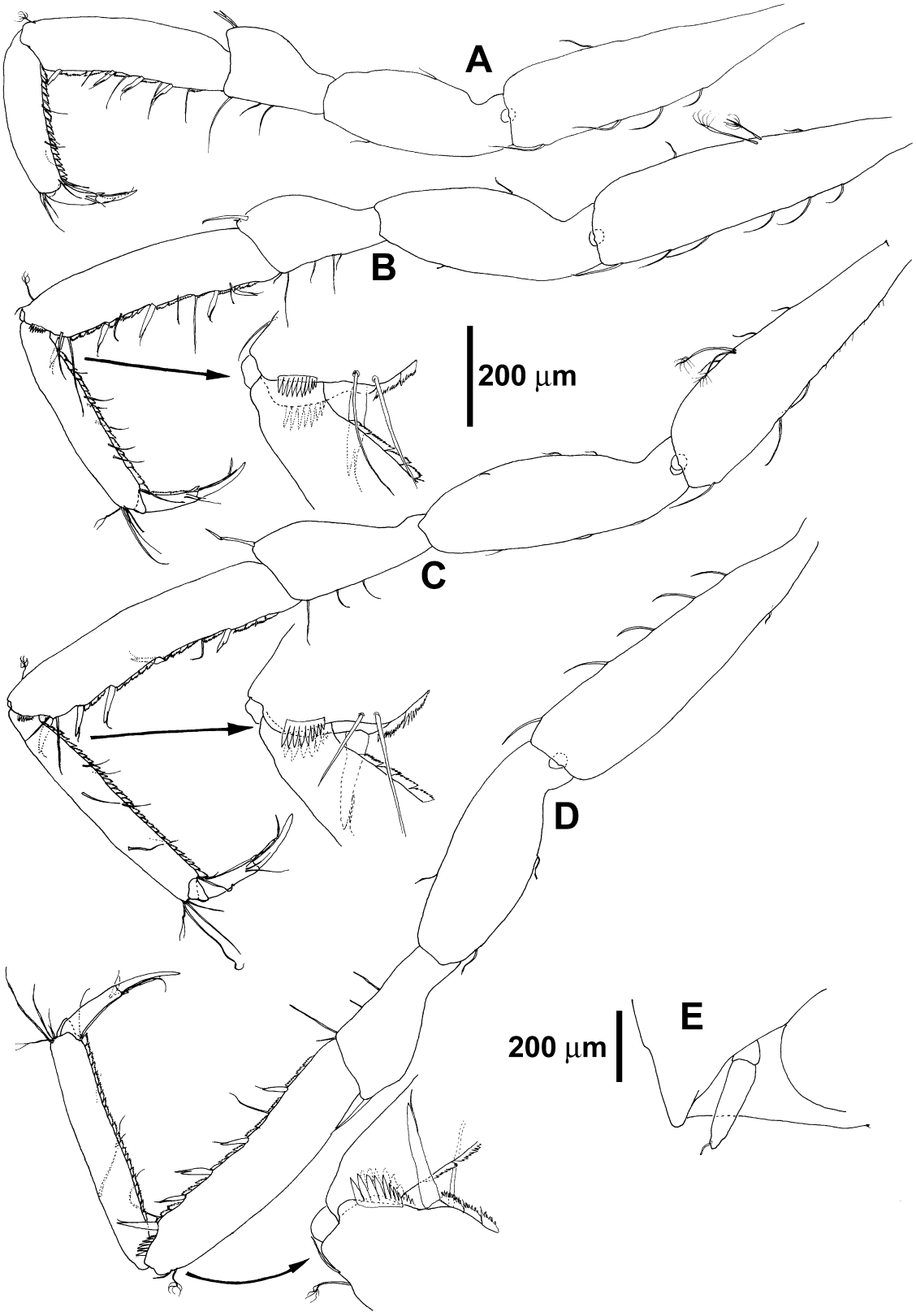

Figure 23. ***Haploniscus procerus*** **sp. nov.**, paratype, female, K40764, 7.6 mm: A, pereopod 1; B, pereopod 2; C, pereopod 3; D, pereopod 4; E, uropod.

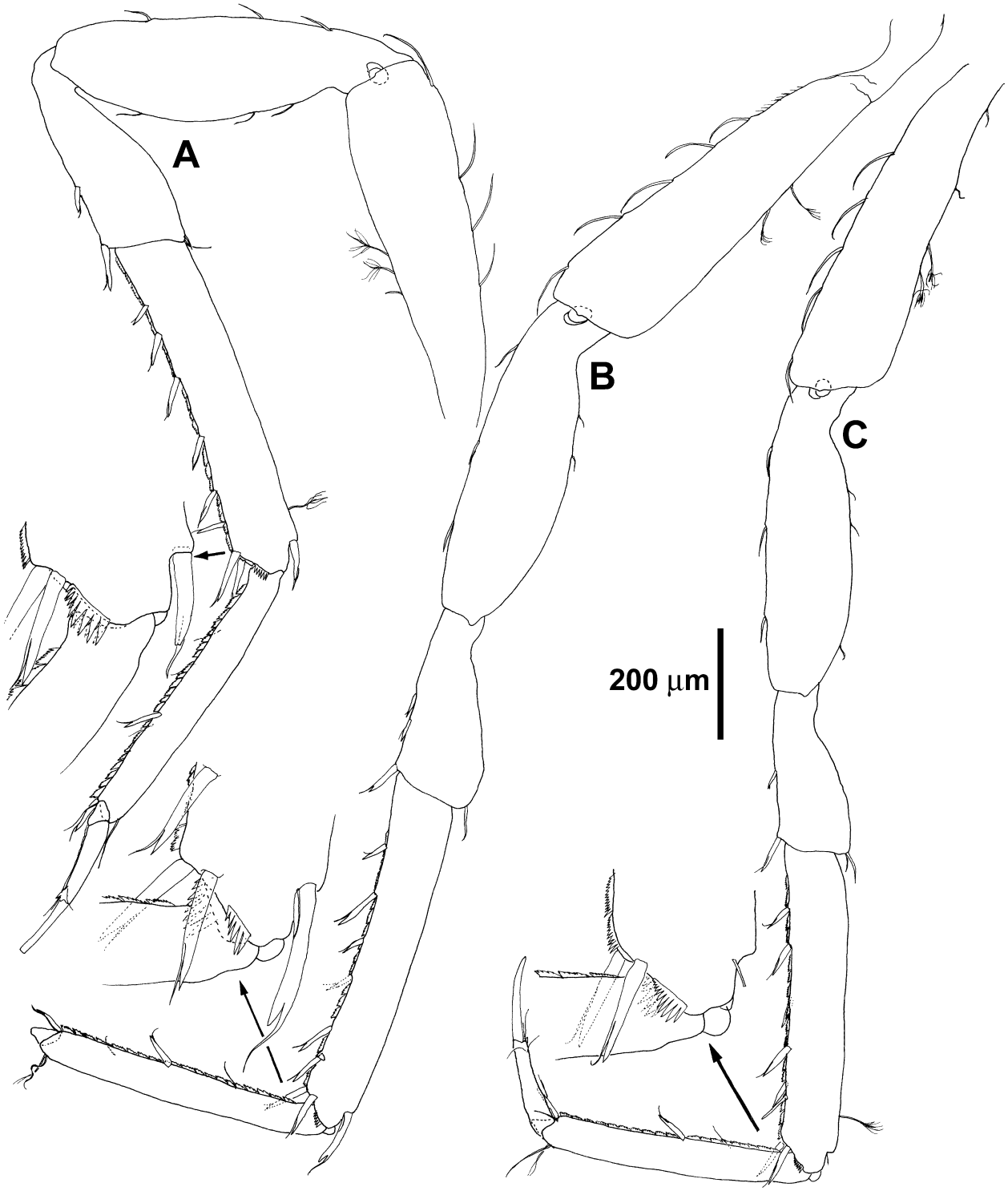

Figure 24. ***Haploniscus procerus*** **sp. nov.**, paratype, female, K40764, 7.6 mm: A, pereopod 5; B, pereopod 6; C, pereopod 7.

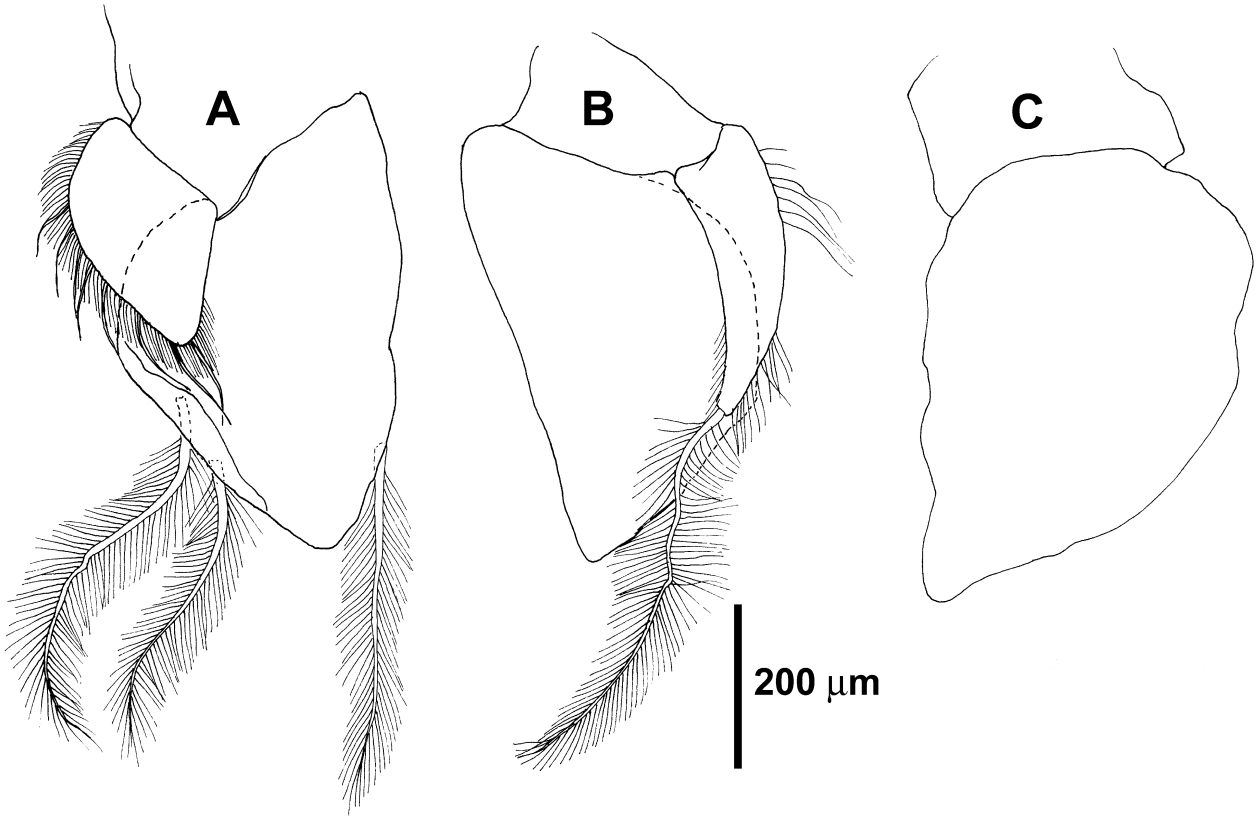

Figure 25. ***Haploniscus procerus*** **sp. nov.**, paratype female, K40764, 7.6 mm: A, pleopod 3; B, pleopod 4; C, pleopod 5.

Maxilliped (Fig. 22) with three retinacula.

Pereopods (Figs 23, 24): Basis with 4–6 setae ventrally. Merus of pereopods 1–4 with 2–3 simple medioventral setae, of pereopods 5–7 with 1–2 medioventral flagellate setae. Carpus of pereopods 1–4 with 4–5 ventral flagellate setae, of pereopods 5–7 with 7–8 ventral flagellate setae, dorsal apical flagellate seta on carpus of pereopods 5–7 (broken off on pereopod 7).

Description of male: No males of this species are known.

Remarks: Besides the above described species three juvenile specimens of a *Haploniscus* species possessing the characteristic rostrum were found at station 131 together with the two adults of *H. procerus*. These possess a much shorter rostrum than *H. procerus* and could not be allocated clearly to one of the newly described species.

HAPLONISCUS KYRBASIA SP. NOV.
(FIGS 26–31, 40E)

Holotype: Male, 5.7 mm; station 141-10, 58°15.98–16.28′S, 24°53.73–54.09′W, 4183 m depth; ZMH K40765.

Etymology: Kyrbasia is the name of a Persian hat with peaked crown; the name refers to the rostrum.

Diagnosis: Body oval, length 3.0× width. Head width 3.0× length, frontal margin concave, with prominent rostrum; rostrum covered with small tubercles, with dorsal depression and acute upturned frontal tooth, a deep ventral indentation between rostrum and frontal margin of head. Pereonites 3–5 broadest. Lateral margins of pleotelson convex basally, concave distally, posterolateral processes short, not reaching terminal margin; dorsal surface of pleotelson with two sharp longitudinal keels, ventral surface with cuticular bulge surrounding the branchial chamber and tapering towards anus. Antenna 1 with four flagellar articles. Maxilliped with three retinacula. Carpus of pereopods 1–4 with four flagellate setae, of pereopods 5–7 with 5–6 flagellate setae, apical and ventral combs of carpus spinose, carpus of pereopods 5 and 6 with dorsal flagellate seta. Pleopod 1 with nearly continuous distal margin. Endopod of pleopod 2 as long as basipod.

Description of male holotype: H. kyrbasia differs from *H. cassilatus* in the following characters.

Head (Figs 26, 40E) width 3.0× length. Rostrum slightly larger, less tapering, curved slightly stronger dorsally in lateral view. Pleotelson (Fig. 25) lateral margins convex basally, concave distally, distance between pleotelson processes 1.5× anterior margin width.

Antenna 1 (Fig. 27) flagellar articles 3 and 4 with one aesthetasc each.

Antenna 2 (Fig. 27) article 4 length 0.9× article 3 length, 1.4× width, article 5 length 1.8× article 3 length, about as long as article 6, length 2.6× width, article 6 length 1.8× article 3 length.

Mandibular (Fig. 27) palp article 3 with ten serrated setae.

Maxilliped (Fig. 28) with three retinacula.

Pereopods (Figs 29, 30): Basis with four ventral setae. Merus with two medioventral setae. Carpus of pereopods 1–4 with four flagellate setae, of pereopods 5–7 with 5–6 flagellate setae. Propodus of pereopods 5–7 with one ventral flagellate seta.

Description of female: Only the male holotype of this species is known.

HAPLONISCUS NUDIFRONS SP. NOV.
(FIGS 32–35)

Holotype: Female, 11.3 mm; station 129-2, 59°52.21–52.20′S, 59°58.75–58.63′W, 4076 m depth; ZMH K40766.

Etymology: The name refers to the absence of the rostrum that is characteristic for the other species of the *Haploniscus cucullus* complex; the Latin *nudus* meaning 'naked'.

Diagnosis: Body oval, length 3.0× width. Head width 2.5× length, frontal margin concave, without rostrum. Pereonites 3–5 broadest. Lateral margins of pleotelson convex, posterolateral processes short, not reaching terminal margin; dorsal surface of pleotelson with two sharp longitudinal keels, ventral surface with cuticular bulge surrounding the branchial chamber and tapering towards anus. Carpus with 3–4 flagellate spine-like setae, apical and ventral combs of carpus spinose, carpus of pereopods 5 and 6 with dorsal flagellate seta. Pleopod 2 of female without setae on lateral margins. Uropods reaching terminal margin of pleotelson.

Description of female holotype: H. nudifrons differs from *H. cassilatus* in the following characters.

Head (Fig. 32) without rostrum.

Distance between pleotelson processes 1.7× pleotelson anterior margin width.

Distal articles of antennae (Fig. 35) lost.

Maxilliped with three retinacula.

Pereopods (Figs 33, 34): Merus with 1–2 medioventral setae. Carpus with 3–4 ventral flagellate setae.

Pleopod 2 (Fig. 35) lateral margins, without setae, distal margin with about 20 setae.

Uropods (Fig. 32) reaching terminal margin of pleotelson.

Description of male: Only the female holotype of this species is known.

HAPLONISCUS MICROKORYS SP. NOV.
(FIGS 36–39, 40F)

Holotype: Male, 4.3 mm; station 134-3, 65°19.20–19.05′S, 48°03.77–02.92′W, 4553 m depth; ZMH K40767.

Etymology: From the Greek words *micros* meaning small and *korys* meaning helmet; the name refers to the rostrum, which is smaller than in most species of the *Haploniscus cucullus* complex.

Diagnosis: Body oval, length 3.0× width. Head width 2.5× length, frontal margin concave, with triangular rostrum; rostrum pointing ventrally with acute frontal tooth, a deep ventral indentation between rostrum and frontal margin of head. Pereonites 3–5 broadest. Lateral margins of pleotelson convex basally, concave distally, posterolateral processes short, not reaching terminal margin; dorsal surface of pleotelson with two sharp longitudinal keels, ventral surface with cuticular bulge surrounding the branchial chamber and tapering towards anus. Antenna 1 with five flagellar articles. Maxilliped with three retinacula. Carpus of pereopod 1 with six ventral flagellate setae, of pereopods 2–7 with 7–11 ventral flagellate setae, apical and ventral combs of carpus spinose, carpus of pereopods 5 and 6 with dorsal flagellate seta. Pleopod 1 with nearly continuous distal margin. Endopod of pleopod 2 as long as basipod.

Description of male holotype: H. microkorys differs from *H. cassilatus* in the following characters.

Rostrum (Figs 36, 40F) smaller, pointing ventrally, triangular in dorsal view, without dorsal depression.

Lateral margins of pleotelson (Fig. 36) convex basally, concave distally, distance between processes 2.0× anterior margin width.

Antenna 1 (Fig. 37) with five flagellar articles, articles 3 and 4 with one aesthetasc, article 5 with two aesthetascs.

Antenna 2 (Fig. 37) article 4 length 0.5× article 3 length, 0.9× width, article 5 length 0.8× article 6 length, 3.3× width, article 6 length 1.9× article 3 length, 5.6× width.

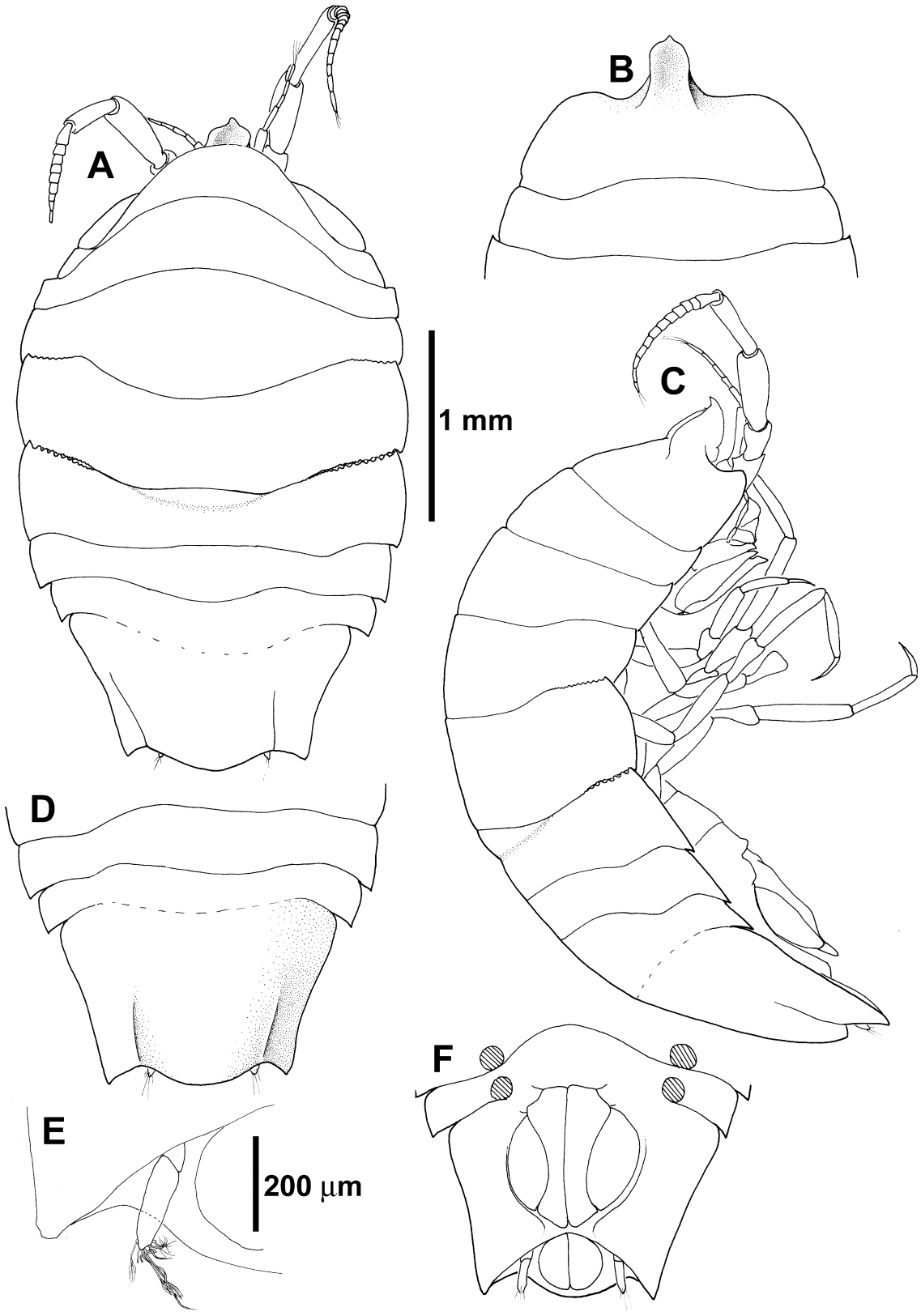

Figure 26. ***Haploniscus kyrbasia*** **sp. nov.**, holotype, male, K40765, 5.7 mm: A, dorsal view; B, anterior body, straight dorsal view; C, lateral view; D, posterior body, straight dorsal view; E, uropod; F, posterior body, ventral view.

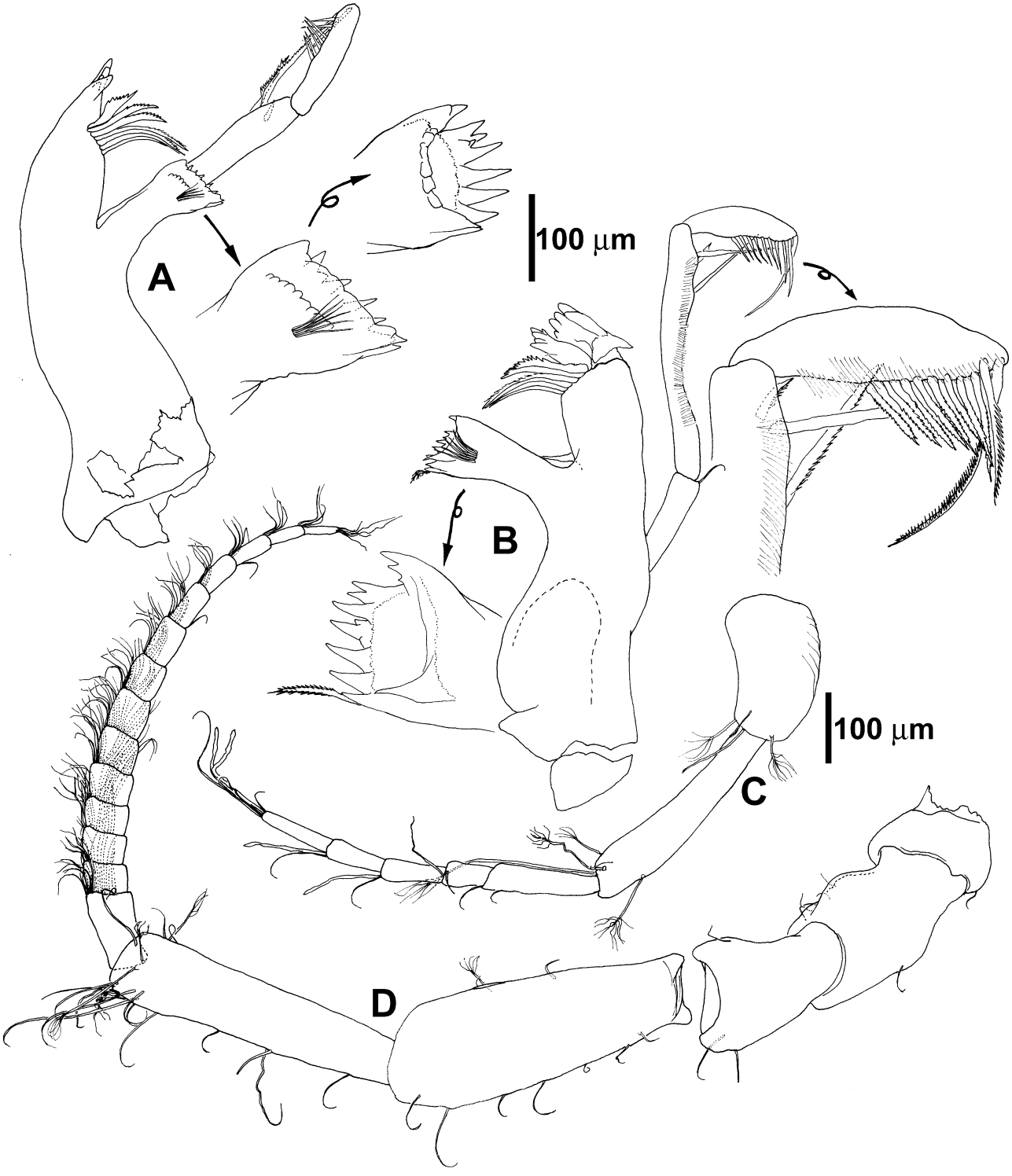

Figure 27. ***Haploniscus kyrbasia*** **sp. nov.**, holotype, male, K40765, 5.7 mm: A, right mandible; B, left mandible; C, antenna 1; D, antenna 2.

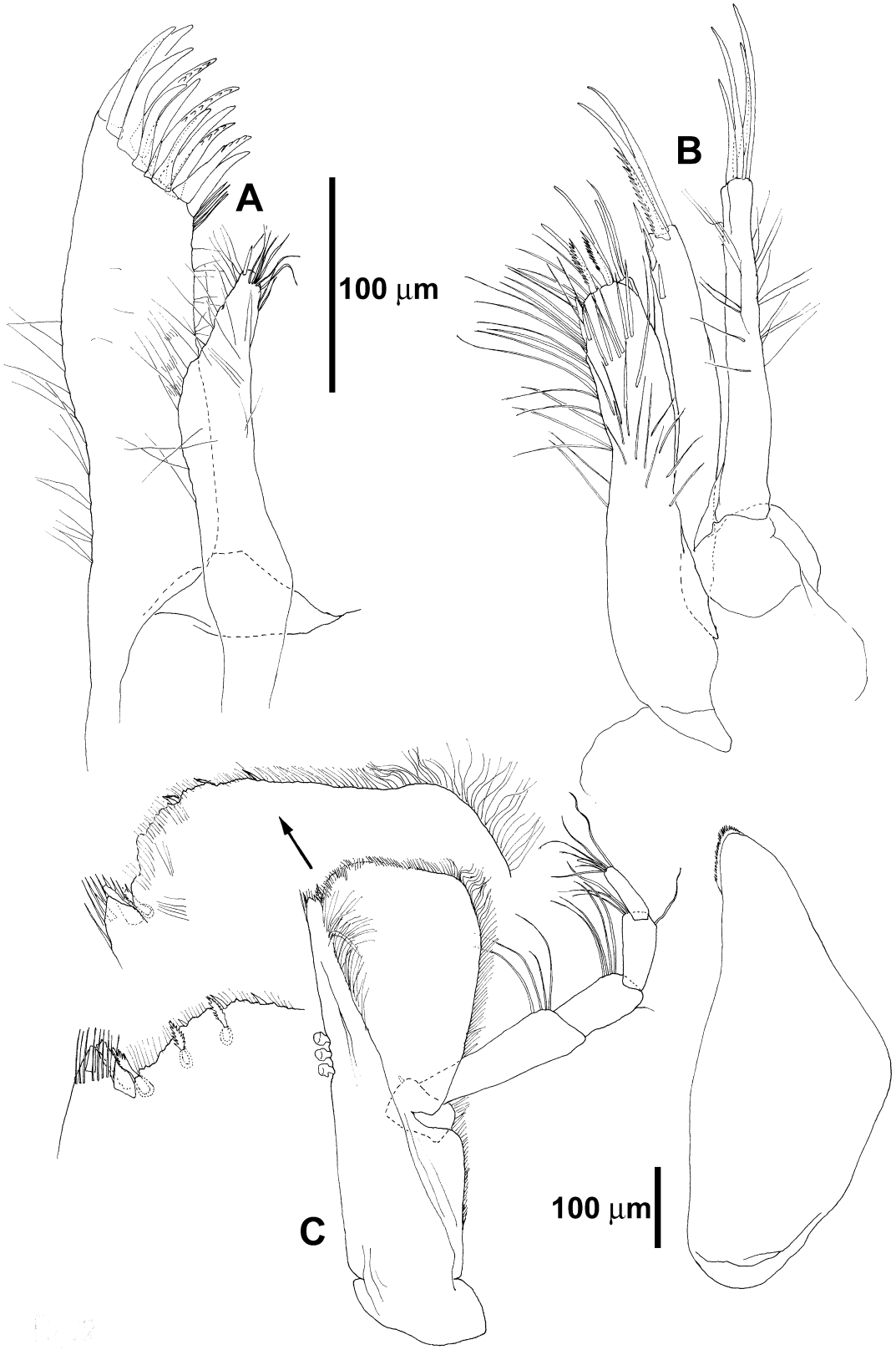

Figure 28. ***Haploniscus kyrbasia*** **sp. nov.**, holotype, male, K40765, 5.7 mm: A, maxilla 1; B, maxilla 2; C, maxilliped, distal margin in dorsal and ventral view.

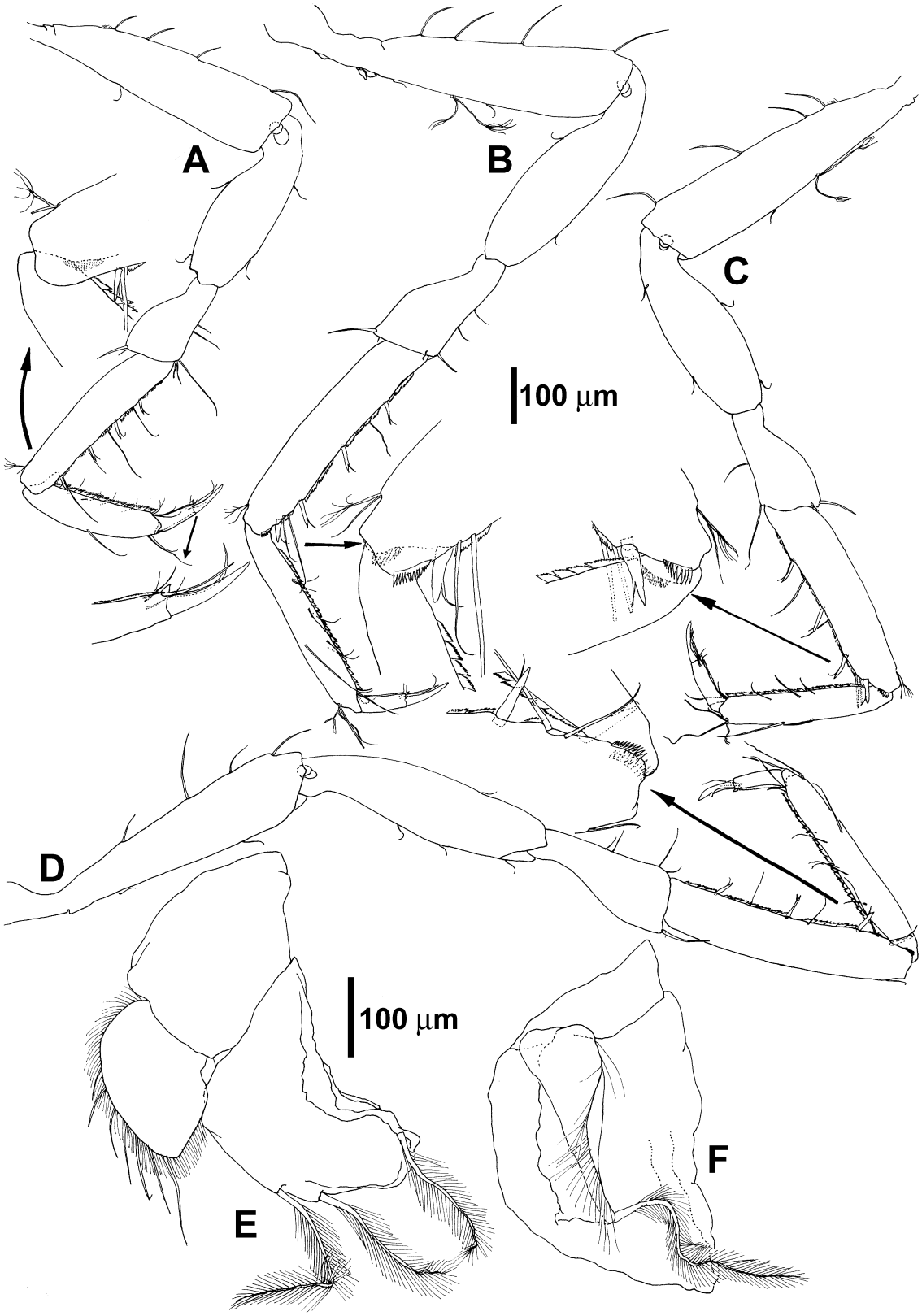

Figure 29. ***Haploniscus kyrbasia*** **sp. nov.**, holotype, male, K40765, 5.7 mm: A, pereopod 1; B, pereopod 3; C, pereopod 2; D, pereopod 4; E, pleopod 3; F, pleopod 4.

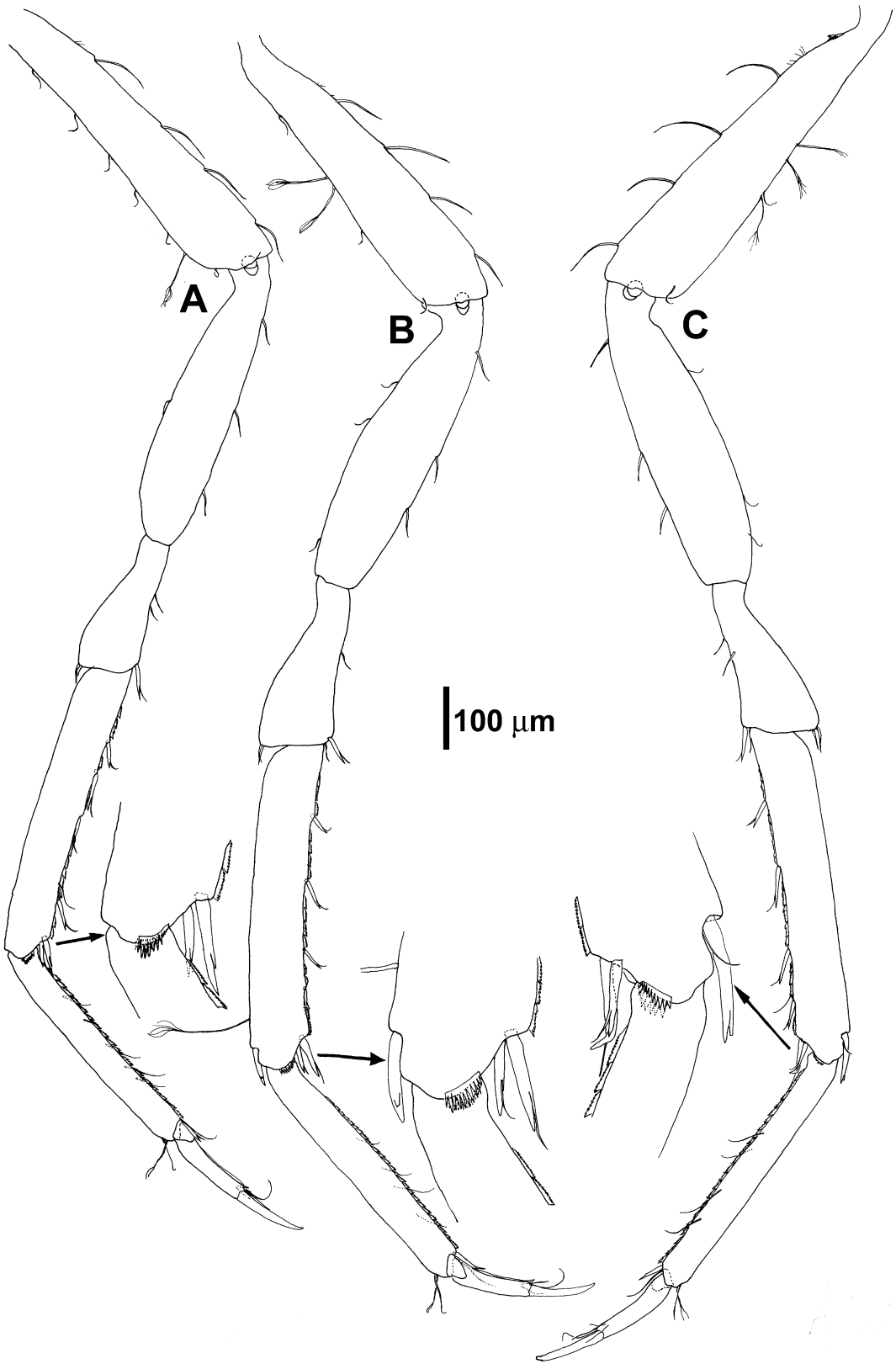

Figure 30. ***Haploniscus kyrbasia*** **sp. nov.**, holotype, male, K40765, 5.7 mm: A, pereopod 7; B, pereopod 5; C, pereopod 6.

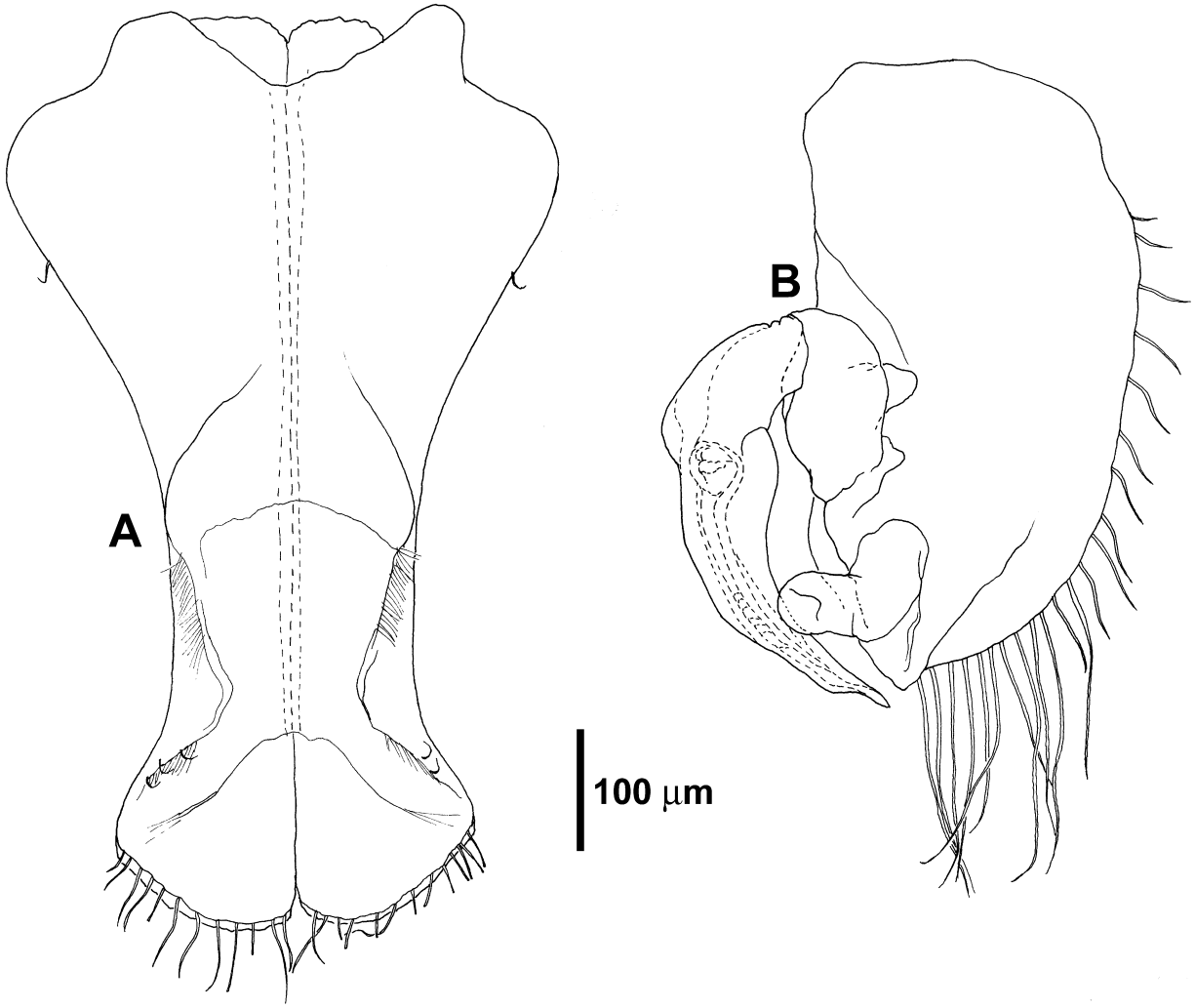

Figure 31. ***Haploniscus kyrbasia*** **sp. nov.**, holotype, male, K40765, 5.7 mm: A, pleopod 1; B, pleopod 2.

Mandibular (Fig. 37) palp article 3 with 11 serrated setae.

Maxilliped with three retinacula.

Pereopods (Figs 38, 39): Basis with 4–7 ventral setae. Ischium with 3–6 ventral setae. Merus of pereopods 1–4 with 3–4 medioventral simple setae, of pereopods 5–7 with three medioventral flagellate setae. Carpus of pereopod 1 with six ventral flagellate setae, of pereopods 2–7 with 7–11 ventral flagellate setae. Propodus of pereopods 2–4 with almost 20 simple setae ventrally, propodus of pereopods 5–7 with 1–2 ventral flagellate setae and several simple setae.

Exopod of pleopod 3 (Fig. 37) with 12 setae.

Description of female: Only the male holotype of this species is known.

MOLECULAR STUDIES

DNA could be extracted and sequenced from five of the seven species of the *Haploniscus cucullus* complex (see tables). The sequenced fragment of the mitochondrial large-subunit rRNA gene is AT rich, as it is typical for this gene (e.g. France & Kocher, 1996; Wetzer, 2001; Wetzer, Martin & Trautwein, 2003). Average base frequencies are pi(A) = 32%, pi(C) = 15%, pi(G) = 21% and pi(T) = 32%, while the 18S rDNA data set shows a slightly increased G-content: pi(A) = 24%, pi(C) = 23%, pi(G) = 28% and pi(T) = 25%. However, both alignments show no significant differences in base composition [χ^2 test 16S rDNA (18S rDNA): d.f. = 66 (18), $P = 1.00$ (0.99)]. The AIC suggests the use of the TVM model with gamma-distributed rates and no invariant sites for the 16S rDNA data set (alpha = 0.3755, $R_{(AC)} = 1.00$,

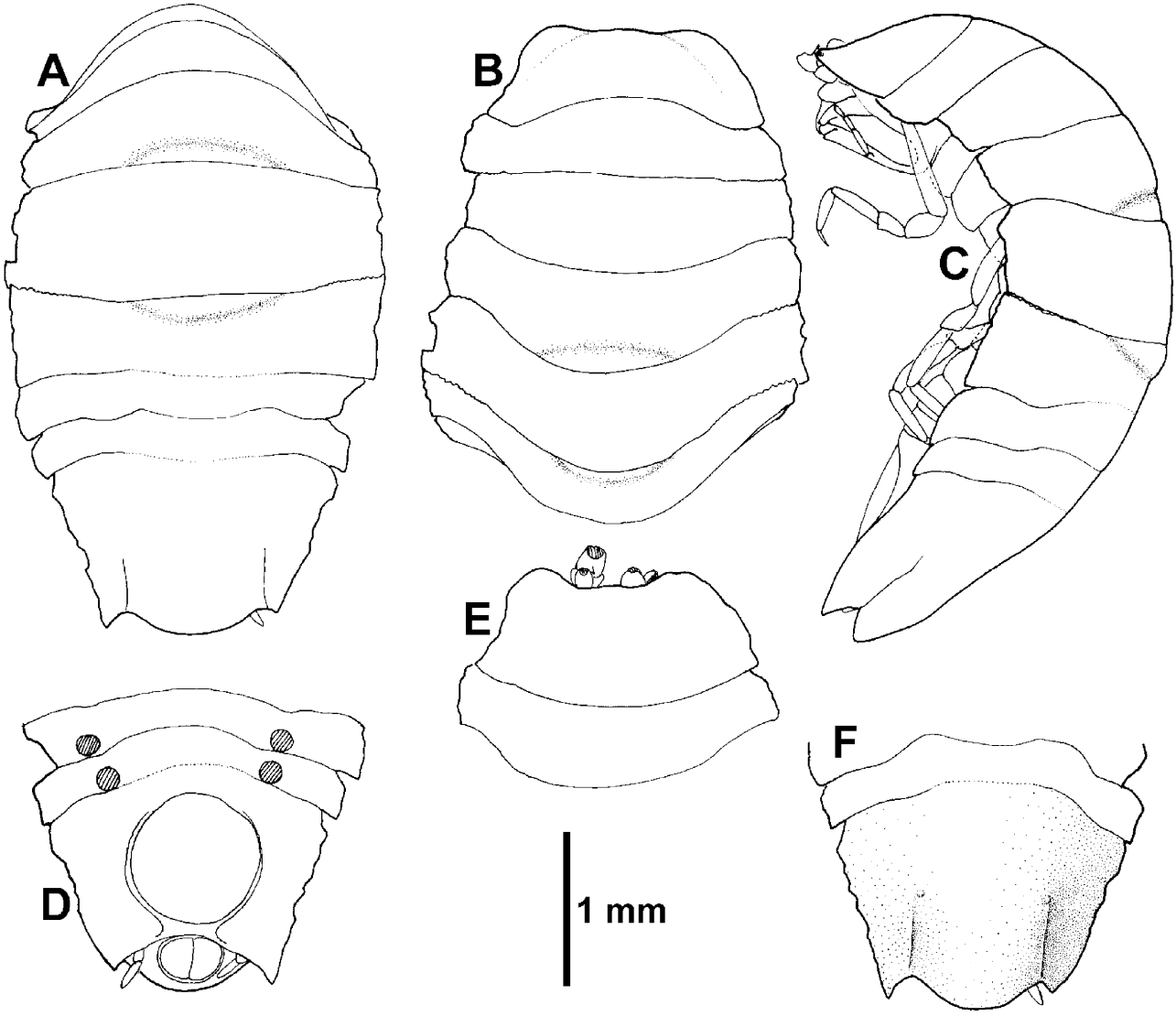

Figure 32. ***Haploniscus nudifrons*** **sp. nov.**, holotype, female, K40766, 11.3 mm: A, posterior body, dorsal view, B, anterior body, dorsal view; C, lateral view; D, posterior body, ventral view; E, anterior body, straight dorsal view; F, posterior body, straight dorsal view.

$R_{(AG)} = 4.01$, $R_{(AT)} = 0.90$, $R_{(CG)} = 0.16$, $R_{(CT)} = 4.01$, $R_{(GT)} = 1.00$), which were used as parameters for the Bayesian analysis. In addition, the AIC suggests the GTR model with gamma-distributed rate variation across sites and a proportion of invariable sites (alpha = 0.7877, $p_{invar} = 0.7595$, $R_{(AC)} = 0.83$, $R_{(AG)} = 1.82$, $R_{(AT)} = 1.42$, $R_{(CG)} = 0.50$, $R_{(CT)} = 3.13$, $R_{(GT)} = 1.00$) for the analysis of the 18S rDNA data set.

Figure 42 shows the 50% majority rule consensus tree of the 16S rDNA data set recovered using the Bayesian approach. Topologies were rooted with *Antennuloniscus armatus* Menzies, 1962. Both data sets (16S and 18S alignments) resulted in identical tree topologies. However, within the *Haploniscus* clade all posterior proabilities of the 18S rDNA data set appear somewhat lower than those of the 16S rDNA data set. All species with more than one sequenced specimen appear to be monophyletic; the sequenced *Haploniscus* species form a monophyletic group. One of its clades includes *Haploniscus cucullus*, *H. microkorys* and *H. nudifrons*, the latter two representing sister taxa. The second, strongly supported clade includes *Haploniscus weddellensis* and *H. cassilatus*.

The uncorrected distances (*p*-distances) between the species of *Haploniscus* range from 0.0732 to 0.1456 across all 16S rDNA sequences (*d*-distances: 0.0914–0.2298) and 0.0140–0.0330 (*d*-distances: 0.0143–0.0340) for the complete 18S rDNA sequences (see Tables 2, 3).

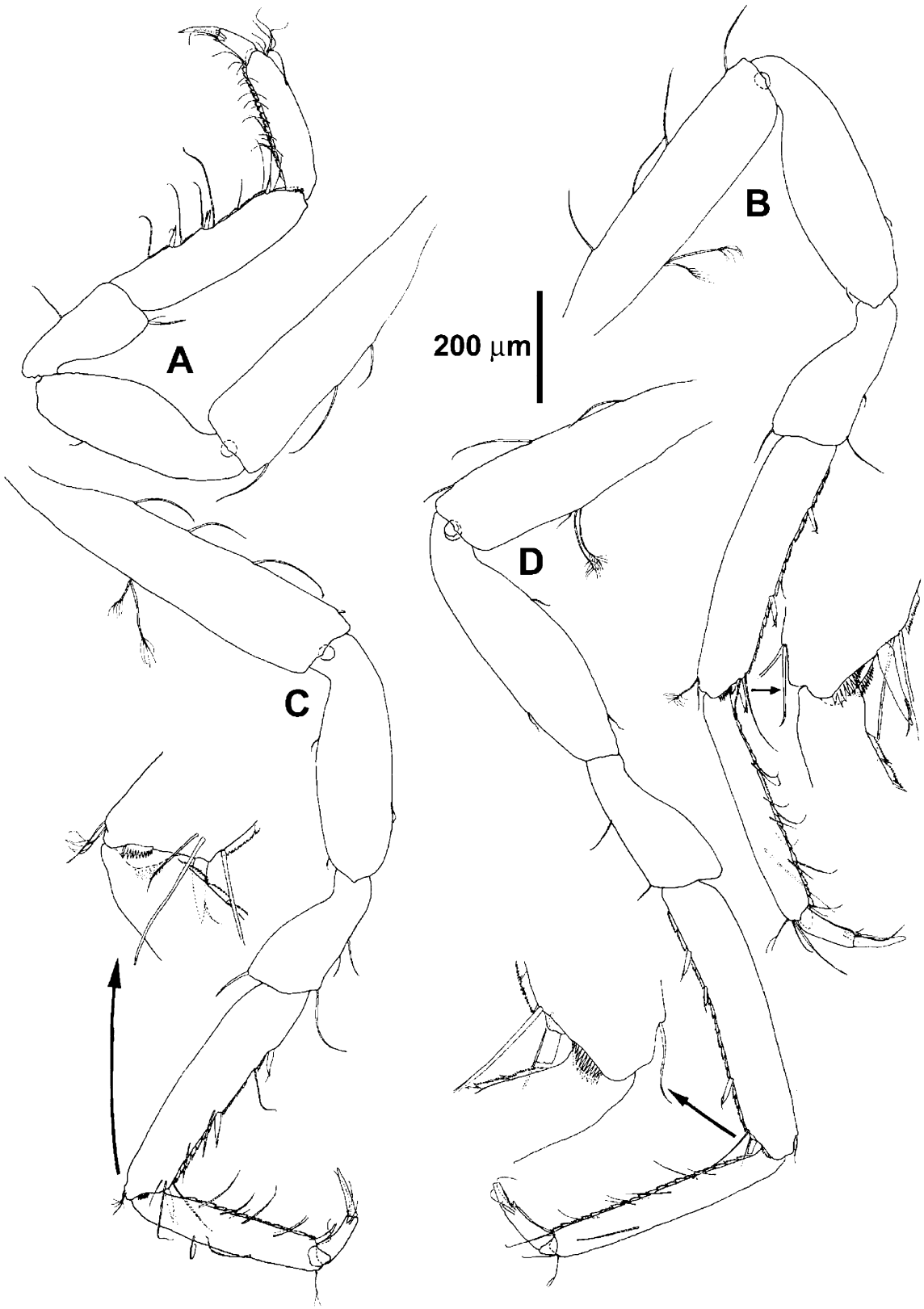

Figure 33. ***Haploniscus nudifrons*** **sp. nov.**, holotype, female, K40766, 11.3 mm: A, pereopod 1; B, pereopod 3; C, pereopod 2; D, pereopod 4.

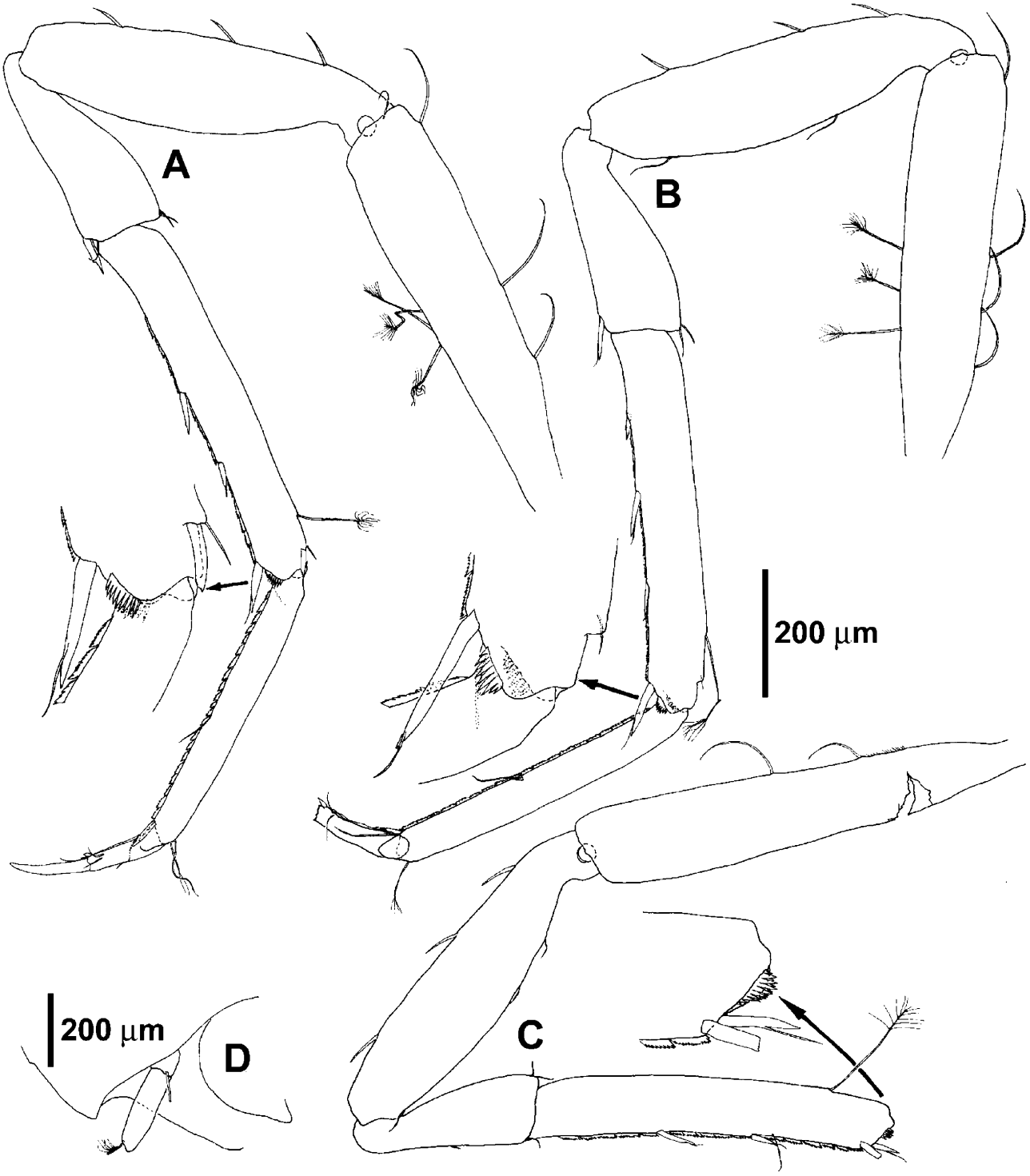

Figure 34. ***Haploniscus nudifrons*** **sp. nov.**, holotype, female, K40766, 11.3 mm: A, pereopod 5; B, pereopod 6; C, pereopod 7; D, uropod.

DISCUSSION

Within the genus *Haploniscus* a number of species share characters with species of the *Haploniscus cucullus* complex: the relatively broad body shape, the relatively short pleotelson processes, and the flagellate setae on the ventral margin of merus, carpus and propodus. Many of these species also possess

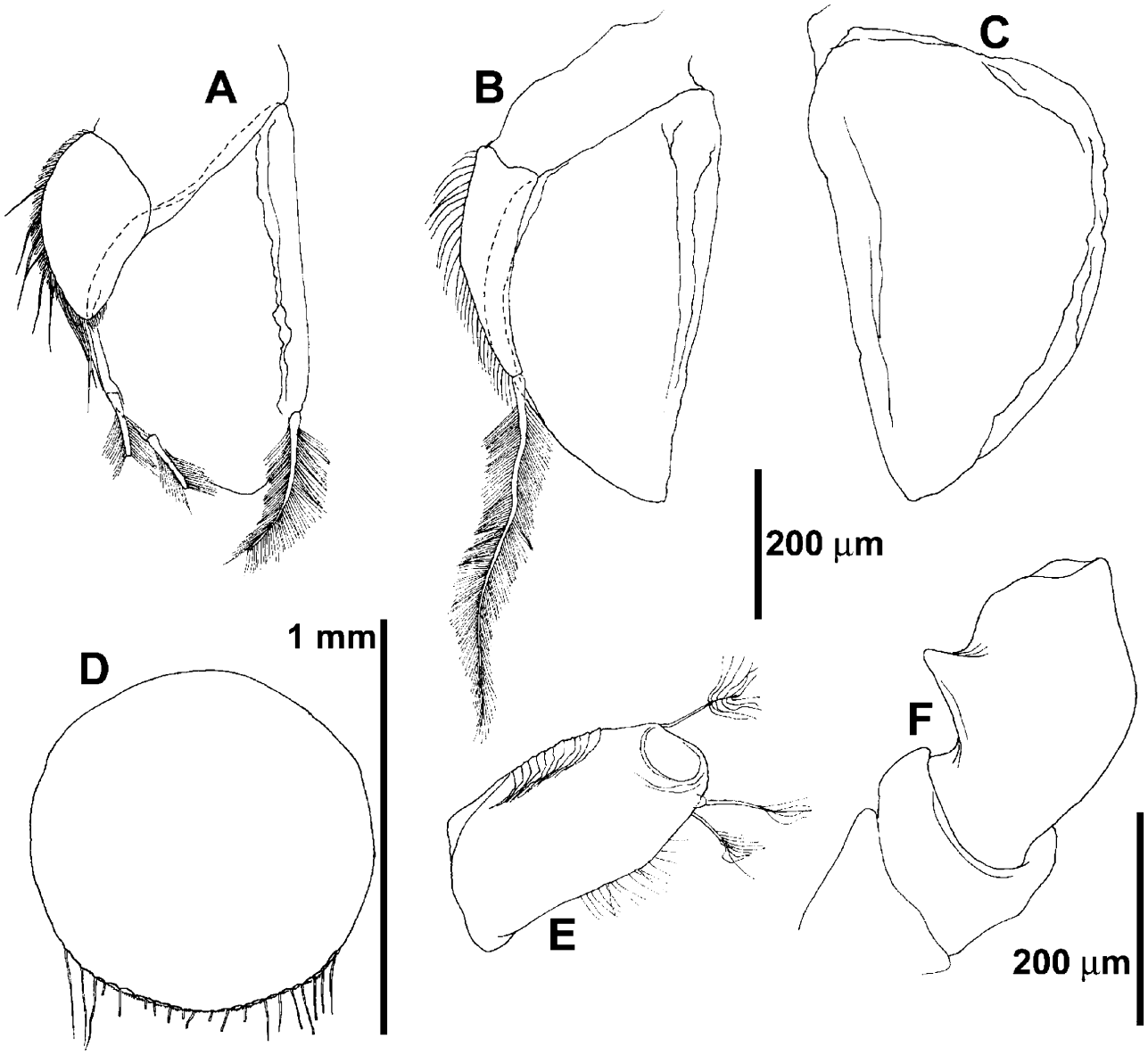

Figure 35. ***Haploniscus nudifrons*** **sp. nov.**, holotype, female, K40766, 11.3 mm: A, pleopod 3; B, pleopod 4; C, pleopod 5; D, pleopod 2; E, antenna 1, article 1; F, antenna 2, articles 1–3.

a rostrum, sometimes resembling the rostrum of species of the *Haploniscus cucullus* complex. These species have to be regarded as potential relatives of the species described above, but no genetic information is available for most of them. *Haploniscus charcoti* Chardy, 1975 closely resembles the rostrum-bearing species of the *Haploniscus cucullus* complex, but apparently lacks the acute produced tip of the rostrum, and the two pereopods illustrated by Chardy seem to lack the typical flagellate setae. In addition, it was found in the North Atlantic and as the different populations of this species complex sampled at nearby stations in the Southern Ocean proved to belong to different species, it is hardly plausible that one of the species described above could belong to *H. charcoti*. *Haploniscus nondescriptus* Menzies, 1962 is most similar to *H. nudifrons*, but differs in the shape of pleopods 3–5. Also, the known specimens of *H. nondescriptus* are distinctly smaller than the specimen of *H. nudifrons*, about 3–4 mm, and the cuticle of *H. nudifrons* is much stronger. Nevertheless, the two species might be closely related. *H. capensis* Menzies, 1962, *H. tridens* Menzies, 1962, *H. tricornis* Menzies, 1962, *H. tricornoides* Menzies, 1962 and *H. piestus* Lincoln, 1985a also resemble species of the *Haploniscus cucullus* complex, but differ clearly in the shape of

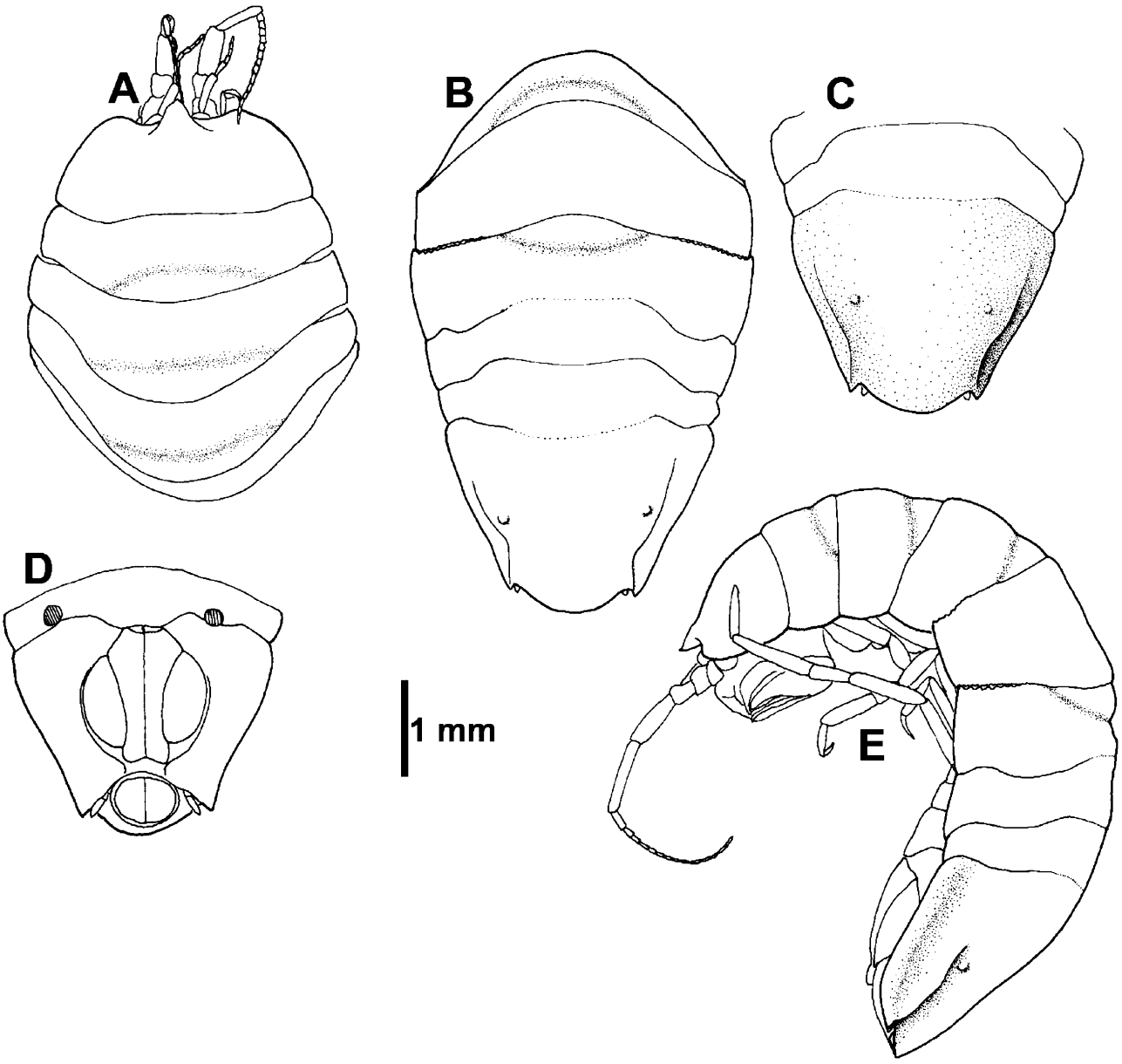

Figure 36. ***Haploniscus microkorys*** **sp. nov.**, holotype, male, K40767, 4.3 mm: A, anterior body, dorsal view; B, posterior body, dorsal view; C, posterior body, straight dorsal view; D, posterior body, ventral view; E, lateral view.

the rostrum. Further potential members are *H. laticephalus* Birstein, 1968 and *H. similis* Birstein, 1968, but the illustrations by Birstein are not sufficient for detailed investigations.

Haploniscus cucullus, *H. cassilatus*, *H. weddellensis*, *H. procerus* and *H. kyrbasia* show only little morphological differences, especially in the basic shape of the rostrum, and therefore it seems likely that these species are siblings. The morphological differences to *H. nudifrons* and *H. microkorys* are more obvious. These latter two species and *H. cucullus* are grouped within one clade according to both molecular data sets, whereas *H. cassilatus* and *H. weddellensis* form a second clade, which is the sister group of the first. These findings, indicating a high degree of morphological plasticity within the *Haploniscus cucullus* complex, suggest that it might contain yet further species.

The intention of the present molecular study was to help resolve phylogenetic relationships within a group of morphological similar Antarctic Haplonisciidae as well as to test the value of DNA sequences for the identification of the described species. Owing to amplification problems, additional analyses using the

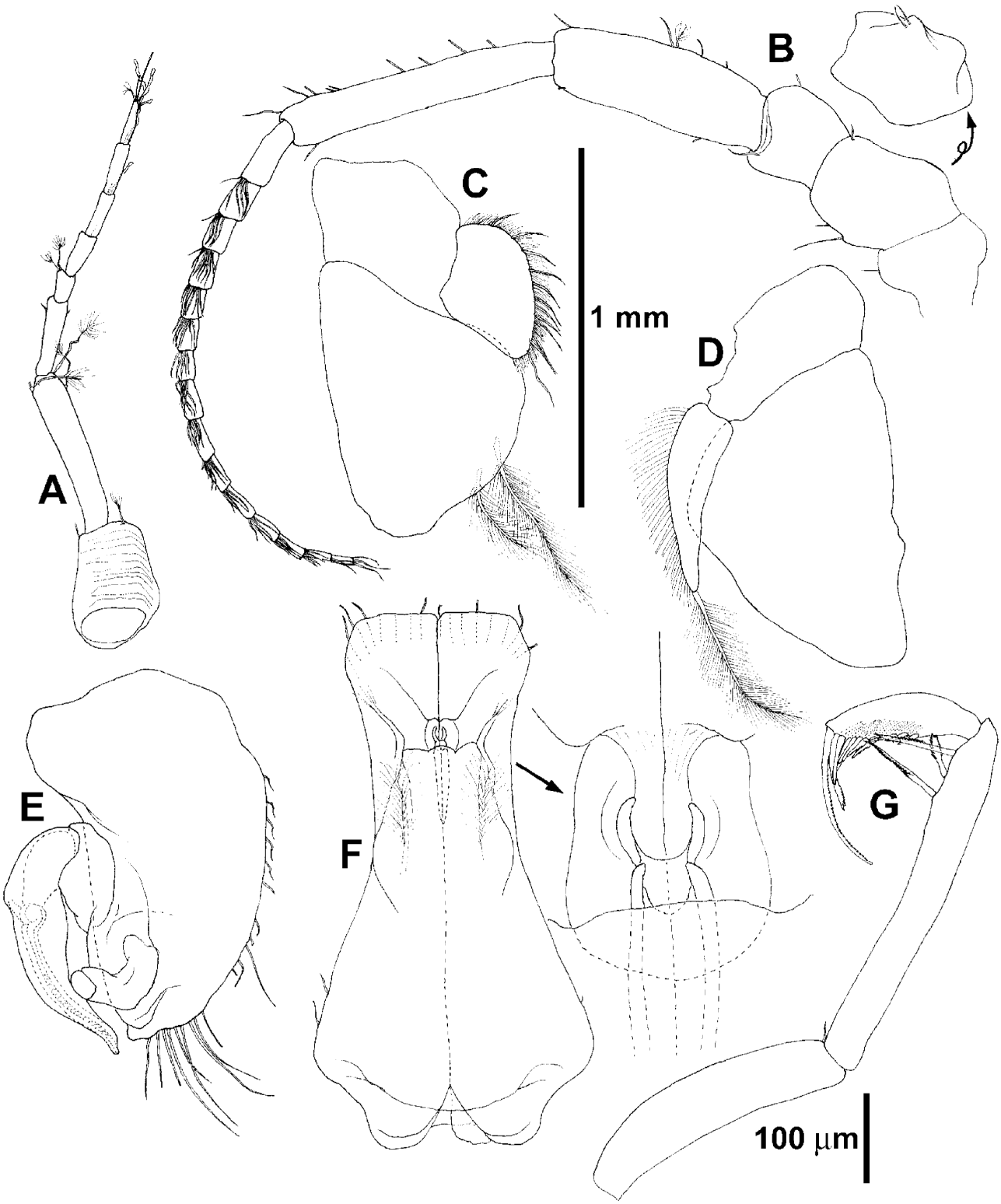

Figure 37. ***Haploniscus microkorys*** **sp. nov.**, holotype, male, K40767, 4.3 mm: A, antenna 1; B, antenna 2; C, pleopod 3; D, pleopod 4; E, pleopod 2; F, pleopod 1; G, mandibular palp.

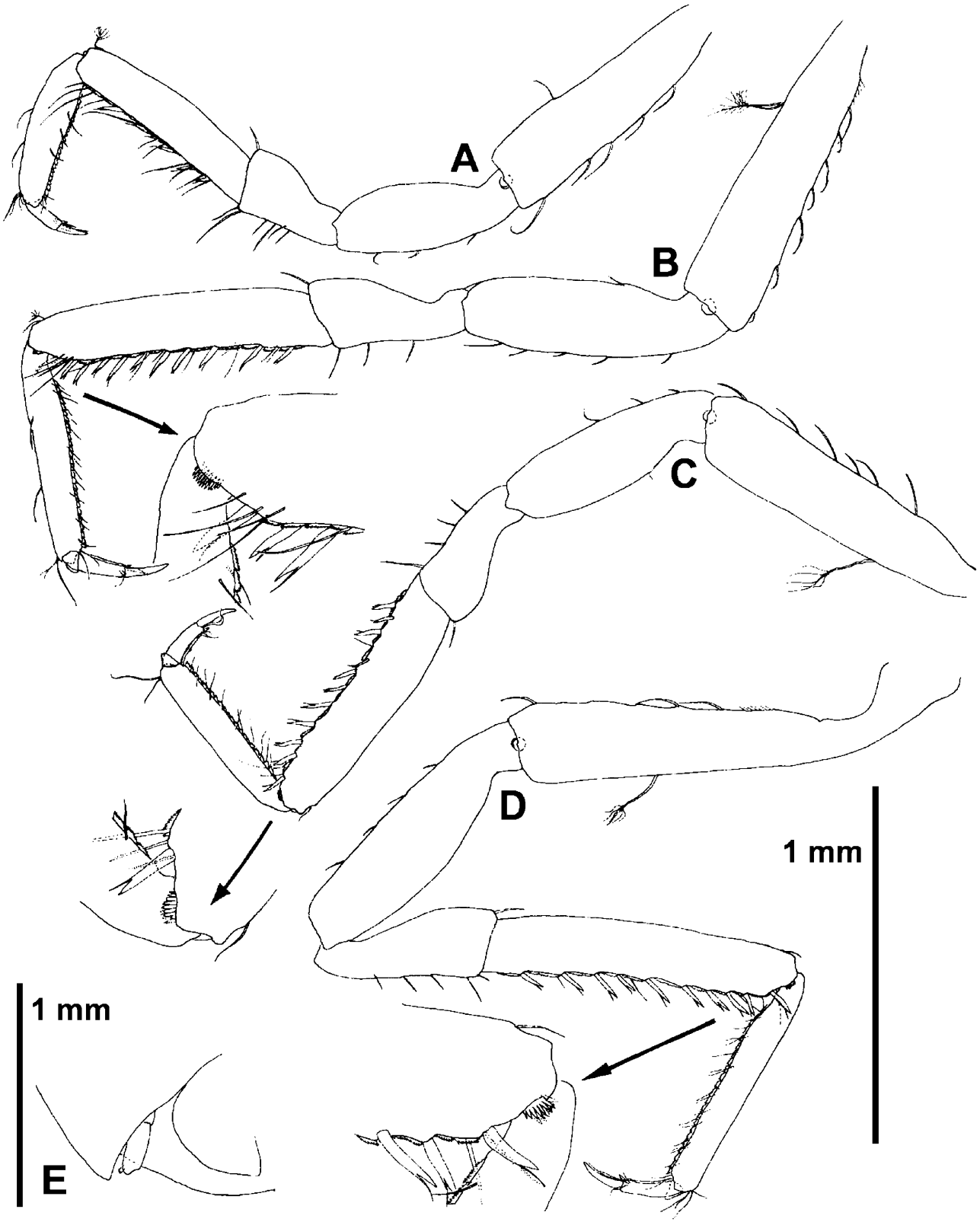

Figure 38. ***Haploniscus microkorys*** **sp. nov.**, holotype, male, K40767, 4.3 mm: A, pereopod 1; B, pereopod 3; C, pereopod 2; D, pereopod 4; E, uropod.

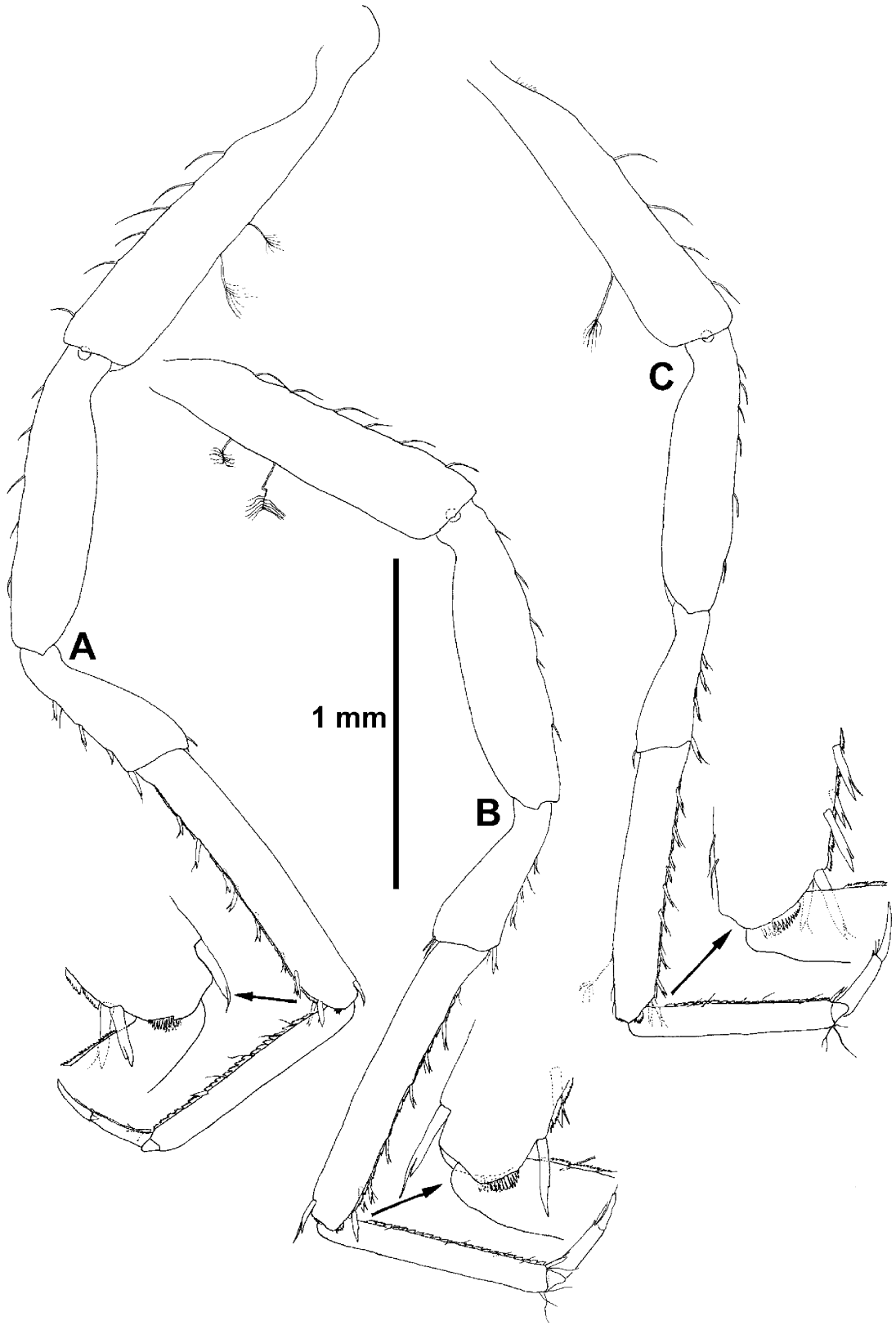

Figure 39. ***Haploniscus microkorys*** **sp. nov.**, holotype, male, K40767, 4.3 mm: A, pereopod 5; B, pereopod 6; C, pereopod 7.

Table 2. Pairwise genetic distances of haplotypes of mitochondrial 16S rDNA sequences (above: *p*-distances, below: *d*-distances)

	H. cassilatus (*N* = 6)	*H. cucullus* (*N* = 8)	*H. microkorys* (*N* = 1)	*H. nudifrons* (*N* = 1)	*H. weddellensis* (*N* = 4)
H. cassilatus	0–0.0060				
(*N* = 6)	0–0062				
H. cucullus	0.1345–0.1456	0.0020–0.0102			
(*N* = 8)	0.2052–0.2298	0.0020–0.0104			
H. microkorys	0.1150–0.1190	0.0826–0.0887	0		
(*N* = 1)	0.1679–0.1774	0.1088–0.1157			
H. nudifrons	0.1322–0.1362	0.1036–0.1097	0.0732	0	
(*N* = 1)	0.2035–0.2141	0.1433–0.1543	0.0914		
H. weddellensis	0.0816–0.0878	0.1333–0.1396	0.1195–0.1217	0.1322–0.1362	0–0.0020
(*N* = 4)	0.1059–0.1171	0.2042–0.2186	0.1827–0.1876	0.2153–0.2206	0–0.0020

N = number of specimens.

Table 3. Pairwise genetic distances of complete 18S rDNA sequences (lower triangle; above: *p*-distances, below: *d*-distances)

	H. cassilatus	*H. cucullus*	*H. microkorys*	*H. nudifrons*	*H. weddellensis*
H. cassilatus	–	29/42	26/24	29/28	16/15
H. cucullus	0.0324	–	24/41	28/44	31/35
	0.0334				
H. microkorys	0.0228	0.0298	–	32/22	29/27
	0.0233	0.0306			
H. nudifrons	0.0260	0.0330	0.0246	–	23/34
	0.0266	0.0340	0.0251		
H. weddellensis	0.0140	0.0301	0.0256	0.0260	–
	0.0143	0.0310	0.0261	0.0266	

Upper triangle: number of observed genetic distances. transitions (left) vs. transversions (right).

cytochrome oxidase subunit I gene (COI), the classical gene for DNA barcoding, were not possible. Obviously the priming sites of CO1 appear to be highly variable among the Haloniscidae, hindering the application of a universal primer. This problem is also known from other animal species (e.g. Vences *et al*., 2005a, b). However, our study strongly validated the efficacy of both analysed genes for phylogenetic studies and species identification within the *Haloniscus cucullus* complex. The comparison of 16S rDNA and 18S rDNA sequences of the same species shows that mitochondrial DNA is more variable, a fact which is ascribed among other reasons to the higher metabolic rate of mitochondria, causing a higher mutation rate within mitochondrial genes (e.g. Martin & Palumbi, 1993).

Mitochondrial gene sequences have been successfully used for analysing the phylogenetic relationships between closely related species (e.g. Schubart, Diesel & Hedges, 1998; Schubart, Cuesta & Rodríguez, 2001; Near, Pesavento & Cheng, 2003). Owing to its higher mutation rate, the 16S rRNA gene may reveal more support for younger phylogenetic events than 18S rRNA gene sequences, which can be used more properly in identifying older processes (Hillis & Dixon, 1991). Both aspects can be observed in our study. The two data sets resulted in identical tree topologies, but whereas the 16S rDNA data set supports nodes within the genus *Haloniscus* with high values, posterior probabilities of the 18S rDNA data have lower values. Most studies dealing with genetic differentiations within populations and the identification of sibling species only use mitochondrial DNA, which can have some possible pitfalls. Mitochondrial polymorphism might be caused by persistent ancestral polymorphisms, by introgression or by isolation (e.g. Theimer & Keim, 1994; Mason, Butlin & Gacesa, 1995; Bernatchez *et al*., 1996; Wares, 2001). Nevertheless, our approach combines mitochondrial, nuclear and morphological data. We found *p*-distances of at least

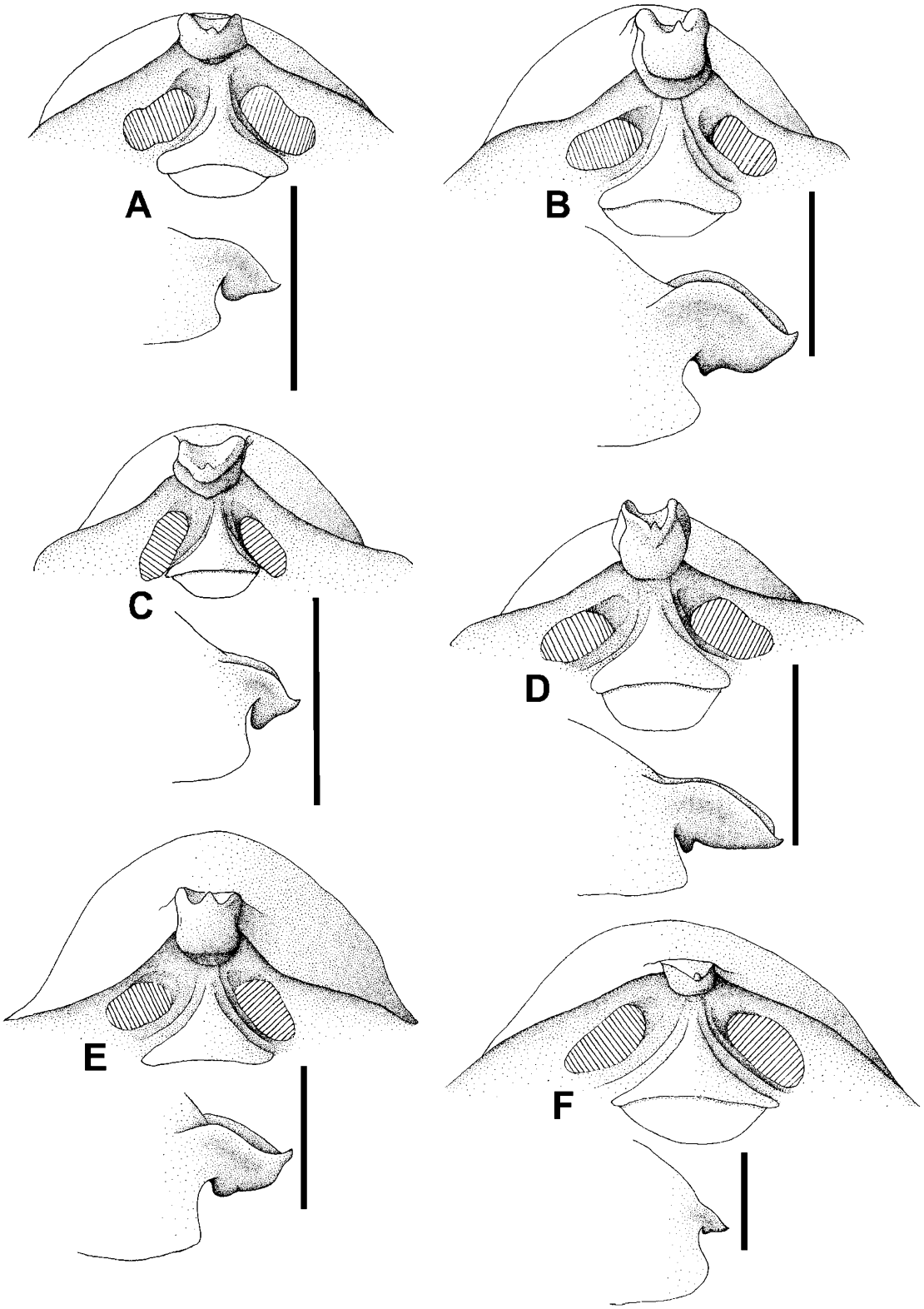

Figure 40. Frontal and lateral view of rostral processes: A, ***Haploniscus cassilatus* sp. nov.**, paratype, male, K40757, 3.6 mm; B, ***H. cucullus* sp. nov.**, holotype, K40758, male, 5.3 mm; C, ***H. weddellensis* sp. nov.**, holotype, male, K40761, 3.0 mm; D, ***H. procerus* sp. nov.**, holotype, female, K40763, 7.6 mm; E, ***H. kyrbasia* sp. nov.**, holotype, male, K40765, 5.7 mm; F, ***H. microkorys* sp. nov.**, holotype, male, K40767, 4.3 mm. Scale bars = 500 μm.

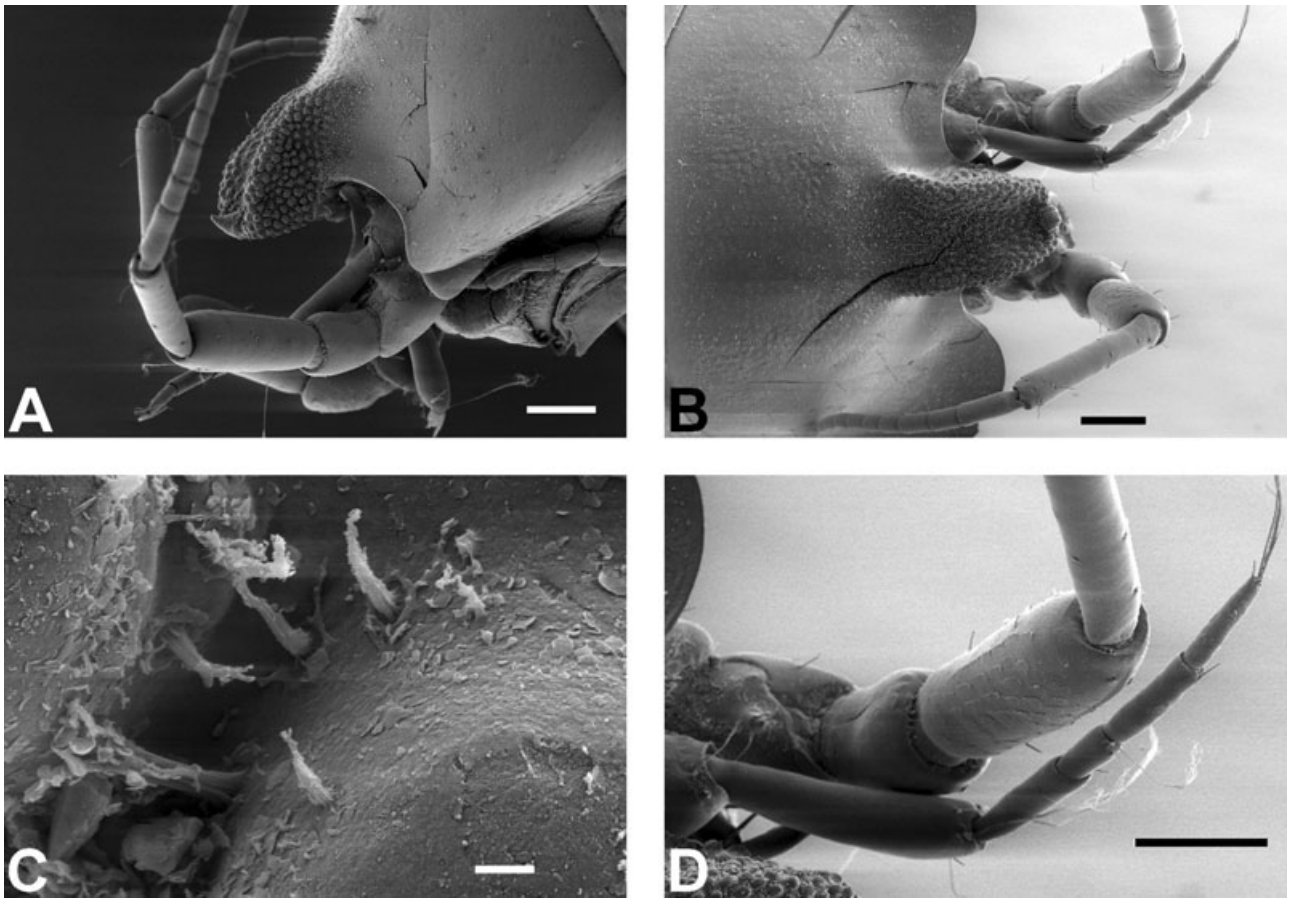

Figure 41. ***Haploniscus cucullus*** **sp. nov.**, SEM: A, rostrum and antennae, lateral view; B, rostrum and antennae, dorsal view; C, detail of dorsal rostrum structure; D, detail of B, showing antennal scales. Scale bars = 100 μm (A, B, D), 1 μm (C).

0.0732 (*d*-distances: 0.0914) for the 16S rDNA (between *Haploniscus microkorys* and *H. nudifrons*, two species that show greater morphological differences than the other five species) and 0.0140 (*d*-distances: 0.0143) for the 18S rDNA (between *Haploniscus cassilatus* and *H. weddellensis*) between species. These values should be used as guidelines for further studies of the genetic variability and the definition of distinct species within deep-sea asellote isopods, and especially the Haploniscidae.

All species possessing the characteristic rostrum seem to have a very limited distribution and were only found at stations relatively close the Antarctic Peninsula, suggesting a local radiation. The specimens found at stations 42-2 and 43-8 belong to the same species, *H. cucullus*. The two stations are located relatively closely together (about 120 km apart) in the Scotia Sea and have similar depths. The other species were each found at one station only without any distributional overlap. Preliminary studies of material obtained during the ANDEEP III expedition in 2005 showed that species possessing the characteristic rostrum were not contained in samples from the eastern Weddell Sea, but occurred at several stations in the western Weddell Sea. The depth distribution of the two clades in Figure 42 within the *Haploniscus cucullus* complex is rather different. *H. weddellensis* and *H. cassilatus* are found at depths of about 1100 and 2900 m, respectively, while species of the other clade (*H. cucullus*, *H. nudifrons*, *H. microkorys*) were found below 3600 m only.

Although patterns of deep-sea biodiversity at species level have been documented from local to global scales (Rex, Etter & Stuart, 1997; Rex, Stuart & Coyne, 2000), research on the genetic foundation of this biodiversity is just beginning. Quattro *et al*. (2001) identified several morphologically cryptic but genetically distinct clades in the deep-sea gastropod *Frigidoalvania brychia*, while Weinberg *et al*. (2003) analysed genetic differences within and between species of the deep-sea crab *Chaceon*. Allozyme studies and analyses of mitochondrial DNA (Bucklin,

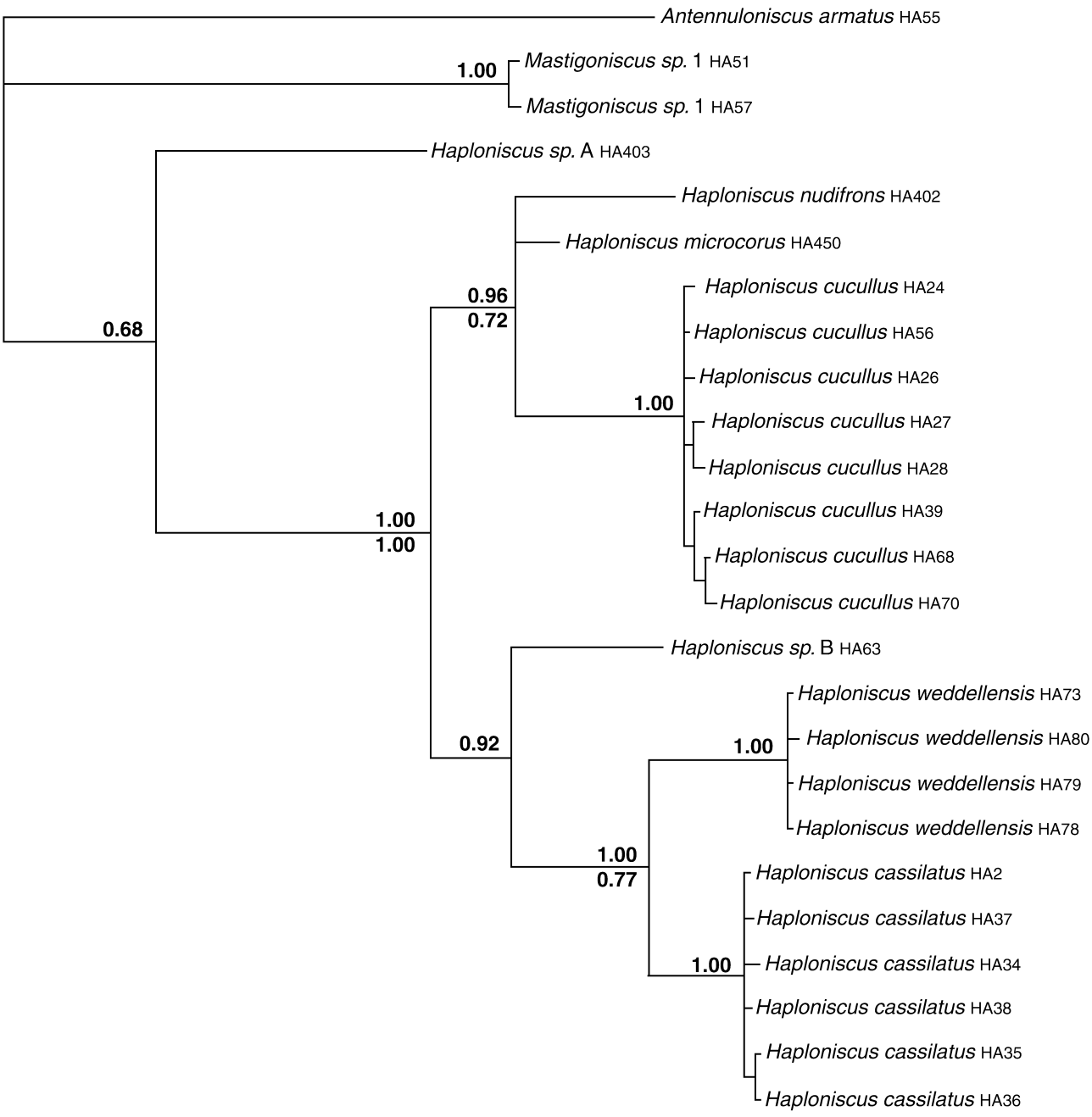

Figure 42. Bayesian 50% majority rule consensus tree of the 16S rDNA data set. Model choice based on AIC: TVM model with gamma distributed rates (alpha = 0.3755) and no invariant positions (see text for more details). Values above the branches are posterior proabilities of the 16S rDNA data set, values below of the 18S rDNA data set (if applicable).

Wilson & Smith, 1987; France & Kocher, 1996) reveal distinct populations within the amphipod *Eurythenes gryllus*. In contrast, recent molecular studies in four species of protobranch bivalves reveal a decrease of population differentiation with depth (Etter *et al*., 2005). However, all studies support the theory of high species diversity in the deep sea. With an unexpected diversity of species the deep sea provides a challenging target for both morphological and molecular taxonomy.

ACKNOWLEDGEMENTS

We would like to thank Professors Angelika Brandt and Johann-Wolfgang Wägele for their support during the ANDEEP project and helpful discussions.

The manuscript benefited from the comments of Drs Marina Malyutina and Gary Poore. We are grateful to Professor Dieter Fütterer, chief scientist, and all participants of the ANDEEP cruises. Furthermore we would like to thank all pickers and sorters of the ANDEEP material and also Renate Walter for her assistance in obtaining the SEM pictures. This study was supported by the German Science Foundation (DFG Br 1121/20, Wa 530/26). This is ANDEEP publication no. 59.

REFERENCES

Akaike H. 1974. Information theory and an extension of the maximum likelihood principle. In: Petrov BN, Csaki F, eds. *Second International Symposium on Information Theory*. Budapest: Akademiai Kiado, 267–281.

Bernatchez L, Vuorinen JA, Bodaly RA, Dodson JJ. 1996. Genetic evidence for reproductive isolation and multiple origins of sympatric trophic ecotypes of whitefish (*Coregonus*). *Evolution* **50:** 624–635.

Birstein JA. 1963a. Isopods from the ultra-abyssal zone of the Bougainville Trench. *Zoologicheskii Zhurnal* **42:** 814–834 (in Russian).

Birstein JA. 1963b. *Deep water isopods (Crustacea. Isopoda) of the north-western part of the Pacific Ocean.* Moscow: Akademiya Nauk, SSSR (in Russian, English translation by the Indian National Scientific Documentation Centre, New Delhi, 1973).

Birstein JA. 1968. Deep-sea Asellota (Isopoda) from the Antarctic and Subantarctic. *Biological reports of the Soviet Antarctic Expedition (1955–1958)* **4:** 141–152.

Birstein JA. 1971. Additions to the fauna of isopods (Crustacea, Isopoda) of the Kurile-Kamchatka Trench. Part II. Asellota 2. *Trudy Instituta Okeaonogiya* **92:** 162–238 (in Russian).

Brenke N. 2005. An epibenthic sledge for operations on marine soft bottom and bedrock. *Journal of the Marine Technology Society* **39:** 13–24.

Brökeland W, Wägele JW. 2004. Redescription of three species of Haploniscus Richardson, 1908 (Isopoda, Asellota, Haploniscidae) from the Angola Basin. *Organisms, Diversity and Evolution* **4** (Electronic suppl. 7)**:** 1–40.

Bucklin A, Wilson RR Jr, Smith KL Jr. 1987. Genetic differentiation of seamount and basin populations of the deep-sea amphipod *Eurythenes gryllus*. *Deep-Sea Research* **34:** 1795–1810.

Bucklin A, Bentley AM, Franzen SP. 1998. Distribution and relative abundance of *Pseudocalanus moultoni* and *P. newmani* (Copepoda: Calanoida) on Georges Bank using molecular identification of sibling species. *Marine Biology* **132:** 97–106.

Chardy P. 1974. Les Haploniscidae (Crustacés Isopodes Asellotes) de l'Atlantique. Description de huit espèces nouvelles. *Bulletin du Muséum national d'Histoire naturelle, 3^e série* **no. 243, Zoologie 167:** 1137–1166 (in French).

Chardy P. 1975. Isopodes nouveaux des campagnes Biaçores et Biogas IV en Atlantique Nord. *Bulletin du Muséum national d'Histoire naturelle, 3^e série* **no. 303, Zoologie 213:** 1137–1167 (in French).

Chardy P. 1977. La famille des Haploniscidae (Isopodes, Asellotes): discussion systématique et phylogénique. *Bulletin du Muséum national d'Histoire naturelle 3^e série* **no. 476, Zoologie 333:** 879–906 (in French).

Dreyer H, Wägele JW. 2001. Parasites of crustaceans (Isopoda: Bopyridae) evolved from fish parasites: molecular and morphological evidence. *Zoology* **103:** 157–178.

Dreyer H, Wägele JW. 2002. The Scutocoxifera tax nov. (Crustacea, Isopoda) and the information content of nuclear SSU rDNA sequences for reconstruction of isopod phylogeny (Peracarida: Isopoda). *Journal of Crustacean Biology* **22:** 217–234.

Edgar RC. 2004. MUSCLE: multiple sequence alignment with high accuracy and high throughput. *Nucleic Acids Research* **32:** 1792–1797.

Etter RJ, Rex MA. 1990. Population differentiation decreases with depth in deep-sea gastropods. *Deep-Sea Research* **37:** 1251–1261.

Etter RJ, Rex MA, Chase MC, Quattro JM. 1999. A genetic dimension to deep-sea biodiversity. *Deep-Sea Research Part I* **46:** 1095–1099.

Etter RJ, Rex MA, Chase MR, Quattro JM. 2005. Population differentiation decreases with depth in deep-sea bivalves. *Evolution* **59:** 1479–1491.

France SC, Kocher TD. 1996. Geographic and bathymetric patterns of mitochondrial 16S rRNA sequence divergence among deep-sea amphipods, *Eurythenes gryllus*. *Marine Biology* **126:** 633–643.

George RY. 2004. Deep-sea asellote isopods (Crustacea, Eumalacostraca) of the north-west Atlantic: the family Haploniscidae. *Journal of Natural History* **38:** 337–373.

Hansen HJ. 1916. Crustacea. Malacostraca III. *Danish Ingolf Expedition* **3:** 1–262.

Hebert PDN, Cywinska A, Ball SL, deWaard JR. 2003. Biological identifications through DNA barcodes. *Proceedings of the Royal Society of London Series B* **270:** 313–321.

Hillis DM, Dixon MT. 1991. Ribosomal DNA: molecular evolution and phylogenetic inference. *Quarterly Review of Biology* **66:** 411–453.

Huelsenbeck JP, Ronquist F. 2001. MrBayes: bayesian inference of phylogenetic trees. *Bioinformatics* **17:** 754–755.

Knowlton N. 1993. Sibling species in the sea. *Annual Reviews in Ecology and Systematics* **24:** 189–216.

Knowlton N. 2000. Molecular genetic analyses of species boundaries in the sea. *Hydrobiologia* **420:** 73–90.

Kussakin OG. 1988. Marine and brackish-water Crustacea (Isopoda) of cold and temperate waters of the Northern Hemisphere. 3. Suborder Asellota 1. Janiridae, Santiidae, Dendrotionidae, Munnidae, Haplomunnidae, Mesosignidae, Haploniscidae, Mictosomatidae, Ischnomesidae. *Opredeliteli Po Faune SSSR, Akademiya Nauk, SSSR* **125:** 1–501 (in Russian).

Lincoln RJ. 1985a. The marine Fauna of New Zealand: Deep-sea Isopoda Asellota, family Haploniscidae. *Memoirs of the New Zealand Oceanographic Institute* **94:** 1–56.

Lincoln RJ. 1985b. Deep-sea asellote isopods of the north-east Atlantic: the family Haploniscidae. *Journal of Natural History* **19:** 655–695.

Martin AP, Palumbi SR. 1993. Body size, metabolic rate, generation time, and the molecular clock. *Proceedings of the National Academy of Sciences of the USA* **90:** 4087–4091.

Mason DJ, Butlin RK, Gacesa P. 1995. An unusual mitochondrial DNA polymorphism in the *Chorthippus biguttulus* species group (Orthoptera: Acrididae). *Molecular Ecology* **4:** 121–126.

Menzies RJ. 1956. New abyssal tropical Atlantic isopods, with observations on their biology. *American Museum Novitates* **1798:** 1–16.

Menzies RJ. 1962. The Isopods of abyssal depths in the Atlantic Ocean. *Vema Research Series* **1:** 79–206.

Menzies RJ, George RY. 1972. Isopod Crustacea of the Peru-Chile Trench. *Anton Bruun Report* **9:** 1–124.

Near TJ, Pesavento JJ, Cheng C-HC. 2003. Mitochondrial DNA, morphology, and the phylogenetic relationships of Antarctic icefishes (Notothenioidei: Channichthyidae). *Molecular Phylogenetics and Evolution* **28:** 87–98.

Palumbi SR, Martin A, Romano S, McMillan WO, Stice L, Grabowski G. 1991. *The simple fool's guide to PCR*, Version 2. Honolulu: University of Hawaii Press.

Posada D, Crandall KA. 1998. MODELTEST: testing the model of DNA substitution. *Bioinformatics* **14:** 817–818.

Quattro JM, Chase MR, Rex MA, Greig TW, Etter RJ. 2001. Extreme mitochondrial DNA divergence with populations of the deep-sea gastropod *Frigidoalvania brychia*. *Marine Biology* **139:** 1107–1113.

Raupach MJ, Wägele JW. 2006. Distinguishing cryptic species in Antarctic Asellota (Crustacea: Isopoda) – a preliminary study of mitochondrial DNA in *Acanthaspidia drygalskii*. *Antarctic Science* **18:** 191–198.

Raupach MJ, Held C, Wägele JW. 2004. Multiple colonization of the deep sea by the Asellota (Crustacea: Peracarida: Isopoda). *Deep-Sea Research II* **51:** 1787–1795.

Rex MA, Etter RJ, Stuart CT. 1997. Large-scale patterns of species diversity in the deep-sea benthos. In: Ormond RFG, Gage RD, Angel MV, eds. *Marine biodiversity: patterns and processes*. Cambridge: Cambridge University Press, 94–121.

Rex MA, Stuart CT, Coyne G. 2000. Latitudinal gradients of species richness in the deep-sea benthos of the North Atlantic. *Proceedings of the National Academy of Science of the USA* **97:** 4082–4085.

Richardson H. 1908. Some new isopoda of the superfamily Aselloidea from the Atlantic coast of North America. *Proceedings of the US National Museum* **35:** 71–86.

Sanger F, Nicklen S, Coulson AR. 1977. DNA sequencing with chain-terminating inhibitors. *Proceedings of National Academy of Science of the USA* **74:** 5463–5467.

Sars GO. 1877. Prodomus descriptionis Crustaceorum et Pycnogonidarum qvae in expeditione Norvegica anno 1876, observatit. *Archiv for Mathematik Og Naturvidenskab* **2:** 237–271 [in Latin].

Schubart CD, Diesel R, Hedges SB. 1998. Rapid evolution to terrestrial life in Jamaican crabs. *Nature* **393:** 363–365.

Schubart CD, Cuesta JA, Rodríguez A. 2001. Molecular phylogeny of the crab genus *Brachynotus* (Brachyura: Varunidae) based on the 16S rRNA gene. *Hydrobiologia* **449:** 41–46.

Swofford DL. 2001. *PAUP*. Phylogenetic analysis using parsimony (* and other methods)*, Version 4. Sunderland, MA: Sinauer Associates.

Tautz D, Arctander P, Minelli A, Thomas RH, Vogler AP. 2003. A plea for DNA taxonomy. *Trends in Ecology and Evolution* **18:** 70–74.

Theimer TC, Keim P. 1994. Geographic patterns of mitochondrial DNA variation in collared peccaries. *Journal of Mammology* **75:** 121–128.

Vanhöffen E. 1914. Die Isopoden der Deutschen Südpolar-Expedition 1901–1903. *Deutsche Südpolar-Epedition* **15:** 449–598.

Vences M, Thomas M, Bonett RM, Vieites DR. 2005a. Deciphering amphibian diversity through DNA barcoding: chances and challenges. *Philosophical Transactions of the Royal Society of London Series B* **360:** 1859–1868.

Vences M, Thomas M, van der Meijden A, Chiari Y, Vieites DR. 2005b. Comparative performance of the 16S rRNA gene in DNA barcoding of amphibians. *Frontiers in Zoology* **2:** 5.

Wägele JW. 1983. The homology of antennal articles in Isopoda. *Crustaceana* **45:** 31–37.

Ward RD, Zemlak TS, Innes BH, Last PR, Hebert PDN. 2005. DNA barcoding Australia's fish species. *Philosophical Transactions of the Royal Society of London Series B* **360:** 1847–1857.

Wares JP. 2001. Intraspecific variation and geographic isolation in *Idotea balthica* (Isopoda: Valvifera). *Journal of Crustacean Biology* **21:** 1007–1013.

Weinberg JR, Dahlgren TG, Trowbridge N, Halanych KM. 2003. Genetic differences within and between species of deep-sea crabs (*Chaceon*) from the North Atlantic Ocean. *Biological Bulletin* **204:** 318–326.

Wetzer R. 2001. Hierarchical analysis of mtDNA variation and the use of mtDNA for isopod (Crustacea: Peracarida: Isopoda) systematics. *Contributions to Zoology* **70:** 23–39.

Wetzer R, Martin JW, Trautwein SE. 2003. Phylogenetic relationships within the coral crab genus *Carpilius* (Brachyura, Xanthoidea, Carpiliidae) and of the Carpiliidae to other xanthoid crab families based on molecular sequence data. *Molecular Phylogenetics and Evolution* **27:** 410–421.

Wolff T. 1962. The systematics and biology of bathyal and abyssal Isopoda Asellota. *Galathea Report* **6:** 1–320.